NTNU
Norwegian University of
Science and Technology

Faculty of Engineering
Science and Technology
Department of Hydraulic
and Environmental Engineering

CONTACT FILTRATION OF HUMIC WATERS IN EXPANDED CLAY AGGREGATE FILTERS

By

Torgeir Saltnes

A Dissertation submitted to
the Faculty of Engineering Science and Technology,
the Norwegian University of Science and Technology,
in partial fulfillment of the requirements for the degree of
Doctor Engineer

Trondheim, Norway, March 2002

SUMMARY

This study deals with contact filtration of humic waters using expanded clay aggregates as filter media. The main objective of the work was to identify the desired characteristics of the filter media, and optimise the efficiency when used in a filter bed. Emphasis has been on removal of humic substances from drinking water.

Humic substances
Humic substances are large, organic molecules resulting from the degradation of plants and animals. When these molecules are washed out from the soil and end up in the water sources, a lake or river, they are causing a brownish colouring of the water. Water with high levels of humic substances, might not be harmful to drink, but there are other problems connected to these organic compounds. Micro-pollutants in the water (like pesticides) might be associated with the humic molecules and if chlorination is used for disinfection, carcinogenic by products are formed.

Because the humic substances are molecules, they have to be pre-treated to create filterable particles before filtration in a depth filter. Deep bed granular filtration is a treatment method where particles are removed by sedimentation on, interception of, or diffusion to filter grains, and stored in the depth of the filter bed. In direct filtration the coagulant is added in a rapid mixing device, before flocculation to enhance floc growth, and filtration. In contact filtration the flocculation step is omitted, and particle formation takes place inside the filter pores.

The filter media
In this study expanded clay aggregates (Filtralite) are used as the granular filter media in deep bed contact filtration. Testing of settling velocity for clay aggregates with different densities unveiled that Filtralite could be used as the only media in a dual media filter bed. Down flow filter beds usually consist of two media or more with different size ranges, with the direction of flow towards smaller grain sizes to enhance particle removal. A common design is a layer of anthracite coal grains on top a layer of smaller sized sand grains. The density of the top layer (large) grains must be lower than for the bottom layer (small) grains to avoid intermixing of the two after settling from a backwash.

Due to the porous structure of the expanded clay aggregates they adsorb water. Especially the Filtralite NC (Normal density, crushed) material gives an increase in particle density when water penetrates the air-filled pores. Water uptake is rapid the first weeks, and after this a slow increase in settling velocity is observed for about half a year. The Filtralite HC (High density, crushed) material shows the same behaviour as anthracite, with only a small water uptake in the first few days. The increase in density for Filtralite NC is of importance for the design of a filter bed and might lead to washout of media if not treated with caution the first weeks after wetting. One possible solution is pre-wetting of the material before it is taken into service in order to reduce the loss of media. Attrition tests involving 100 hours of backwashing with both air and water have shown that both HC and NC materials have sufficient resistance to attrition.

Pilot plant

A number of contact filtration experiments were performed in a pilot plant consisting of two parallel filter columns. Raw waters used in the experiments have been tap water added humic concentrate from an ion-exchange plant, and/or bentonite clay suspension. The raw water was pH adjusted with HCl prior to coagulant addition. The in-line mixer provided a head loss of about 0,2 m for proper mixing of the coagulant. Water was then lead to the two filter columns. One filter used as a reference filter consisted of a top layer of 60 cm anthracite (0,8-1,6 mm), on top a 35 cm deep layer of sand (0,4-0,8 mm). In the other filter there was 47 cm Filtralite NC (1,6-2,5 mm) on top 47 cm Filtralite HC (0,8-1,6 mm). Later in the experimental part of the study the Filtralite filter was changed, by increasing the bed depth. This was done to see if it was possible to compensate for the larger grains by increasing filter depth. Turbidity, pH, flow and head loss in the filter bed was measured on-line, and data were logged and saved on a computer. Raw, coagulated and filter effluent water were sampled for each experiment and analysed in the laboratory.

Optimisation experiments

The initial series of experiments were carried out to study coagulation optimisation for the Filtralite filter. Since this filter had coarser media than the reference filter, it was necessary to find the coagulant type, dose and pH conditions that were optimal in order to create flocs that were filterable and storable in this media. Coagulation/filtration of humic waters give generally short filter runs, and it was of high priority to find a way to utilise the storage capacity of the coarse Filtralite filter.

Four coagulants were tested in the dose/pH optimisation, which focused on the removal of organic matter (humic substances). Aluminium sulphate, iron chloride sulphate, poly-aluminium chloride and the biopolymer chitosan were all tested at 3-4 different doses and pH of coagulation. The optimisation experiments were performed in the pilot filter plant by taking out water samples after steady effluent turbidity conditions had been obtained. Generally four raw waters were used in the optimisation tests, RW15 and RW50 (colour levels of 15 and 50), and RW15/3 and RW50/3 (same colour levels but with increased turbidity up to 3 NTU added as bentonite clay). The tap water had a turbidity of about 0,2 NTU. Effluent water quality was evaluated by analysis of residual turbidity and residual metal concentration (when a metal salt was used for coagulation), as well as removal of true colour and TOC (total organic carbon).

The experiments showed that the water quality produced by the filters is affected by pH and dose for all four coagulants. Coagulation of coloured, low turbidity raw waters with a metal salt, was found to be dependent on the formation of positively charged metal species that can interact with the negatively charged humics, or precipitates of metal hydroxide form and act as adsorbers. A common problem experienced when using metal salts is too high metal residuals. Metal penetrate the filter as soluble (strongly pH dependent) or as colloids/particulates, which are not removed. This means that pH has to be within certain limits (dependent on the coagulant used) to comply with residual metal limitations. If soluble metal is kept at a low level by pH adjustment, this is, however, not always the optimum pH for particulate removal. Hydroxide precipitates (which show as turbidity in the effluent) may contribute considerably to high levels of residual metal.

The colour and TOC removal was found to be higher for the metal salts than for chitosan. Removals of more than 90% colour and 70% TOC was achievable with metal-based coagulants. Chitosan however, was able to remove up to 80% colour and 40% TOC with the doses used in this study. The relatively lower TOC removal for chitosan was most likely caused by the fact that about 60wt% of chitosan is organic matter, which might contribute to effluent TOC. Optimum pH for aluminium-based coagulants was about 6, but this is a compromise between low levels of turbidity and residual metal. Iron chloride sulphate had an optimum pH of about 5,5. The optimum doses were more or less proportional, on mol basis, to the level of organic matter content in the raw water. However, generally lower removals were observed for RW15 than for RW50 at equal specific doses. Higher levels of turbidity in the raw water (RW15/3 and RW50/3) did not increase the coagulant demand (in relation to

removal of organics) to any great extent, implying that humic substances are much more coagulant demanding than clay particles.

The experiments did not reveal any differences with respect to optimum pH and dose between the filters. What were seen however, were differences in effluent turbidity and residual metal caused by the grain size difference in the two filters. Aluminium sulphate used to coagulate RW50 produced an effluent turbidity from the Filtralite filter of about 0,5 NTU compared to 0,13 NTU for the anthracite/sand filter at optimum conditions. The removal of organic matter did not differ to the same extent. The other metal coagulants and especially chitosan performed much better in the Filtralite filter as compared to aluminium sulphate. For raw waters containing higher levels of turbidity the difference in effluent water quality between the coarse Filtralite filter and the anthracite /sand filter was much less than for low turbidity raw waters. The filterability of the flocs created with clay particles was higher than the flocs with only humics. This is probably due to an increased density of the flocs, which make them more separable by sedimentation on the filter grains. The more filterable flocs created with clay particles gave in addition low metal residuals. This is due to the possibility one has by increasing pH, to enhance precipitation and reduce the fraction of soluble metal, without too much turbidity leaking through the filter.

Filtration experiments

At the optimum conditions for each coagulant and raw water, full filter runs were performed in the pilot plant until termination by breakthrough or head loss. The results obtained in these experiments were evaluated on the basis of filter run time, solids storage capacity, total head loss, head loss distribution in the filter bed and effluent turbidity.

Raw water that produced low levels of solids after coagulation gave relatively longer filter runs than coagulated waters high in suspended solids. For RW15 the larger pore volumes in the Filtralite filter could be utilised, and the slow head loss development with time gave long runs before termination, in most cases by breakthrough. The anthracite sand filter had a much more rapid head loss development due to the smaller grains, and was usually head loss limited before the storage capacity was utilised. Chitosan for coagulation was superior to the other coagulants with respect to effluent water turbidity and run length. However, this coagulant gives a higher head loss per weight unit of solids loaded to the filter. This is a significant advantage in combination with the coarse Filtralite filter, due to the large available head loss.

For the raw waters containing higher levels of colour and/or turbidity, filter run times were short (usually less than 5 hours) with the exception of experiments with chitosan. With this coagulant and RW50, which was the most difficult raw water to treat, run lengths of about 21 and 14 hours were obtained in the Filtralite filter and anthracite/sand filter respectively, before breakthrough (Filtralite) and head loss (anth./sand) limitation occurred. From both filters, effluent turbidity was below 0,06 NTU.

Inspection of head loss gradients distribution in the filter bed (cm head loss per cm bed depth), show that citosan can build up much higher gradients than a metal salt. This indicates that the humic flocs formed with chitosan are stronger than the ones from metal salt coagulation. The head loss gradients that build up in the filters are generally higher for raw waters with colour and low turbidity than for raw waters with higher levels of turbidity. This is caused by the more voluminous flocs and deposits formed with the humics for raw waters low in turbidity. In the anthracite/sand filter the gradient for the top section of anthracite and sand was very high while the bottom sections within each layer experienced only a small increase in head loss. In the Filtralite filter the head loss gradients showed a much more even distribution in the depth of the filter.

The experiments on deeper Filtralite filter demonstrated that it was possible to produce equally low effluent turbidity from that filter as from the anthracite/sand filter when poly-aluminium chloride and chitosan were used as coagulants. By increasing the depth of the filter bed, the run length is prolonged, but the relationship is not necessarily linear.

Filtration rate have an influence on effluent water quality and filter run time. The coarse Filtralite filter was more sensitive, with regard to effluent water quality, to higher filtration rates than the anthracite/sand filter when a metal salt was used for coagulation. Both filters showed almost no increase in effluent turbidity for filtration rates between 7,5 and 20 m/h when chitosan was used as coagulant. An increased filter bed depth made the filter more resilient at higher filtration rates. The relationship between filter run time and filtration rate was not proportional, and relatively longer runs were obtained at low rates. This implies that a higher filtration rate decreases the utilisation of the filters storage capacity. Analysis of head loss gradients in the filter bed depth demonstrated that more solids were deposited further down in the filter bed at higher filtration rates. This resulted in a lower utilisation of the top section of the filter, where storage capacity was high compared to the bottom filter layer (sand or Filtralite HC).

By analysing head loss gradients as a function of time for each layer of a filter, a dynamic picture of the contact filtration process can be seen. In the first period after start up of a filtration run, the top sections of the filter bed were active while the bottom sections showed no increase in head loss. These bottom sections of the bed were taken into use one by one, as the storage capacity of the upper adjacent layer was exhausted. When a head loss gradient was detected in the bottom layer, an increase in effluent turbidity was immediately seen, indicating an incipient breakthrough. The depth of the active layer was dependent on the filter bed characteristics, filtration rate and the character of the suspension to be filtered.

The different raw waters tested showed the same trend when filter run times were analysed as a function of solids load to the filters. However, a significant difference was observed between experiments where a metal salt was used and where chitosan was used for coagulation. The relationship between solids load and run time can be used to predict run times, when suspended solids concentration in the influent to the filters is known. Coagulation of coloured raw water creates deposits in the filter that occupy more pore space per solids load than deposits from raw water with higher levels of turbidity. This implies that the humic flocs/deposits are more voluminous than the humic-clay particle flocs/deposits.

One way to overcome the problem of short filter runs when a metal salt is used to coagulate humic waters is the addition of a polymer as filter aid. A filter aid can be used in situations where filter runs are limited by breakthrough before head loss limitation is reached. After coagulation, a reaction time of a few minutes was needed before polymer was added just prior to filtration. A non-ionic, high molecular weight polymer was used (Magnafloc LT20). The results showed that effluent turbidity and filter run length could be considerably improved by using small doses of filter aid. A dose of 0,05 mg/l of polymer in combination with 3,0 mg/l Al as aluminium sulphate, reduced effluent turbidity from the Filtralite filter from 0,53 NTU without polymer to 0,2 NTU, and a run time of 15 hours was achieved with RW50. Even longer filter runs could be obtained with a higher polymer dose, because the run was still terminated by breakthrough before the available head loss was reached. Polymer addition in experiments where aluminium sulphate was used as coagulant gave the best results. In the experiments where polymer was used, visible flocs were observed in the water above the filter media, which was not the case without polymer.

Modelling

A model to predict clean bed removals of different particles in filter beds was implemented for the three filters tested in this study. The predictions showed that removal of small and light particles was low in the two coarse Filtralite filters compared to the anthracite/sand filter. When trying to predict experimentally measured removals for contact filtration in the three filters, the model failed. Generally, the difference in performance between the anthracite/sand filter and the Filtralite filters was too high. This might be an indication of the influence of other mechanisms than particle removal in contact filtration.

In this study head loss in sections of the filter bed was measured during all the filtration experiments. With this data, and a model relating head loss to specific deposit volume, the effect of different filter bed porosities on the character of deposits were studied. The model was able to predict equal specific deposit volumes for equal increase in head loss gradient in the two different filters implemented (Filtralite and anthracite/sand). This indicates that deposit volumes increased more rapidly with time in the coarse Filtralite filter, giving the deposits a lower density (if equal SS removal is assumed).

Using capacity calculations from adsorption column theory, good fit was found between predicted and experimental values. This was tested on experiments where the same conditions had been used in the deeper and the normal Filtralite filter. It was possible to predict turbidity capacities for one filter using experimental values from the other by multiplying with the two filters depth ratio. When tested on an experiment where detention time and polymer addition was used, the scale up failed. This indicates that the capacity for turbidity storage in contact filtration, is proportional to bed depth (or grain surface area), when using the same filter media. This relationship seems to be independent of suspension, coagulant type and filtration rate.

ACKNOWLEDGEMENTS

I would like to thank my supervisors, professor Hallvard Ødegaard and Bjørnar Eikebrokk for guiding me through these four years at the University. It has been ensuring to know that professional help has been just around the corner, while struggling to fill the many holes in knowledge and understanding.

To my colleges at the Department of Hydraulic and Environmental Engineering, thank you for your support and friendship. Thanks to Magnar Katla and the other Dr. of Engineering students for friendship and company in off work activities.

Thanks to Hans and Arne at the workshop for helping me with the pilot plant, and Gøril and Heidi at the lab.

Many thanks to Magnhild Føllesdal and Oddvar Hyrve at Optiroc Group AB for giving me the opportunity and help along the way.

To my family August, Erle and Ingunn, sincerely thanks for putting up with all the late hours and encouraging me all the way. I would not have made this without you!

TABLE OF CONTEST

LIST OF SYMBOLS

A	filter surface area (m^2)
A_S	effect of bed porosity on particle transport
C	concentration (kg/m^3 or mg/l)
C_0	influent concentration, L=0 (kg/m^3 or mg/l)
C_D	drag coefficient
C_{limit}	limiting concentration (mg/l or NTU)
D	diffusion coefficient (m^2/s)
d_{10}	10^{th} percentile grain diameter (mm)
d_g	filter grain diameter (mm)
d_p	particle diameter (μm)
f	filter bed porosity
f_0	initial filter bed porosity, t=0
f_b	buoyancy force (N)
f_d	drag force ($N=kgm/s^2$)
f_g	gravity force (N)
f_p	porosity of deposited particles
g	gravitational acceleration (m/s^2)
G	velocity gradient (s^{-1})
H	head loss (m or cm)
H_0	initial head loss, t=0 (m or cm)
H_{limit}	limiting total head loss (m or cm)
I	head loss gradient (cm/cm bed depth)
I_0	initial head loss gradient, t=0 (cm/cm bed depth)
k	head loss per solids load ($cm/(g\ SS/m^2)$)
k_B	Boltzmann's constant ($1{,}38 \cdot 10^{-23}$ J/K)
k_H	Hamaker constant (J)
L	filter bed depth (cm or m)
N_G	effect of sedimentation on particle transport
N_L	effect of interception on particle transport
N_{Lo}	effect of dispersion forces on particle transport
N_{Pe}	effect of Brownian diffusion
p	permeability (m/s)
P	power dissipation ($W=kgm^2/s^3$)
Pe	Peclet number
Q	flow rate (m^3/s)
Re	Reynolds number
T	temperature (°K or °C)

t	time (s or h)
t_b	time equivalents (turbidity capacity)
S_A	grain surface area (mm^2/mm^3)
UC	uniformity coefficient
v	filtration rate (m/h)
V	volume (m^3)
v_s	settling velocity (cm/s)

Greek letters

α	collision efficiency factor
β	geometric constant related to filter grain packing
γ	solids concentration in deposits (g SS/l deposit)
η	overall single collector efficiency
η_D	single collector efficiency for diffusion
η_G	single collector efficiency for sedimentation
η_I	single collector efficiency for interception
λ	filter coefficient (m^{-1})
λ_0	initial filter coefficient, t=0 (m^{-1})
μ	dynamic viscosity (kg/m s)
ρ	density of water (kg/m^3)
ρ_g	grain density (kg/m^3)
ρ_p	particle density (kg/m^3)
σ	specific deposit
σ'	bulk specific deposit
σ_m	specific deposit mass (g/l)
σ_u	saturation value of specific deposit (ultimate specific deposit)
σ_v	specific deposit volume (l/l)
ψ	shape factor (sphericity)
ψ_A	electrostatic attractive forces
ψ_R	electrostatic repulsive forces

1 INTRODUCTION

1.1 Background for the study

In 1997 Norsk Leca AS (now Optiroc AS) made a settlement with NTNU in Trondheim to finance a Doctor of Engineering project dealing with the use of expanded clay aggregates in water treatment. The project started in January 1998, with professor Hallvard Ødegaard (NTNU) and research director Bjørnar Eikebrokk (SINTEF) as supervisors.

Bjørnar Eikebrokk and co-workers at SINTEF, had been testing expanded clay aggregates (Filtralite) in pilot scale deep bed filters for some time before this study started. It was extensively tested as the top layer of a dual media filter bed, together with sand, in coagulation/contact filtration of humic waters. The results of these tests showed that Filtralite was a good alternative compared to a top layer of anthracite. The water quality produced by the Filtralite/sand filter was as good as an anthracite/sand filter, run in parallel, for a number of coagulants and operational conditions. The head loss in the Filtralite/sand filter bed was in most cases less than in the anthracite/sand reference filter.

Due to the possibility of making clay aggregates in different densities, tests were made with two different types of Filtralite material with the goal of creating a dual media filter using only clay aggregates. Initial testing showed that intermixing of the two layers was a problem if filter grain sizes were identical to the anthracite/sand filter bed. These tests resulted in the development of a dual media filter using only Filtralite, which is now registered as a patent pending.

This thesis is an extension of the work described above.

1.2 The need for water filtration

Since the first municipal water filtration plant was build in Paisly, Scotland in 1832, the process has developed to be the most extensively used processes for water purification throughout the world. The process has been under continuous improvement along with the increasing demand of water quality and supply.

There have been some major improvements of the water filtration process since the first plants was built. One has been the introduction of chemical pre-

treatment to enhance filterability of suspensions. The rapid deep bed filters was introduced in America around 1890, primarily to increase water production. The use of multi media filters for increased solids storage capacity in down flow filters, is one of the latest major innovations in water filtration. Today most water filtration treatment plants are built with all these facilities.

In drinking water treatment, membrane filtration has been introduced as an alternative to traditional filtration, and has gained a lot of attention over the last decades. Granular media filtration and membrane filtration have advantages that make one more feasible than the other, both economically and in terms of water quality, in different situations. However, the process of membrane filtration is not yet as well documented as traditional filtration. Due to the increasing water demand, deterioration of source waters and higher quality standards, the different processes for water purification and combinations of them will be needed more and more in the years to come.

A survey done during the early 1990's revealed that 1200 of Norway's 1600 registered water works needed an upgrade to produce satisfactory water quality (Folkehelsa, 1997). In Norway, which traditionally has been regarded as a country with generally good source water quality, the treatment of drinking water is in most cases related to the removal of humic substances, corrosion control and disinfection. Humic substances are large molecules, which must be chemically pre-treated before granular bed filtration. An increase in organic matter content of source waters over the last decades have been observed in Norway, as in other parts of the world. This has resulted in a growing number of locations without organics removal, which are now faced with the fact that their water source is not satisfactory. Because of this a number of plants should be built in the near future.

2 SCIENTIFIC BASIS

The scientific basis found in this section is discussed in more detail in (Ives, 1975), (Letterman(Ed.), 1999) and (McEwan (Ed.), 1998) among others.

2.1 Humic substances in water

Humic substances in drinking water is the result of microbial and chemical degradation of plants (Gjessing, 1982). They are macromolecules, which are formed over a long period of time. The term NOM, natural organic matter, is commonly used to describe all natural occurring organic matter, and humic substances is the fraction of NOM associated with humic and fulvic acid.

2.1.1 Formation, incidence and consumer related problems

Dead plants and to some extent animals are continuously degraded in nature. The products of this clean-up operation are large macromolecules that are very slow biologically degradable. Most humic substances originate from soil, and they are therefore influenced by different area specific chemical conditions in the soil. Water transports the humic substances through the soil, where they end up in rivers, lakes or in the ocean. There will be a dominance of water-soluble compounds for the humic substances that are brought to these water sources, where they will be further degraded in a new environment.

For some parts of the world the water sources are mainly humic surface waters. This is true for areas with a cold climate. Gjessing (1982) suggested that areas with a temperature in the summer above 0 ^{0}C and a winter temperature below 0 ^{0}C are exposed to humic substances.

Humic substances give the water a brown colour, in some places it can look almost like beer. This colouring may not be harmful in it self, but it certainly makes it unattractive to drink and use in households. The colour can stain sinks and other appliance in contact with water, and cause problems to the washing of cloths. High concentrations can also give the water taste and odour. Another problem can be the ability of humic substances to corrode metals. This may lead to unacceptable concentrations of the metal used in piping in the tap water. Biological growth and cement corrosion in distribution systems are other problems connected to NOM. Micro-pollutants in the water, like pesticides, might be associated with NOM and carried trough to the consumers (Van der Hoek et. al., 1999).

When chlorine is used for disinfection of humic waters, chlorinated organic compounds are produced. These compounds are called disinfection by products (DBP), such as trihalomethanes (THM) and haloacetic acids (HAA), and they are harmful to human helth (Singer, 1999). As a result of this the US Environmental Protection Agency (US EPA) has set maximum contaminant levels for the sum of these compounds in drinking water (Singer, 1999). In the new Norwegian regulations a limit of 50 µg/l is set for these compounds (Helsedepartementet, 2001). Usually the content of these compounds have been regulated by maximum allowable concentrations of colour and TOC (total organic carbon), due to insufficient analytical equipment for their detection. Humic substances also react with ozone to produce compounds that contribute to the content of biodegradable organic carbon (BOC). These components like aldehydes and aldo- and ketoacids, can lead to regrowth in the water distribution system if they are not properly controlled.

2.1.2 Physical and chemical characterisation

Classes of organic matter

Data on classification of NOM differs some from one publication to another. This might have to do with the different separation and analytical procedures used, but it is also an expression of the natural variation in composition. In Table 2.1 a generally accepted classification of organic matter in natural freshwater is presented (Thorsen, 1999).

From Table 2.1 one can see that NOM is divided into two main groups, which is humic substances, and non-humic substances. In natural water there is usually more fulvic acid than humic acid, in contrast to what is the case for soil.

Physical and chemical characteristics

NOM has a very complex chemical composition, influenced by site-specific conditions. The two main components of humic substances, humic and fulvic acid differ in chemical composition as well as in physical properties. In general humic substances consist of mostly cyclic and aromatic polymeric chain fractions that are connected with covalent bonds (van der Waals and electrostatic). Fulvic acid is composed mostly of benzene rings, often substituted by carbonic acid and phenolic groups. Molecular weight for fulvic acid is in the range of 300 up to about 10 000 D. The chemical composition of humic acid varies more, but the chains are less substituted. The polymeric chains are longer and more strongly bound than for fulvic acid, and are assumed to have molecular weights between 500 and 100 000. Some rings in humic acid

are connected with double bonds, which is the major cause of the brown colour (Thorsen, 1999).

Name of group		Subgroup	Solubility character	Water affinity	Colour	% of total carbon		Other
HUMIC SUBSTANCES	Humin	Total	Insoluble	H.phobic	Brown	5-20		
	Humic acid	Total	Acid soluble Alkali insoluble	H.phobic	Brown	2-15		
		Brown	Not precipitated with electrolyte	H.phobic	Dark brown	-	35-70	
		Grey	Precipitated with electrolyte	H.phobic	Gray black	-		
	Fulvic acid	Total	Acid insoluble Alkali soluble	H.phobic	Light	10-35		
		Generic	As above	H.phobic	Yellow	-		Coloured part of fulvic acid
Non-humic substances		Total	Not adsorbed on h.phobic surface	H.philic	Low	-		
		Hy.philic acids	Ion dissociating	H.philic	Low	10-40	30-65	
		Hy.phobic neutral	Not dissociating	H.philic	Low	10-40		

Table 2.1 Organic matter classes in natural freshwater. (Summarised by Thorsen, 1999)

Light absorbency in the visible and ultra violet wavelength range, is the easiest method for analysis of humic substances in water. These wavelengths are related to the colour of humic substances created by double bonds with oxygen and nitrogen. In this study colour is mainly measured at a wavelength of 410 nm. Measurement of colour will to some extent underestimate the content of humic substances because the method is more sensitive to large molecules. Fulvic acid that is the dominating fraction of aquatic humics, consist mainly of smaller molecules, and contribute less to the colour of water.

Humic substances have a large number of charged groups, because of this there is repulsion between the molecules. Under natural circumstances the molecules are negatively charged in water, and the charge density increase with pH. In Figure 2.1 it is shown that colour change with pH. This is probably due to an increase in molecular weights (molecular size) for the humic substances. When the pH is increased H^+-ions from the functional groups will dissociate, and the

negative surface charge will increase. This increase the repulsion between the functional groups and the molecule will stretch out.

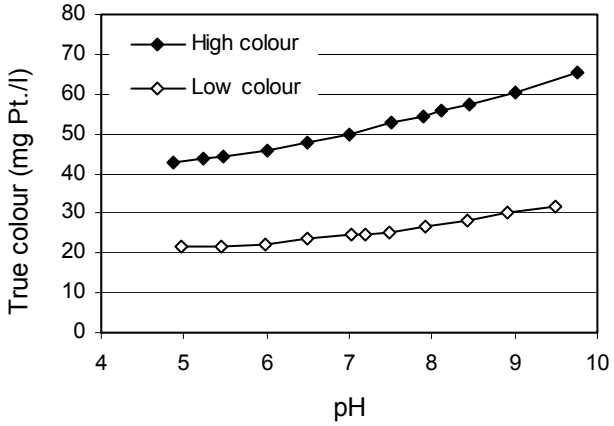

Figure 2.1 The pH dependency of colour (Machenbach, 2002).

2.2 Coagulation and flocculation

Coagulation is used as a pre-treatment step in most water treatment plants for the removal of particles and dissolved substances such as organic matter (NOM). The purposes of coagulation are primarily:

- to destabilise particles
- to make organic matter and other dissolved substances removable in a later treatment step
- to improve flocculation

There is a growing concern about disinfection by-products such as THM's (trihalomethans) when treating water containing organic matter. In some countries (like USA) this has lead to a shift in the main focus for coagulation optimisation from removal of particles (turbidity) to the removal of NOM (colour). Pathogenic organisms like *Giardia Lamblia*, *Cryptosporidium parvum* and *Legionelle* are given much attention in the water treatment industry (Edzwald and Kelly, 1998), (Ribas et. al., 2000). These organisms are of such a state (charge and size) that they usually relay on proper coagulation to be removed in traditional water treatment processes.

Raw water quality dictates which particle removal processes, and coagulation conditions that are optimal. There are different needs for coagulant types, -doses and pH conditions for each raw water and treatment process. In general, coagulation is used to destabilise and aggregate suspended particles, and to precipitate or adsorb NOM in such a way that the product can be removed in the following process.

Coagulation is a two-step process that involves 1) addition of chemicals to destabilise particles and react with NOM, 2) transport of particles to the vicinity of others. Chemical reactions are a part of the coagulation process. Following coagulation there is usually flocculation, which means the process of aggregation of coagulated particles resulting in floc formation. Flocculation is a way to alter the floc size and make it suitable for the specified removal process.

2.2.1 Inorganic coagulants

Aluminium salts

Aluminium sulphate (alum) is the most widely used coagulant for water treatment. When alum is added to water it is an acid, and reacts with alkalinity in the water. A simplified reaction equation is shown below.

$$Al_2\left(SO_4\right)_3 \cdot 14H_2O \rightarrow 2Al^{3+} + 3SO_4^{2-} + 14H_2O \tag{2.1}$$

Normally, the soluble fraction of aluminium in water is in equilibrium with precipitated aluminium hydroxide. If organic or inorganic substances are present in the water they can react with the aluminium ions, increasing its solubility. Simplified hydrolysis reactions for the most common Al species are listed below (water molecules involved in the reactions are omitted).

$$Al^{3+} + 3OH^- \rightarrow Al(OH)_3(am) \tag{2.2}$$

$$Al^{3+} \rightarrow AlOH^{2+} + H^+ \tag{2.3}$$

$$AlOH^{2+} \rightarrow Al(OH)_2^+ + H^+ \tag{2.4}$$

$$Al(OH)_2^+ \rightarrow Al(OH)_3(aq) + H^+ \tag{2.5}$$

$$Al(OH)_3(aq) \rightarrow Al(OH)_4^- + H^+ \tag{2.6}$$

Dependent on pH these aluminium species exist in the coagulated water. The amount of dissolved and precipitated aluminium can bee studied in a solubility plot as a function of pH. This is shown in Figure 2.2. The lines indicate total soluble aluminium concentration in equilibrium with amorphous aluminium hydroxide at 25 °C and 5 °C. Above the lines are areas where $Al(OH)_3(am)$ exist. Alum is normally used in a dosage that exceeds the solubility. As seen from Figure 2.2 the solubility depends on pH, temperature and concentration of Al (dose).

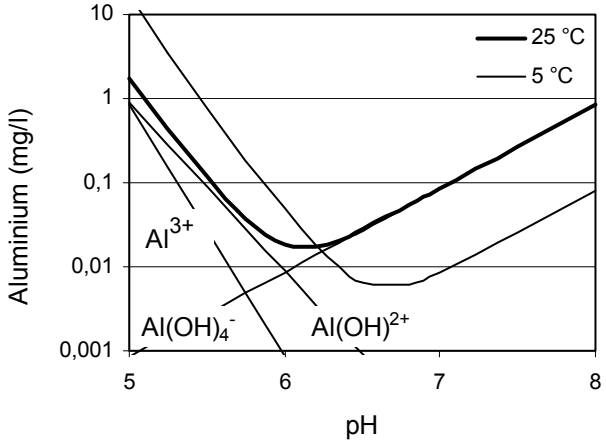

Figure 2.2 Theoretical solubility of aluminium in equilibrium with $Al(OH)_3(am)$ at 25 °C and 5 °C. For 25 °C the dominant species are shown.

Aluminium species carry a positive or negative charge dependent of pH. At low pH, below pH of minimum solubility the dominant species are Al^{3+} and $Al(OH)^{2+}$ (positively charged), and in the region above pH of minimum solubility the dominant specie is $Al(OH)_4^-$. At a pH just above 6 aluminium is most insoluble, and coagulation at this pH minimises the residual aluminium concentration. If a water is treated at a constant pH of 6 the year around, the residual aluminium concentration is higher at colder water temperatures. However, if the pH of coagulation is higher than the pH of minimum solubility, increased temperature leads to increased solubility.

Iron salts

Iron salts act and behave in a similar way as alum. In water they are acids and they hydrolyse. Ferric precipitates are formed at the proper pH and coagulant dose conditions. Compared to aluminium the precipitates from iron salts are much less soluble, and the pH range of low solubility is wider. Iron salts

consume less alkalinity than alum, calculated per weight of Me. Precipitation of iron hydroxide is described as:

$$Fe^{3+} + 3OH^- \rightarrow Fe(OH)_3(s) \qquad (2.7)$$

The pH of minimum solubility is at about 7-8, and the dominating species at lower pH is positively charged. Because of the generally lower solubility of iron, metal residuals should be a minor problem when iron salts are used for coagulation.

The electrical double layer

Particles in water are surrounded with a double layer of ions. Most particles carry a negative charge in water, and they have an adsorbed rigid layer of positive ions on the surface (Stern layer). The outer surface of the Stern layer is called the plane of shear, and the charge of this layer is the zeta-potential of the particle. Outside this layer is the diffuse layer of loosely "connected" ions of different charge. In the diffuse layer the concentration of positive ions decrease from the plane of shear and outwards, while the concentration of negative ions increase. The diffuse layer is a result of electrostatic attraction and repulsion between ions. The electrical double layer is schematically illustrated in Figure 2.3.

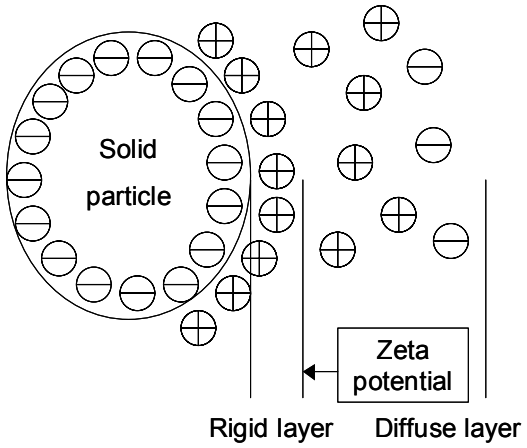

Figure 2.3 Schematic illustration of the electrical double layer.

Interaction between two particles can be evaluated by looking at the energy needed to bring them close together. When two charged surfaces approach each other, their diffuse double layers begin to interact. The sum of the interaction

energy (ψ_R-ψ_A) as shown in Figure 2.4 is produced by attractive van der Waals forces (ψ_A) and repulsive forces from overlapping double layers (ψ_R).

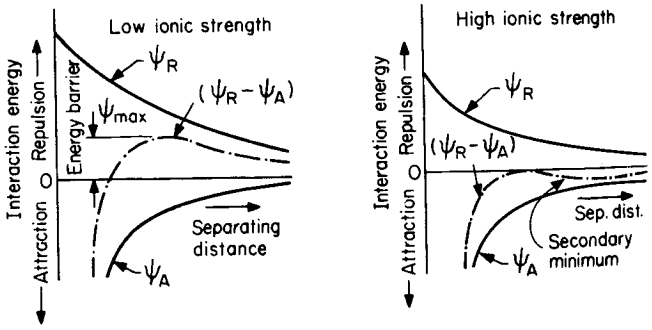

Figure 2.4 Total interaction energy as a function of distance from particle surface. (From Letterman (Ed.), 1998)

In an electrostatically stabilised system the repulsive energy is dominating and only very slow coagulation take place. In waters of high ionic strength the interaction energy is generally lower and there is often a secondary minimum in the net energy. Particles can be caught in this secondary minimum and this state is often referred to as flocculated particles. If two particles approaching each other overcome the energy barrier, the attractive forces will dominate and the net energy falls down to the primary minimum. In this state the two particles are strongly attached and will act as one.

Coagulation mechanisms

The main mechanisms involved in coagulation of particles and NOM with metal salts are shown bellow.

- Charge neutralisation
- Sweep coagulation
- Adsorption

In *charge neutralisation* the soluble metal hydrolysis products bind with sites on the surface of particles and on soluble natural organic substances. If the sites on particles and NOM are abundant relative to the amount of hydrolysed metal species, all the metal will react irreversible with the surface. The hydrolysed metal products that have already reacted are not available for precipitation. Natural particles and NOM usually have a negative surface charge, they can be neutralised by positively charged metal species, and the suspension are said to be destabilised. This mechanism is dependent on the presence of positively

charged (for negatively charged particles) metal species in the water. In general this is fulfilled at low pH, about 5-5,5, and relatively low coagulant doses two prevent precipitation. From Figure 2.2 we can see the area were Al^{3+} and $Al(OH)^{2+}$ are the dominating species.

If metal is added in a sufficient amount and pH is in the precipitation range according to Figure 2.2, hydroxide solubility is exceeded. Hydroxide precipitate begins to form when the coagulant demand for charge neutralisation is essentially satisfied. If the water contains NOM, the organic macromolecules can *adsorb* on the surface of the colloidal precipitates and in humic waters create a coagulant demand. The net charge of the precipitate is negative and will remain stable and dispersed when NOM is in majority. An increase in coagulant dose will increase the available surface area for adsorption, and at some point there is a shortage of NOM for the stabilisation of the precipitate. At this point the suspension starts to flocculate and filterable flocs are produced. The mechanism of *sweep flocculation*, or enmeshment, actuates when the coagulant dose exceeds the stabilisation point. Under these conditions, the negatively charged colloidal particles or the NOM are entrapped in the precipitating $Al(OH)_3(am)$. The particles in the water are catalysts for hydroxide precipitation. Sweep coagulation occurs at high dosages and pH about 6-8.

As demonstrated by Eikebrokk (2001), considerable NOM removal takes place in contact filter beds for hours after coagulant dosing is stopped. This is taken as an indication that NOM adsorption to metal hydroxide and/or previous deposits plays an important role in contact filtration systems.

In most practical cases coagulation is a combination of the above-mentioned mechanisms. Especially in waters containing both particles and NOM, which influence the solubility of the metal hydroxide, the coagulation process is quite complex.

Poly-aluminium coagulants

When metal salts like alum are added to water the hydrolysis reaction produces H^+-ions that consume alkalinity. In the poly-aluminium products, base is added in the production process to pre-hydrolyse the coagulant. The degree of pre-hydrolysation is described by the ligand ratio r, which is the molar concentration of hydroxide ($[OH^-]$) to the total molar concentration of aluminium ($[Al_{total}]$) in the solution. The ratio r usually has values between 0,3 and 2,5 for commercial products, which equals basicities between 10 and 83 percent according to the equation below.

$$Basicity(\%) = \left(\frac{100}{3}\right) * \frac{\left[OH^-\right]}{\left[Al_{total}\right]} \quad (2.8)$$

The species formed when poly-aluminium coagulants are dissolved in water depends on the basicity of the product. They are called poly-aluminium coagulants because some of the species formed are poly-nuclear. For a basicity less than 33 % positively charged monomeric Al species (Al^{3+} and $AlOH^{2+}$) dominate as in the case with alum. For higher basicity a polymeric cation ($Al_{13}O_4(OH)_{24}^{7+}$) is known to be formed (Parthasaraty and Buffle, 1985). This specie is often said to be the dominant specie for products with basicity higher than about 40 %. At higher basicities aluminium hydroxide is formed. The coagulation mechanism for the Al_{13} polymer is charge neutralisation, and the high positive charge result in a strong adsorption to negative colloids. Gregory and Rossi (2000) found that flocs formed with poly-aluminium coagulants were bigger and stronger than those formed with alum.

2.2.2 Organic coagulants (polymers)

Polymers are widely used in water treatment as coagulants and/or flocculants. In filtration, low molecular weight, cationic polymers are normally used as primary coagulants and high molecular weight, non-ionic or anionic polymers can be used as filter aids to increase filterability, e.g. filtration run times. The polymers most widely used are the synthetic organic ones as poly(DADMAC) and polyacrylamide based polymers. Also polymeric coagulants made from natural organic compounds are used. One example of this is the cationic biopolymer chitosan made from crab and shrimp shells, which is used in this study. Polymers used in water treatment are characterised by charge, charge density, molecular weight and the chemistry of the functional groups.

There are generally two models describing the mechanisms of coagulation with polymers, and that is the charge neutralisation model and the interparticle bridging model. The charge neutralisation model is based on adsorption of oppositely charged polymers on particle surfaces. The polymer dose needed to destabilise a suspension is proportional to the concentration of particles, and overdosing can lead to positively charged, restabilised particles. Waters containing low levels of turbidity experience few particle collisions, and a polymer would not be very effective for such waters. Gregory (1989) developed the patch model for particle destabilisation by polymers. The model describes how polymer molecules adsorb unevenly on the particle surface, giving patches

of positive charge. Flocs are formed by electrostatic attraction between positive patches and negative, polymer free, areas. This is why complete destabilisation is not needed.

Anionic and non-ionic polymers are normally used as coagulant aids and filtration aids after the addition of a conventional metal salt. These polymers are characterised by a high molecular weight and thereby long chains, which give them the opportunity to reach beyond the double layer thickness and attach to other particles. The non-ionic and anionic polymers adsorb on particles because of electrostatic forces, hydrophobic properties and hydrogen bonding.

2.2.3 Mixing and flocculation

The destabilisation reaction rate is controlled by the chemical reaction rate and the flow conditions in the mixer. Normally high intensity mixers creating turbulent conditions are needed for coagulant addition, because the reaction rate of destabilisation is fast. Rapid mixing is obtained either by internally or externally generated turbulence. Internally generated mixing is normally accomplished by head loss, which is the case for this study. In-pipe mixing is discussed in the following section.

In-pipe mixing
Using a rapid mixing tank for coagulant dispersion often leads to short-circuiting and mass rotation of flow. Because of this there is an increased use of in-pipe mixing for coagulants that destabilise by charge neutralisation. Pipe constriction and injection of the coagulant in the back eddy of the constriction has proven to be an effective way of dispersion. Klute (1990) found that since the hydrolysis reaction and the destabilisation was very fast and essentially irreversible, complete distribution of metal salts within 0,1 s was required for charge neutralisation. In practise this is almost impossible to accomplish. When the mechanism is sweep coagulation short dispersion times and high turbulence mixing is not that important. He also found that the poly-metal coagulants (i.e. poly-aluminium chloride) are less sensitive to poor mixing conditions. Studies by Eikebrokk (2000) indicated that the intensity of mixing was of minor importance for NOM removal and effluent water quality in contact filtration of humic waters, also at low water temperatures. This is indicating that charge neutralisation plays a minor role in contact filtration of humic waters.

Flocculation
Destabilised particles start to aggregate because of Brownian motion and this is called *perikinetic* flocculation. If some physical stirring is introduced to

destabilised particles it will enhance the flocculation process. From the stirring, velocity gradients are induced in the water creating relative motion in the suspension increasing particle collisions. This type of flocculation is called *orthokinetic*. In most cases the velocity gradient is variable because of a non-uniform shear field. The gradient is described by an average value G, representing the power dissipated per unit water volume (P/V). The mean velocity gradient is given by:

$$G = \left(\frac{P}{V\mu} \right)^{1/2} \tag{2.9}$$

Where P is the power dissipated, V is the volume and μ is the viscosity of the fluid.

In this study, dealing with contact filtration there is no separate flocculation step before filtration and the pre-flocculation is thus limited to a few meters of filter inlet pipe (about 25-75 seconds at G=5-30 s^{-1}) and the volume of water above the media in the pilot filter columns (some minutes detention time). The pipe gives low G-values for a short period of time and the orthokinetic flocculation is probably negligible. The volume above the filter media giving some minutes of residence time (depends on head loss in the filters and is increasing with time of filtration) introduces some flocculation before filtration. This is very much influenced by the concentration and characteristics of the particles in the suspension. Few and large particles decrease the rate of perikinetic flocculation caused by Brownian motion.

Filter pore flocculation

Flow in the filter pores is usually laminar in deep bed filtration. There are however local velocity gradients in the pores creating water drag past the particles enhancing particle flocculation. The pores in the filter bed can be compared to a stack of small-bore tubes with a head loss, which can be calculated from the Kozeny-Carman equation (see Equation (2.37)). If this equation is combined with Equation (2.9), and an expression for P in a tube with laminar flow, the G-value for flow in a deep bed filter can be presented as (McEwan(Ed.),1998):

$$G = \frac{13,4v(1-f)}{f^2 d_g} \tag{2.10}$$

v is filtration rate, f is bed porosity and d_g is grain diameter. If this formula is used on the pilot plant filters in this study, the results are as presented in Table 2.2. The residence time is calculated from:

$$t = \frac{fAL}{Q} = \frac{fL}{v} \tag{2.11}$$

Where A is filter surface area, L is filter depth and Q is volumetric flow rate.

Table 2.2 Calculated filter pore flocculation parameters for the pilot plant filters.

Filter layer	**v** (m/h)	**f_0**	**d_{10}** (mm)	**L** (m)	**t** (s)	**G** (s^{-1})
Filtralite NC (top)	7,5	0,7	1,65	0,47	158	10,4
Filtralite HC (botom)	7,5	0,6	0,84	0,47	137	36,9
Anthracite (top)	7,5	0,55	0,82	0,6	159	50,6
Sand (botom)	7,5	0,43	0,5	0,35	72	172,1

The calculated G-values for the coarse Filtralite filter are low and therefore large flocs may form. This can be suitable for the particle removal in the larger grain sizes of this filter, but bigger flocs are weaker than smaller ones and floc break-up might be a problem. The higher G-values for the fine-grained anthracite/sand filter will create smaller flocs than in the Filtralite filter, and in this filter large flocs would clog filter pores, which is undesirable. The increasing G-values in the direction of flow (for both filters) are probably a disadvantage, because it might lead to break-up of flocs formed in the top layer. However, the flocculation in the filter pores is accompanied by simultaneous capture of the flocs that are formed, and the deposits result in lower porosities leading to increased G-values. The G-values calculated in Table 2.2 are to be considered as clean bed estimates.

Graham (1988) found that filter pore particle flocculation was a minor significant mechanism of three principal mechanisms of enhanced particle removal. In his study he observed that alteration of particle-grain attachment efficiency and the preferential deposition of particles onto previously deposited particles were the most important factors influencing the removal of kaolin clay particles destabilised by a cationic polymer in a deep bed filter.

2.3 Filtration theory

The capture of particles in suspension by filtration through a porous media is generally divided into two steps, transport and attachment. The filtration process is either a cake filtration (surface) or as deposition within the pores (depth). Surface filtration can take place in a depth filter by straining, this is not desirable and can be avoided by the right choice of filter media and pre-treatment. The flow in the filter pores is laminar, which means that it obeys Darcy's law and that the head loss is proportional to the flow rate. Viscous forces control the water movement and the streamlines do not cross. But the streamlines and viscous forces are not uniform and they vary with time as the pores get clogged with deposits. In laminar flow a particle in a streamline follows this streamline until forces act to move it.

2.3.1 Transport mechanisms

Straining
The dominant mechanism in cake filtration, straining, will also to some extent take place in a depth filter. Straining occurs when the particles are bigger than the pores in the filter media, thus being trapped in the pores. This leads to a complete blocking of the pore, and will create a blanket of deposited particles on top of the depth filter. Head loss will increase exponentially and the capacity of the filter is dramatically reduced. This mechanism is undesirable in depth filtration, and is not considered further.

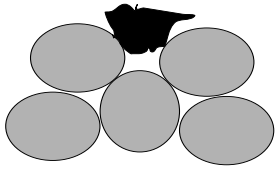

Figure 2.5 Straining

Interception
Some particles follow the streamlines that bend off around a filter grain. If the particle is following a streamline that is close to the grain, it can touch the surface of the grain. The distance from grain to streamline must be less than the particles radius. In interception there are no forces acting on the particles across the streamlines, so it might not be regarded as a transport mechanism.

The efficiency of interception can be characterised by the dimensionless ratio:

$$\frac{d_p}{d_g} \tag{2.12}$$

Where d_p is the particle diameter and d_g is the filter grain diameter. When d_p increase the greater the probability for the particle to touch the grain, and particle capture is more efficient. When the ratio approaches 1 straining is the dominant mechanism. d_g could also have been the pore size of the filter media, because an increasing pore size (as well as an increasing grain size) leads to a less efficient particle capture. In water and wastewater filtration values between 0,0002 and 0,1 is normally obtained for this factor (Ives, 1980).
The grain size distribution is an important filter bed characteristic, and it controls the pore size distribution together with the grain shape. A wide grain size distribution gives a wide range of pore sizes, which in some cases might increase the efficiency of the filter. The grain size (pore size) must in all cases be adapted to the suspension to be filtered.

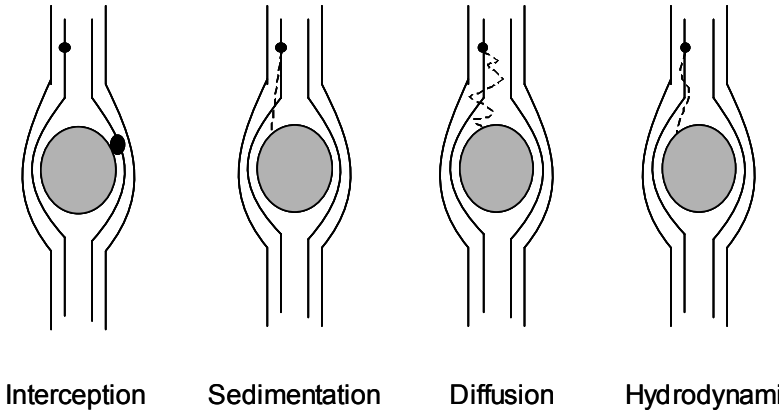

Figure 2.6 Transport mechanisms in filtration

In coagulation/filtration it is reasonable to increase the particle size 100 times by coagulation. To obtain the same effect by decreasing the grain size would require a too small size for practical use.

Inertia
The streamlines in a pore, which are heading towards an underlying grain, have to bend off and go round it. Particles with enough inertia will not follow the streamlines, and this will cause them to collide with the grain. The efficiency of

this mechanism increases with increasing velocity, particle size and density, and decrease with increasing grain size and fluid viscosity. Due to the relatively low velocities used in water filtration, this is not an important transport mechanism.

Sedimentation

Particles that are denser than water and of a size greater than about 5 μm will experience a gravity force resulting in sedimentation. Stokes settling velocity for spherical particles is given by

$$v_s = \frac{g(\rho_p - \rho)d_p^2}{18\mu} \tag{2.13}$$

Where ρ_p and ρ is the particle and water density respectively. The gravity transport mechanism can be expressed by a dimensionless ratio, and it is the settling velocity relative to the approach velocity of filtration, v.

$$\frac{v_s}{v} = \frac{g(\rho_p - \rho)d_p^2}{18\mu v} \tag{2.14}$$

From the dimensionless group it can be seen that the effect of this mechanism increase with density and size of the particles, and decrease with filtration velocity. Flocs and other particles present often have a density close to the density of water, which gives them a low settling velocity, and decreasing the effect of sedimentation. Due to the laminar flow field in the pores, however, the water velocity close to a grain surface is almost zero, but the Stokes velocity is constant everywhere in the filter pores.

Diffusion

Very small particles (<1-2 μm) in liquids exhibit a random movement due to the thermal energy of the water molecules. This movement called Brownian motion increase with higher temperature of the water, which give increased thermodynamic energy to the molecules and a decreased viscous drag on the particles. The Stoke-Einstein diffusion coefficient (mean velocity due to diffusion) gives the total effect.

$$D = \frac{k_B T}{3\pi\mu d_p} \tag{2.15}$$

Where k_B is Boltzmann's constant and T is the temperature in Kelvin. If we divide D by d_g we get the mean velocity due to diffusion over a distance of one grain diameter. Movement of the particle caused by the flow in the pores is proportional to the filtration velocity, v. The effect of diffusion is therefore expressed by the parameter $D/d_g v$. This ratio is the inverse of the Peclet number, Pe.

$$\frac{1}{Pe} = \frac{D}{d_g v} = \frac{k_B T}{3\pi\mu d_p d_g v} \tag{2.16}$$

Hydrodynamic forces

If the particles in the water are not spherical they will fall in a tumbling motion. These motions, which are enhanced by the velocity gradients of the laminar flow field, leads to an increasing probability of contact with a filter grain. Angular filter grains might also lead to irregular flow fields.

This mechanism has been shown experimentally to vary with the Reynolds number Re. A change in Re causes a change in the flow pattern, but it is not a good description because of the complexity of the mechanism. Considering the precaution, the inverse Reynolds number describes the hydrodynamic effect.

$$\frac{1}{\mathrm{Re}} = \frac{\mu}{\rho v d_p} \tag{2.17}$$

The most important filter mechanisms are interception, sedimentation and diffusion. Suspensions to be filtered contain in most cases a range of particle sizes, and different transport mechanisms will influence the different sizes. In Figure 2.7 this is illustrated by looking at the filter removal efficiency for different particle sizes. The small particles, less than 1 μm, are removed by diffusion, and the larger by sedimentation and interception. For particles around 1 μm the removal efficiency is relatively low because they are too large for diffusion and too small for sedimentation and interception.

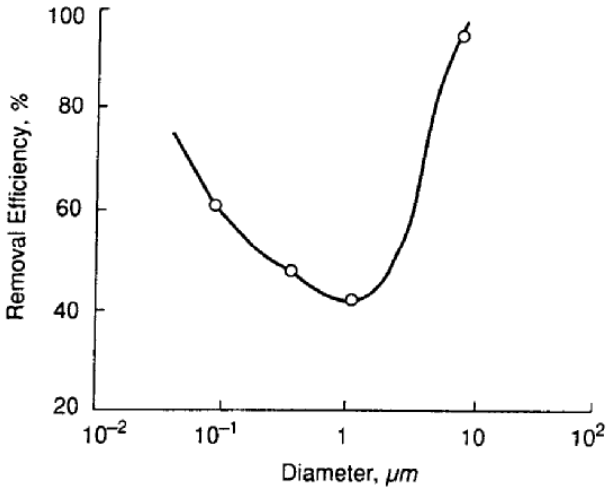

Figure 2.7 **Removal efficiency as a function of particle size. (From Yao et al., 1971).**

2.3.2 Attachment mechanisms

When a particle is transported to the surface of a filter grain or already deposited particles, short-range surface forces between particle and grain decide if attachment occurs. These forces arise from the overlap of electrical double layers on particles and grains, if the particles are not sufficiently destabilised by coagulation. Other surface forces acting on the particles are Van der Waal's attractive forces and forces connected to chemical effects like adsorption.

Electrostatic forces (double layer interaction)
These forces arise from surface potentials (zeta potentials), and create a double layer of ions surrounding particles and grains. Normally, the forces between natural particles and grains are repulsive in water because both are negatively charged. Coagulated flocs are electropositive or negative depending on solution ionic strength and zeta potentials on the particles. Electropositive particles can experience attraction to a negative grain surface. When grains are covered with deposited flocs, further deposition may be hindered by floc-floc repulsion.

Van der Waals forces
This is universally attractive forces between dipoles, created by systems of neutral atoms and molecules with oscillating charges. They lead to attraction

between particles and grains. Van der Waals forces are of limited range, usually less than 50 nm, but very powerful.

Bridging
Mutual adsorption of long chained dissolved polymers leads to links and bridges between particles and grains. The length of the polymer chain needs to be at least as great as the range of the repulsive forces.

Friction forces
Particles hitting a filter grain will in many cases be deformed. If the grain has a rough surface the particle might stick to the grain because of friction forces.

Liquid pressure
For porous filter-grain materials particles can be kept in pores because of the liquid pressure differences. They might also be transported into the pores depending on the capillary suction.

Hydration (Chemical reaction)
Attachment of particles to a filter grain can occur through hydrogen bonding with water molecules to the grain surface.

Hydrodynamic retardation
This is not a mechanism of attachment, rather an effect that prevents attachment when a particle is approaching a grain surface. It is the viscous resistance of the film of water surrounding the particle and the grain. For adhesion to occur this film has to move away from the point of contact.

2.3.3 Detachment mechanisms

In a filter, as the filter pores are filled with deposits, water velocity in the filter pores increase. This will lead to an increasing shear force on the deposited particles. Particles in suspension can also hit the deposited particles and bring them back into the suspension. Moran et al. (1993) showed experimentally that detachment of deposited particles during filtration occurs, and this detachment is perhaps the dominant factor contributing to filter breakthrough.

During backwash of depth filters the adhering particles detach caused by an increased hydraulic shear on the particles and an increased porosity during fluidisation. Backwashing with water alone does not give detachment by grain-to-grain collisions to any significant extent (Amirtharajah, 1978). Air scour and

surface wash promote filter grain collisions and are a much more abrasive cleaning procedure.

Filter media with increased attachment capability might have problems with proper cleaning. If the particles deposited on the grains are not entirely removed during backwash the filter grains might have a reduced removal capacity.

2.3.4 Mathematical description of particle removal in filtration

Models describing particle removal in filtration can be divided into two categories. Macroscopic models make use of a mass balance to describe the rate of particle deposition as a function of time of filtration and depth in the filter medium. Microscopic models, or fundamental models, consider the actual mechanisms of particle transport and attachment to predict particle removal.

Iwasaki's model (1937) proposed that the rate of removal of particles from suspension with respect to filter depth is proportional to the concentration of particles in suspension. This is a much used and widely accepted proposition, and is expressed as:

$$\frac{\partial C}{\partial L} = -\lambda C \tag{2.18}$$

Where λ is the filter coefficient. Equation (2.18) is partial differential because the concentration not only varies with distance in the filter, but also with the time of filtration as deposits alters the porosity of the filter bed.

Microscopic models

Most of the work done have concentrated on modelling the transport mechanisms that bring the particles close to the grain surface. Yao et al. (1971) presented a filtration model used to predict particle removal in packed beds. The model is based on the transport mechanisms sedimentation, interception and diffusion as described earlier. For each mechanism a single collector efficiency (η) is presented, which is the ratio of particles that strike the collector divided by particles that flow towards the collector. The expressions for each transport mechanism are as follows:

$$\eta_D = 4,04 Pe^{-2/3} = 0,9\left(\frac{k_B T}{\mu d_p d_g v}\right)^{2/3} \tag{2.19}$$

$$\eta_I = \frac{3}{2}\left(\frac{d_p}{d_g}\right)^2 \tag{2.20}$$

$$\eta_G = \frac{\left(\rho_p - \rho\right) g d_p^2}{18\mu v} \tag{2.21}$$

Where η_D, η_I and η_G represent the single collector efficiency for diffusion, interception and sedimentation respectively. The overall collector efficiency is the sum of these three.

The performance of a packed bed of grains is related to the efficiency of a single spherical collector. Equation (2.23) is developed using a mass balance for particle removal by an isolated sphere.

$$\frac{dC}{dL} = -\frac{3}{2}\frac{(1-f)}{d_g}\alpha\eta C \tag{2.23}$$

Where f is the bed porosity, L is the bed depth and α is the ratio of collisions leading to adhesion to the total number of collisions between particles and grains. α is influenced by the chemistry of the system, and is equal to 1 in a ideal destabilised system. The equation proposed by Yao et al. has the same form as Equation (2.18) that was introduced by Iwasaki (1937).

The equation of Yao et al. is used to simulate the clean bed efficiency of a filter at the start of a filtration run. When integrated over the distance L in the filter this equation yields:

$$\ln\frac{C}{C_0} = -\frac{3}{2}(1-f)\alpha\eta\left(\frac{L}{d_g}\right) \tag{2.24}$$

By the use of these equations Yao et al. calculated the single collector efficiency for removal of particles of different sizes. They studied the effect of filtration velocity, water viscosity, media size and the density of suspended particles, and found that the density of suspended particles larger than 1 μm influenced significantly on the single collector efficiencies due to settling. Considerably less effect was exerted by the other filtration parameters mentioned. Experimental results showed higher collector efficiencies than the theoretical predictions, but the trends were in reasonable agreement.

From trajectory analysis Rajagopalan and Tien (1976) developed an expression for the single collector efficiency (Equation (2.25)). Logan et al. (1995) compared this model, Yao's model and others with experimental observations, and found best agreement with Rajagopalan and Tien's model.

$$\eta = 4A_S^{1/3}N_{Pe}^{-2/3} + A_S N_{Lo}^{1/8} N_{\mathrm{R}}^{15/8} + (3{,}38\cdot 10^{-3}) A_S N_G^{1,2} N_R^{-0,4} \qquad (2.25)$$

A_S, N_{Pe}, N_{Lo}, N_R and N_G are dimensionless groups representing the effects of bed porosity, convective diffusion (Brownian), dispersion forces, interception and gravity, respectively. They are defined as:

$$A_S = \frac{2(1-p^5)}{w} \qquad (2.26)$$

where $p = (1\text{-}f)^{1/3}$ and $w = 2\text{-}3p+3p^5\text{-}2p^6$

$$N_{Pe} = \frac{d_g v}{D} \qquad (2.27)$$

$$N_{Lo} = \frac{4k_H}{9\pi\mu d_p^2 v} \qquad (2.28)$$

$$N_R = \frac{d_p}{d_g} \qquad (2.29)$$

$$N_G = \frac{v_s}{v} = \frac{(\rho_p - \rho) g d_p^2}{18 \mu v} \tag{2.30}$$

Where k_H is the Hamaker constant and the other parameters are defined earlier. The effect of particle size and density, and grain size on single collector efficiency is presented in Figure 2.8, by the use of Equation (2.25). In Figure 2.8 the fraction removed for each particle size is also presented, and is calculated using Equation (2.24). When comparing removal efficiency between the different grain sizes there is a significant difference for the smallest particle sizes that is influenced mainly by diffusion. For these small particles, an increase in particle density, increasing the effect of sedimentation, does not increase removal efficiency to any large extent. Particle sizes around 1 μm experience low removals, which is in agreement with the transport mechanisms acting on the particles (section 2.3.1) and is shown experimentally by Yao et al. (1971) and others. For low-density particles the removal efficiency is low for large filter grains also when removing large particles (> 10 μm). Particles with a density of 2000 kg/m^3 and a size greater than 30 μm are totally removed with all of the filter grain sizes presented.

The same equations can be used to model the clean bed removal of a dual media filter bed. This was done by O'Melia and Shin (2000) for a dual media anthracite/sand bed. In Figure 2.9 the filter beds used in this study are simulated and grain size, single collector efficiency and C/Co is presented as a function of filter bed depth.

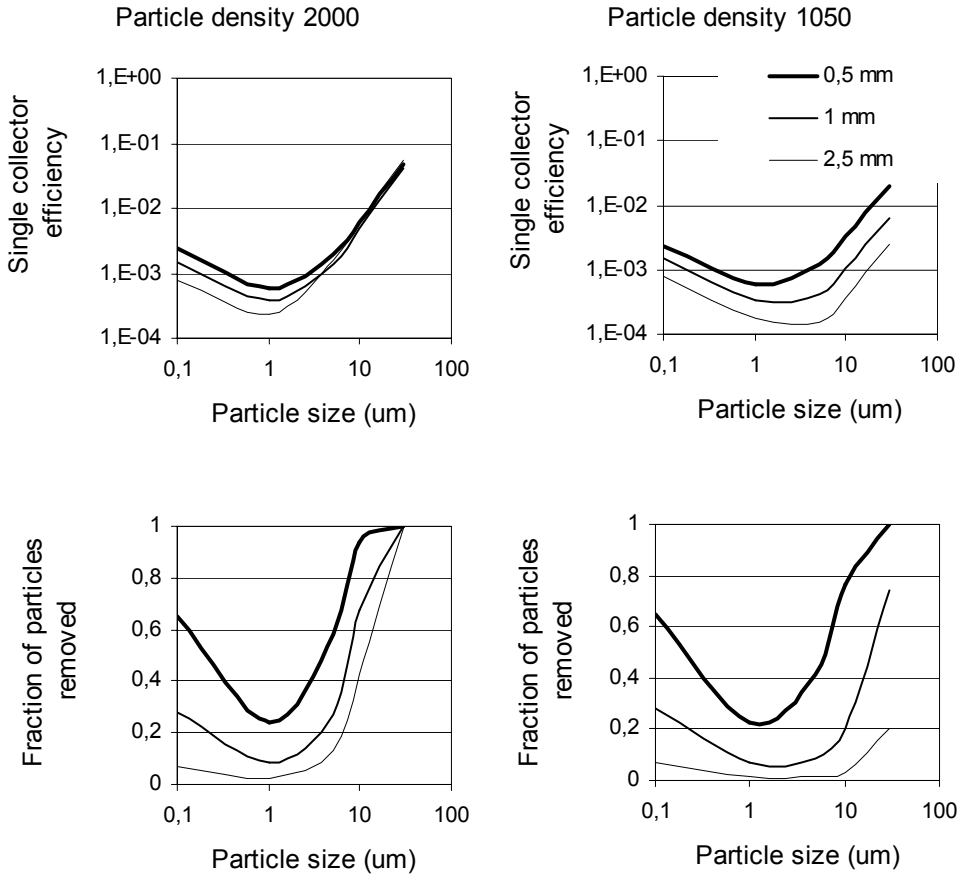

Figure 2.8 Top: Single collector efficiency as a function of particle size for three different filter grain sizes, and two different particle densities. Bottom: Fraction removed for the respective situations. Constants used in the calculations: f=0,5, L=30 cm, v=10 m/h, k_B=1,38e-23 , T=293 °K , k_H=1,0e-20, α=1,0. (Authors own calculations)

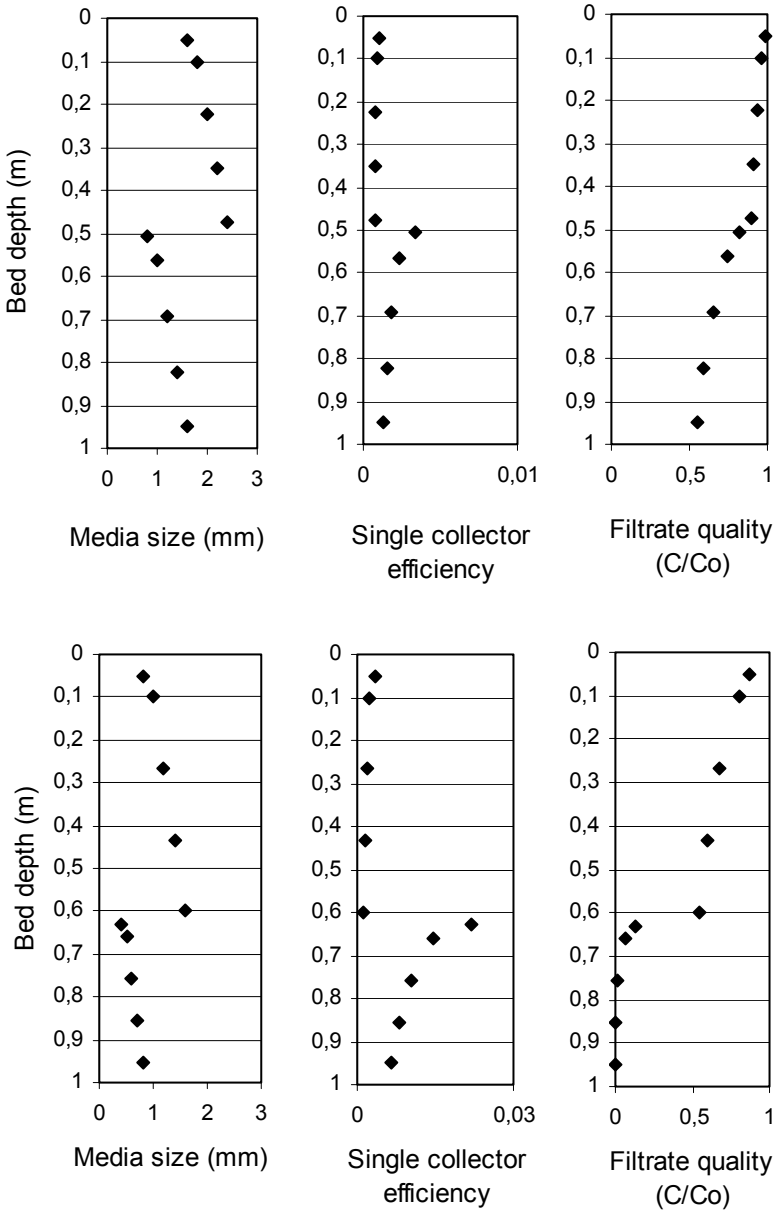

Figure 2.9 Clean bed model used on two filter beds from this study. Top figures: Filtralite NC 1,6-2,5 mm, f=0,7, L=47 cm on top of HC 0,8-1,6 mm, f=0,6, L=47 cm. Bottom figures: anthracite 0,8-1,6 mm, f=0,55, L=60 cm, on top sand 0,4-0,8 mm, f=0,43, L=35 cm. All figures: d_p=20 μm, ρ_p=1050 kg/m3, v=7,5 m/h, α=1,0.

The filter media size distribution is approximated from the sieve curves, and the differences in media size exert great influence on the single collector efficiency. The particle size and density used in this simulation are supposed to represent coagulated humic substances. Interception is the most important transport mechanism for these particles because they are too big for diffusion and to light for sedimentation.

In the top layer of the Filtralite filter there is almost no removal of these particles due to the large grain size. Total removal in this filter is about 50 %. For the anthracite/sand filter the removal of the top layer alone is about 50 % and the rest of the particles are effectively removed in the sand layer. The use of small grain sizes is very important for the removal of light particles. Heavier particles, influenced more by sedimentation, are more easily removed by the large grain sizes of the Filtralite filter, because grain size does not have an influence on the mathematical expression for the effect of sedimentation.

The clean bed model described above can give us an idea of the water quality that a filter is able to produce, but it cannot tell anything about the length of a filter run. To model this one has to consider the change in filter efficiency due to deposited particles in the filter pores.

Macroscopic models

Equation (2.18) proposed by Iwasaki (1937) can be linked with another partial differential equation (Equation (2.31)), derived from a mass balance of the suspended particles, to describe the filtration process. Equation (2.31) was also formulated initially by Iwasaki.

$$-\frac{\partial C}{\partial L} = \frac{1}{v}\frac{\partial \sigma}{\partial t} \tag{2.31}$$

A $\partial C/\partial t$ term is usually negligible and can be omitted (Ives, 1970). σ is the specific deposit, usually expressed as volume of deposit per unit filter volume, and v is the approach velocity. The bulk specific deposit σ' is used to compensate for the porosity of the deposited particles, f_p, this gives:

$$-\frac{\partial C}{\partial L} = \frac{(1-f_p)}{v}\frac{\partial \sigma'}{\partial t} \tag{2.32}$$

These equations are approximations to the exact equations, but they are still preferred by several authors, (Ives, 1970) (Mackie, 1989). If Equation (2.18)

and (2.31) (used instead of (2.32) for simplicity) are combined we get an expression of the time variation of the specific deposit:

$$\frac{\partial \sigma}{\partial t} = \lambda C v \tag{2.33}$$

The filter coefficient λ is a measure of the efficiency of the filter grains for removing the particles in suspension, and is expressed as fraction of particles removed per unit filter bed depth. Ives (1960) proposed that the filter coefficient is not constant during a filtration run due to the deposited particles clogging the filter pores, and suggested an expression for λ as a function of the initial filter coefficient (λ_0) and specific deposit. Other authors like Mints (1970) considered the detachment mechanism to be important, and that a constant value of λ is counteracted by a varying detachment rate throughout the filter run. If we combine Equation (2.18) and (2.23) we get Yao et al.'s (1971) expression for the initial filter coefficient at t=0:

$$\lambda_0 = \frac{3}{2}\frac{(1-f_0)}{d_g}\alpha\eta \tag{2.34}$$

Where f_0 is the initial porosity of the filter bed. As an example of on of the proposed relationships between λ and σ, Ives expression (Ives, 1970), is presented below (Equation (2.35)). This expression consider the increase of specific surface due to coating of deposited particles (first term in brackets), a diminution of specific surface due to deposition in side spaces in pores (second term) and an increase in pore velocity due to a decreasing pore cross section resulting from deposits (third term).

$$\lambda = \lambda_0 (1+\beta\frac{\sigma}{f_0})^y (1-\frac{\sigma}{f_0})^z (1-\frac{\sigma}{\sigma_u})^x \tag{2.35}$$

Where β is a geometric constant relating to the packing of filter grains, σ_u is the saturation value of the specific deposit and y,z,x are empirical exponents. The system of Equation (2.18), (2.31) and (2.35) can be solved mathematically and curves of C/C_0 as a function of bed depth and filtration time can then be produced. Figure 2.10 show these curves for a particular case with mono sized media. It can be seen from the figure that a zone of deposit saturation initially forms in the top section of the filter bed, and that this saturation zone is extended further down in the bed as filtration continues.

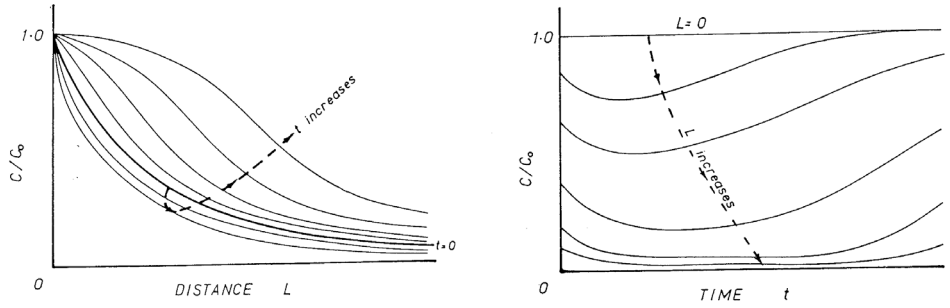

Figure 2.10 C/C_0 for a mono sized filter bed varying with filter bed depth (L) and filter run time (t) (Ives, 1970).

Vigneswaran (1983) concluded that both microscopic and macroscopic models can only be used to predict the performance of individual filtration problems, indicating that model coefficients has to be established from experimental results.

Head loss

The hydraulic gradient (dH/dL) in a filter layer is related to the approach velocity v according to Darcy's law:

$$v = p\left(\frac{dH}{dL}\right) \tag{2.36}$$

Where p is the permeability of the filter layer (m/s), and H is the head loss across the layer (m). When the filter media is clarifying suspension, the pores accumulate deposits leading to reduced permeability and increased resistance to flow. The clean bed resistance to flow can be predicted by the Kozeny-Carman equation:

$$\left(\frac{dH}{dL}\right)_0 = \frac{5\mu v}{\rho g}\left(\frac{6}{\psi d_g}\right)^2 \frac{(1-f_0)^2}{f_0^3} \tag{2.37}$$

Where ψ is the sphericity of the filter grains. This equation is used to calculate the total initial head loss H_0 through the filter layers by summing the contributions from each layer. Attempts to modify the Kozeny-Carman

equation to account for accumulating particles on the filter grains have ended up with a linear relationship:

$$\frac{\partial H}{\partial L} = \left(\frac{dH}{dL}\right)_0 + k\sigma \tag{2.38}$$

Where k is a constant. The hydraulic gradient ($\partial H/\partial L$) at any time and depth in the filter is the sum of the initial gradient $(dH/dL)_0$ and the contribution from the local deposit (σ). Integration of Equation (2.38) first with respect to depth (L) and then with respect to time (t) gives:

$$H = H_0 + kvC_0t \tag{2.39}$$

The total head loss across the filter increase linearly with time, and the slope is represented by kvC_0. In Figure 2.11 (left) the head loss as a function of time is presented. The upward curving line is the result of surface deposits, and is undesirable in depth filtration.

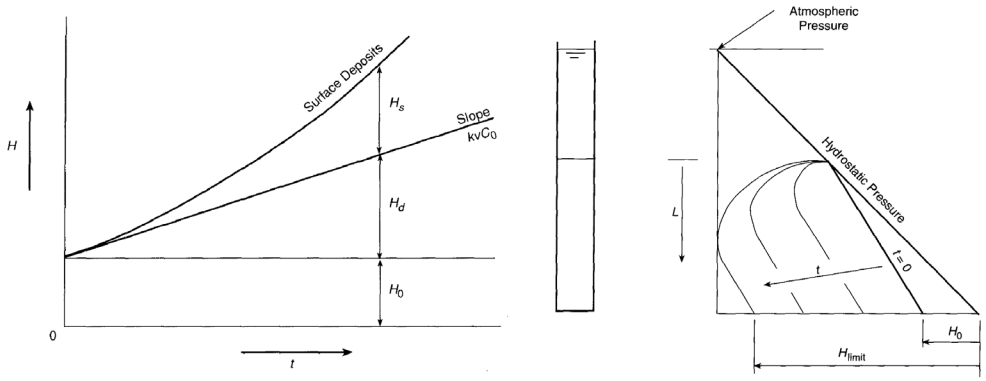

Figure 2.11 Left) Total head loss as a function of time. Right) Head loss distribution curves. (From McEwan (Ed.), 1998).

Figure 2.11 (right) show pressure profiles or head loss distribution curves for a mono media filter bed. Pressure transmitters or manometers at different depths in the filter can record the pressure curves. These curves, called Michau-curves, show were the filter is effective, because the curvature of the lines represent local capture/clogging with deposits. If the slope is determined at any time or depth in the filter and the initial slope deduced, the result is a measure of the

local specific deposit ($k\sigma$). From experimental results a value of k can be calculated from the slope of the total head loss, C_0 and v. From Equation (2.38) a value of σ can then be calculated at any time or depth in the filter. This method of calculating σ from head loss distribution curves is only valid for mono sized filter beds if not C_0 for each layer in a dual media filter is continuously recorded. The H_{limit} value in Figure 2.11 (right) is determined by conditions of less than atmospheric pressure.

2.4 Introduction to direct filtration

Direct filtration is usually used to treat relatively good quality surface water for drinking water production. Over the years different modifications have been tested to optimise the direct filtration process and make it more available. This includes for instance different types of filter media and many different coagulants.

2.4.1 Direct filtration

Direct filtration is a water treatment process that usually includes coagulation, rapid mixing, flocculation and filtration. When the flocculation step is omitted the process is referred to as in-line filtration or contact filtration, where flocculation occur in the filter pores. The goal of the coagulation and rapid mixing steps is to form pinpoint sized and strong flocs (particles), that are easily filterable. The coagulant dosages for direct filtration are generally lower than for conventional treatment where the objective is to create large settleable flocs. Capital costs are lower because no sedimentation tank is required. Low dosages result in lower chemical costs and lower sludge production, which give less cost for sludge treatment and disposal. The main disadvantages of the process is that raw waters high in turbidity and/or colour give short filter run times, and that little time is available for the operator to respond to changes in the raw water.

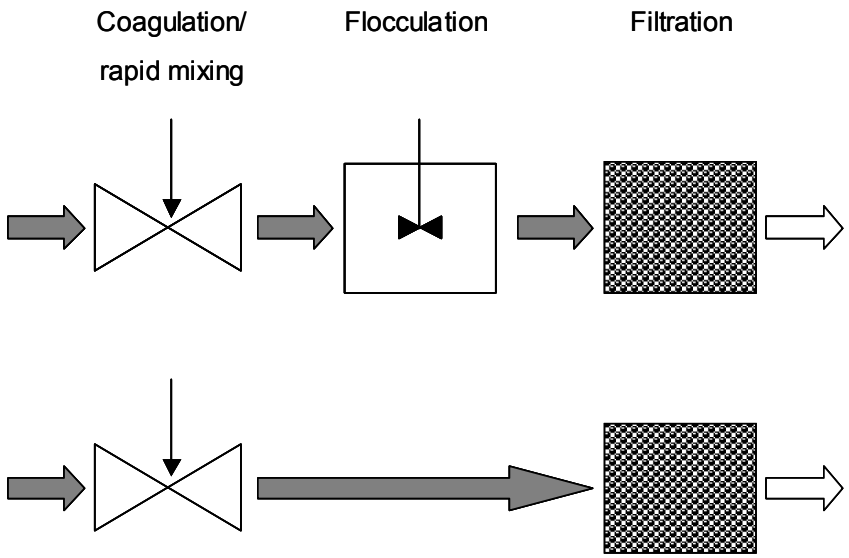

Figure 2.12 Process alternatives for direct filtration. Top: conventional direct filtration, bottom: Contact filtration.

Source waters for direct filtration

Appropriate source waters for direct filtration treatment should have a relatively good quality. When a metal salt is used for coagulation, the coagulant dose that is needed to produce the desired filtrate quality decides if the process is suitable. Especially when NOM containing raw waters are treated by metal salt coagulation and direct filtration, the metal precipitates are the major part of the suspended solids to be removed in the filter. In these cases an increase in coagulant dose will have a crucial effect on filter run times. By the use of polymer as primary coagulant (Eikebrokk and Saltnes, 2000) or in addition to a metal salt as filter aid (Eikebrokk, 1982) (Rebhun et al., 1984), the length of filter runs can be substantially prolonged, and the raw waters can be correspondingly "worse". Filter run times obtained from direct filtration pilot plant experiments can be used as selection criteria for raw water candidates. One way of considering candidates for direct filtration is to study the backwash water volumes relative to the volumes of produced water.

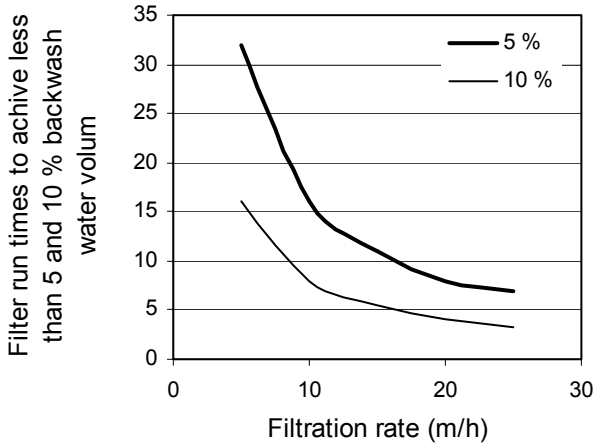

Figure 2.13 Necessary filter run times to achieve backwash water volumes less than 5 and 10 % of produced water volumes as a function of filtration rate. (Backwash water velocity=60 m/h, time for backwash=8 min.)

When studying the desired filter run times it is not sufficient to look at minimisation of the fraction of backwash water. The net water production per unit filter area and time is a more correct parameter, because it optimises water production as a function of filter surface area as well as time (Eikebrokk, 1982). In Figure 2.14 the net water production per hour as a function of filter run time is shown for some filtration rates.

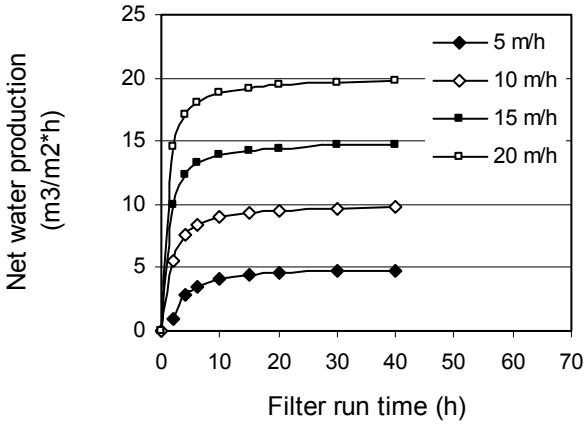

Figure 2.14 Net water production as a function of filter run time. (Same conditions as in Figure 2.13. and with a "valve time" of 4 min. included)

As seen from Figure 2.14 the net water production does not increase much by increasing the filter run times, if the run times are above about 6 hours. This should then be considered as a minimum filter run time for direct filtration.

2.4.2 Contact filtration

In contact filtration the coagulant is added just prior to filtration, normally in a weir or a pipe mixer to ensure complete mixing. Destabilisation has to occur in the short period of time before the filters, because there is no mechanical or hydraulic flocculation. Flocculation in the filter pores can increase the filterability of the flocs to be removed, because the flow in the pores creates velocity gradients (G). Then the filter grains can later remove the destabilised and flocculated particles. The effect of filter pore flocculation is difficult to separate from the effect of particle capture in the filter because both give a reduction in the concentration of particles.

2.4.3 Experiences with contact filtration of humic waters

Few publications are available on contact filtration of humic waters, some of them are mentioned below. The general impression is that the filtration cycles are short, with low capacity to breakthrough, and that especially the alum-humic floc is fragile compared to for instance alum-clay flocs.

Eikebrokk (1982,1999) studied coagulation and direct filtration as well as contact filtration of low turbidity, humic waters. He found that coagulation conditions such as pH and dose are very important in controlling NOM removal and metal residuals. In general, metal residuals at the regulated level of 0,1 mg/l Me controlled the coagulant requirements. There are optimum ranges in pH and dose for NOM removal for each coagulant, and this optimum can be in conflict with turbidity removal and residual metal. He observed early breakthroughs for humic water coagulated with alum and iron salts, leading to filter run times of only a few hours. For poly-aluminium coagulants the water quality was somewhat better but the run times was still quite short (3-4 hours, for raw water with a true colour of 50 mg Pt./l). Polymers as filter aids dramatically increased the obtained filter run times, and allowed the use of increased filtration rates. Beneficial effects of flocculation were obtained for G-values of 100 s^{-1} or higher. Chitosan used as primary coagulant gave low turbidity and relatively good colour removal (60-80 %). Organic carbon was removed to a less extent (20-40 %).

Rebhun, Fuhrer and Adin (1984) studied contact filtration of humic substances and found that a combination of alum and a high molecular weight cationic

polymer in a coarse media filter (1,2 mm grains), could prolong filter run times considerably. They found that for humic-alum flocs the initial attachment was rapid and efficient, but the resistance to detachment was low. Low filter storage capacity and low density of the deposits was also found for alum-coagulated humics, indicating voluminous deposits that easily break off.

Edzwald, Pernitsky and Parmenter (2000) used a small-scale pilot filter with a 0,13 m sand bed to investigate different poly-aluminium coagulants. The direct filtration pilot plant had no flocculation mixing, and coagulant was added just prior to a in-line static mixer. When comparing the performance of alum vs. a high basicity poly-aluminium (PACl) coagulant, for high quality raw water (turbidity < 2, TOC < 3,5), they found good turbidity removal for both coagulants. The head loss however, was lower for the PACl than for the alum. High basicity PACl produced generally lower head loss and better water quality (turbidity and NOM) than alum and the low basicity PACl.

3 LIGHT WEIGHT EXPANDED CLAY AGGREGATES

3.1 Properties of expanded clay aggregates

Expanded clay aggregates are commonly used in building blocks for house building, as insulation material and as road support etc. The aggregates are porous and lightweight, and have proven to be resistant to attrition. Today the aggregates are used in different wastewater processes and in drinking water treatment. Most of the plants that so fare use clay aggregates, use it as a bio-film carrier.

3.1.1 Raw material and production

The clay aggregates used as filter media in this study are produced by Optiroc AS in Rælingen, Norway and are called Filtralite. The raw material is brown and blue clay from the surrounding area of the factory.

The clay is fed into a 65 m long rotary kiln, with a detention time of four hours. In the kiln the clay is first dried and then pelletised with chains and blades. The expansion takes place in the last part of the kiln where the temperature reaches 1200 °C. Expansion is onset by organic matter in the clay that combusts and the gases are generating pores. The aggregates leaving the kiln are from less than 1 to about 30 mm in diameter and they have fairly round shape. They are then sieved, sorted and stored. If required the aggregates are crushed and sieved into the desired size fractions.

3.2 Characterisation of clay aggregates as filter media

Conventional filter media as sand and anthracite are characterised according to different standards and procedures. These procedures can be found in books and articles, and some are published standards for specific countries or areas. The filter grain properties are important for filtration performance and in defining the media. These properties are size, density, porosity and resistance to attrition among others.

In this study two different types of Filtralite were used. Filtralite NC (Normal density, Crushed) grains are lightweight and highly porous, while Filtralite HC (High density, Crushed) grains are heavier compared to NC, and therefore not as porous.

3.2.1 Grain size and size distribution

Filter media grain size is usually specified by a sieve curve, and other parameters withdrawn from the sieve curve. Effective size (ES or d_{10}) is the sieve size that 10 % by weight of the material would pass. If all the grains in a filter were replaced by one size only, this is found to be the grain size that gives the same head loss (hydraulic resistance) as the original size range. Uniformity coefficient (UC) is the ratio of the 60 percentile (d_{60}) to the 10 percentile (d_{10}) sieve size. It describes the shape of the sieve curve. When the UC increase, the grains are less uniform. There are different views on what UC that is best for optimum filter performance, but a value around 1,5 is usually preferred. More mono sized media, lower UC, is generally more expensive, but is better from a filtration performance point of view. The reason for this is that the smallest grains in each layer in a dual media down flow filter will accumulate in the top section of the layer, and this is not beneficial according to filtration theory. A two media filter is designed to be more efficient in the direction of the flow (from large to small filter grains), but within each layer there will be stratification, which is undesirable. Figure 3.1 show sieve curves for the filter media used in this study. In Table 3.1 the other size related parameters are presented along with other characteristics.

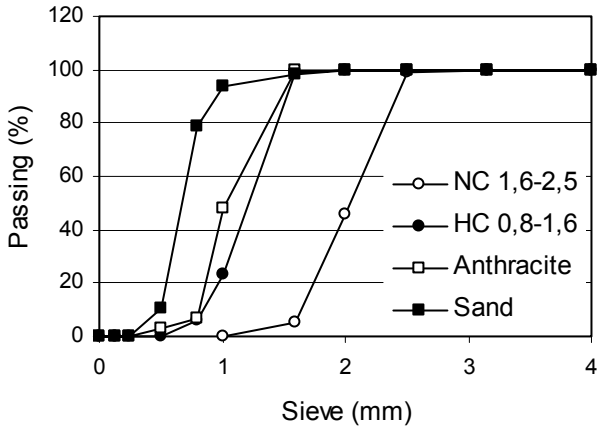

Figure 3.1 Sieve curves for filter media used in the study.

Table 3.1 Filter grain characteristics for the different types used in the pilot experiments.

Media	**Grain size** (mm)	**d_{10}** (mm)	**UC (d_{60}/d_{10})**	**Particle density** (kg/m^3)	**Porosity of filter bed, f_0**
Filtralite NC	1,6-2,5	1,65	1,55	1100	0,7
Filtralite HC	0,8-1,6	0,84	1,29	1780	0,6
Anthracite	0,8-1,6	0,82	1,37	1380	0,55
Sand	0,4-0,8	0,5	1,44	2720	0,43

3.2.2 Density and porosity

The density of granular filter media does not directly affect its filtering abilities. In the design of stratified filters however, information about grain density is vital, and can be used to find the fluidisation behaviour of the filter grains during backwashing. Density of filter grains is normally determined by using a density bottle.

The porosity of a filter bed is defined as pore volume per unit filter volume. It can be used to calculate the mass of media needed to fill a given volume of filter bed. Porosity decrease with increased sphericity of the grains. The porosity data presented are calculated from measured values of particle density and bulk density.

3.2.3 Resistance to attrition

The filter grain's resistance to attrition is an important property, and continuous wearing of grains can lead to serious problems. Filter media that experience attrition would gradually be smaller and eventually washed out of the filter bed. Attrition testing can involve crushing by steel balls, and comparing of media sizes before and after this procedure. Such a test is not very realistic compared to what is actually happening during backwash. Ives (1990) suggested an attrition test, which involves 100 hours of backwashing and calculating weight loss due to attrition. This test can be performed at the actual backwashing conditions the media will experience at a plant. Air and water rates and duration of each can be adjusted. 100 hours of backwashing represent about 3 years of plant operation. Ives also suggests that a weight loss less than 1% is satisfactory, while the British Water standard on granular filtering materials (British Water, 1995) propose that acceptable filter media should not fall in weight by more than 3%.

The 100-hour backwash test has been tried out on the Filtralite material to see if weight loss was acceptable. One of the materials tested was Filtralite NC (0,8-1,6). This material is the lightest and most porous type of Filtralite, and was believed to be the most fragile. The test procedure was 50 hours of air and water wash at 45 and 20 m/h respectively, followed by 50 hours of water only at a rate of about 50 m/h. The weight loss due to attrition was 1,1%, which is an acceptable value.

3.2.4 Chemical composition

The chemical composition of Filtralite is described below in Table 3.2. It is assumed that the material in it self is an inert material without any possibilities of chemical reactions with substances in the water or the water itself. This should be a fair assumption when the material is burned at about 1200^0 C, and the raw material is clay.

Table 3.2 Chemical composition of Filtralite expanded clay aggregates.

SiO_2	Al_2O_3	FeO_3	K_2O	MgO	CaO	Na_2O	C_{Total}
62%	18%	7%	4%	3%	3%	2%	0,02%

3.2.5 Backwash head gradient and bed expansion

During backwash the filter media expand due to friction forces on the grains. The state of fluidisation is reached when the friction drag or the pressure drop across the filter bed is just enough to support the weight of the media (Cleasby et al., 1975). In Figure 3.2 the head loss and filter bed expansion for filter F/F (Filtralite) and A/S (anthracite/sand) are shown. It can bee seen from the curves that fluidisation start at about 12 m/h for the anthracite/sand filter, and at about 28 m/h for the Filtralite filter. A linear increase in head loss for an increasing flow rate before fluidisation start is seen in the figure, as well as the constant head loss pattern after the bed has started to expand.

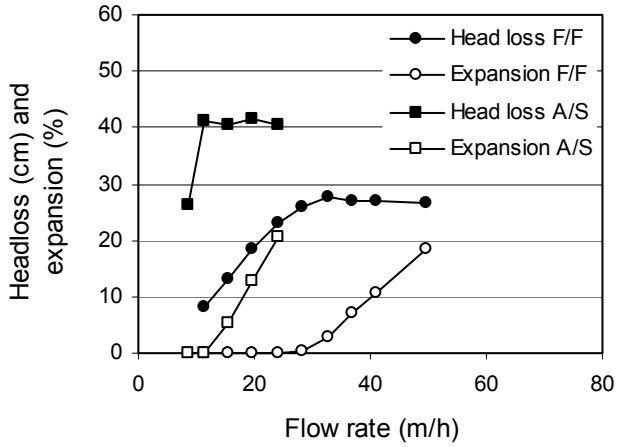

Figure 3.2 Head loss and filter bed expansion during backwash of filter FL (Filtralite) and A/S (anthracite/sand).

3.3 Settling velocity

In a multi layer down flow filter, the grain size and specific weight of the filter grains in the different layers have to match. To achieve good water quality and extensive filter runs, i.e. high solids storage capacity, the water flow has to go in direction of smaller filter grains. To maintain this coarse to fine stratification after backwashing, the filter grains in each layer must have different specific weights as in a conventional sand/anthracite filter. The Filtralite expanded clay aggregates can be produced with different specific weights, and it is therefore possible to create a multi layer filter using clay aggregates as the only filter media.

3.3.1 Theoretical approach

Three different forces influence a filter grain falling in water. These forces are the drag force f_d, buoyancy f_b and gravity f_g. Starting from rest, a grain with a higher density than water will accelerate. Almost immediately the grain reaches its terminal settling velocity, indicating that the drag force equals the effective weight of the particle.

$$f_d = f_g + f_b \tag{3.1}$$

For most theoretical and practical computations of settling velocity, the shape of the falling particle is assumed to be spherical. This gives Equation (3.2).

$$v_s = \left(\frac{4gd_g(\rho_g - \rho)}{3C_d\rho} \right)^{0,5} \quad (3.2)$$

Where v_s = settling velocity, g = gravitational acceleration, ρ_g = specific density of grain, ρ = density of water, d_g = grain diameter and C_D = drag coefficient.

The drag coefficient, C_D, depends on the nature of the flow around the particle. The Reynolds number (Re) usually describes the flow regime.

$$\mathrm{Re} = \frac{\rho v d}{\mu} \quad (3.3)$$

Flow regimes with low Reynolds number, < 1, is laminar flow (C_D=24/Re), and regimes with high Re values, > 1000, is turbulent flow (C_D=0,44). Between these two regions (1<Re<1000) the flow field is transient, and the relationship between C_D and Re is more difficult to represent. The most used representation is:

$$C_D = \frac{24}{\mathrm{Re}} + \frac{3}{\sqrt{\mathrm{Re}}} + 0,34 \quad (3.4)$$

Most of the filter grains used in drinking water treatment experience laminar flow conditions, with Reynolds numbers between 1 and 1000.

3.3.2 Experimental testing

It is known that the clay aggregates adsorb water. Especially the low-density material, Filtralite NC, with large pore space, experiences an increase in density with time spent in water. This made it more difficult to characterise the grains and modified methods had to be used.

Settling velocity information will determine the stratification behaviour of filter grains if water alone is used for the final backwash phase. In the example presented in Figure 3.3 the intermixing and layering of a three media filter bed is demonstrated by plotting settling velocity vs. sieve size for the grains. The shaded areas indicate overlapping settling velocity for two adjacent media layers, with the risk of intermixing.

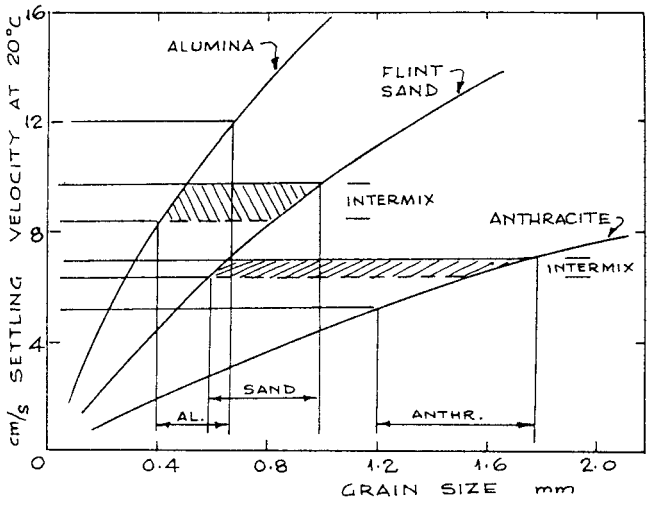

Figure 3.3 Intermixing and layering of a three-layer filter based on settling velocity as a function of grain size (Ives, 1990).

The settling velocity of the Filtralite grains have been determined by timing a 1 m fall of 30 individual grains in a plexiglass column filled with water. The 10 cm in diameter column was 1,4 m long, with about 20 cm acceleration zone before the 1 m timing distance. Initial testing of the Filtralite grains showed quite large differences in settling velocity for grains of the same sieve size. This is due to differences in shape and density from one grain to another.

Image analysis was used as a sizing tool for the grains, trying to relate the projected area of a grain to the settling velocity. This is shown in Figure 3.4 for the two Filtralite types and for some sand and anthracite grains. The results show much scatter in settling velocity, due to shape and density differences. Because of this it was decided to test 30 grains in one size range, (i.e. Filtralite NC 1,6-2,5 mm), and some sand and anthracite grains as references. The average settling velocity value minus the standard deviation (STD) is plotted against the smallest grain size (i.e. 1,6), and the average plus the STD is plotted against the largest grain size (i.e. 2,5). This gives a straight line in direction of increasing grain size and settling velocity, comparable to the lines in Figure 3.3. Figure 3.5 shows settling velocity curves for the four filter media used in this study (pre-wetted until stable settling velocity was achieved).

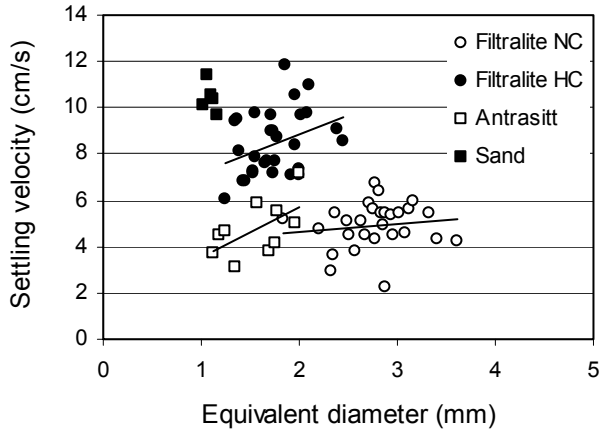

Figure 3.4 Settling velocity as a function of projected area of filter grains from image analysis for the four different media used.

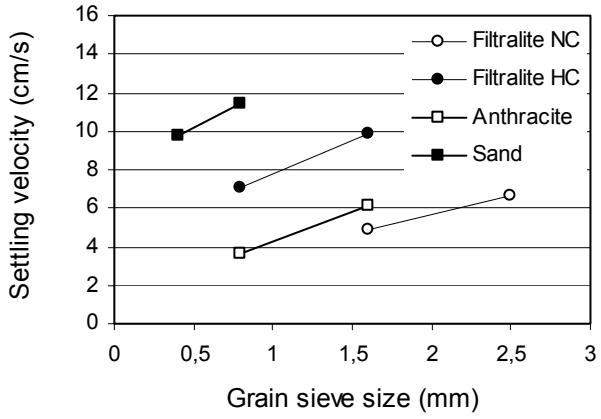

Figure 3.5 Settling velocity as a function of grain size for the four different media used.

The settling velocity for the two types of Filtralite show no overlapping areas, but the smallest HC grains and the largest NC grains do have quite similar settling velocity. For the grains in the reference filter there is a gap in settling velocity between the largest anthracite grains and the smallest sand grains, indicating a safety margin against intermixing.

The settling velocities presented in Figure 3.5 are also seen in Figure 3.6 for the two types of Filtralite media (NC and HC). The measured values are used as

reference to try to match a calculated settling velocity curve from the theoretical equations. The fit of the curve is obtained only by adjusting the grain density, while a combination of Equation (3.2), (3.3) and (3.4) are solved simultaneously to create the curves. These curves for the Filtralite filter grains can be used to select filter media types and sizes that can be combined in a dual or multi-media filter. The grain specific density (in kg/m^3) used for the calculations for each material is specified in the legend of the figure.

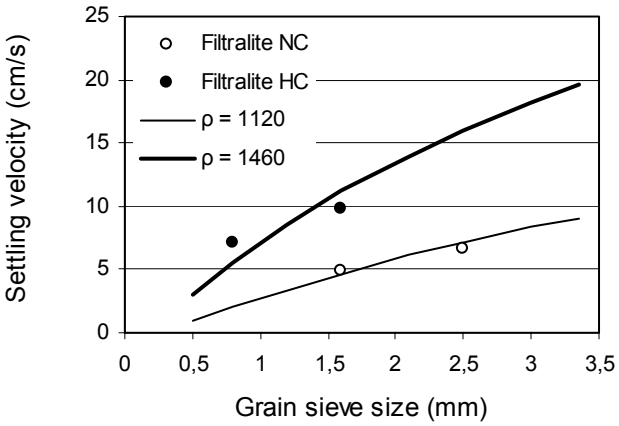

Figure 3.6 Settling velocity models for three different Filtralite media types as a function of grain size.

3.3.3 Water adsorption

The increase in settling velocity was used as a measure of water uptake by the filter grains. The 30 Filtralite grains of each type were stored separately in water, and the settling velocity was measured at different time intervals. The measurements were performed on the same 30 grains each time because of the differences from one grain to another.

Figure 3.7 show an increase in settling velocity for all the filter media except sand, because of water uptake. For anthracite and Filtralite HC there is an increase in settling velocity the first few days after they were soaked in water. These two materials have few pores available for water uptake. For Filtralite NC the settling velocity does not stabilise until the grains are soaked in water for about 6 months, however, the increase is rapid in the first period, and slows down after some weeks. The Filtralite NC grains are very porous, and when they are crushed the pores are easily available for water penetration. In the initial few weeks the large pores available from the surface of the grains adsorb

water and the increase in settling velocity is rather rapid. After this phase the internal pores that are connected to the surface pores starts to receive water, but this is a slow process because the air in these small pores has to escape before the water can get in.

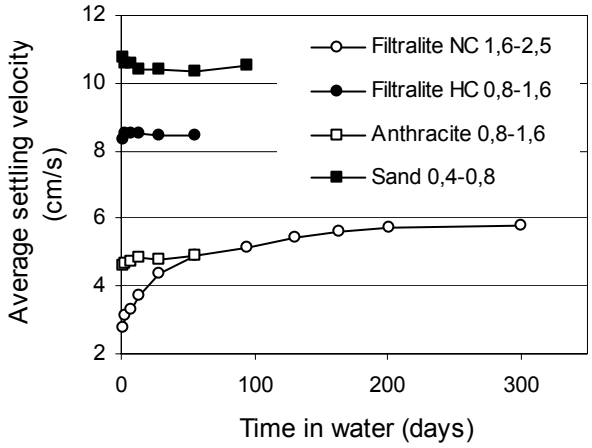

Figure 3.7 Settling velocity as a function of days in water for the different filter media.

The increase in settling velocity is caused by an increase in density when water replaces air in the filter grain pores. Density is a function of mass to volume, and the water uptake process increase the mass of each filter grain, while the volume is constant. The increase in density is calculated by combining Equation (3.2), (3.3) and (3.4), and inserting the measured settling velocities. This is shown in Figure 3.8 for Filtralite NC and HC, and the calculations are done using the d_{50} values from the sieve curves for the two media types. It must be noted that this is an approximation since the theoretical equations assume spherical grains. However, the increase in settling velocity is only due to an increase in grain density. For Filtralite NC the average increase in density is from 1038 kg/m^3 after one day in water to 1115 kg/m^3 after 300 days. Filtralite HC average density increase from 1428 to 1439 when soaked in water for 1 up to 28 days.

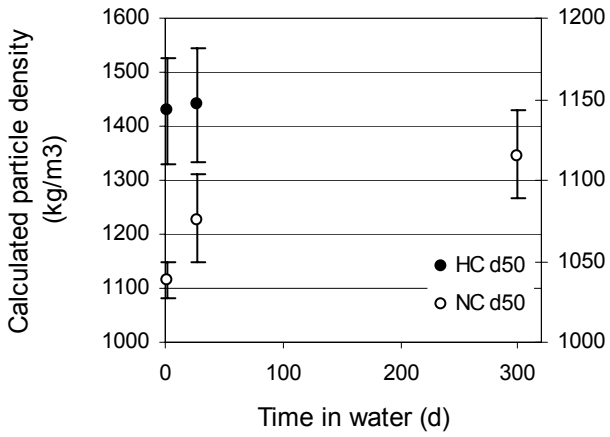

Figure 3.8 Calculated specific density for filter grains as a function of days in water for Filtralite NC grains (left axis), and Filtralite HC grains (right axis).

4 EXPERIMENTS AND EXPERIMENTAL SET-UP

4.1 Filtration pilot plant

Most of the experimental work in this study is carried out on a pilot scale coagulation/contact filtration plant as seen in Figure 4.1. The plant is designed on the basis of experiences from Eikebrokk (1982,1999 and 2000). The pilot plant filtration experiments were conducted for about one and a half years, and were run by the author exclusively.

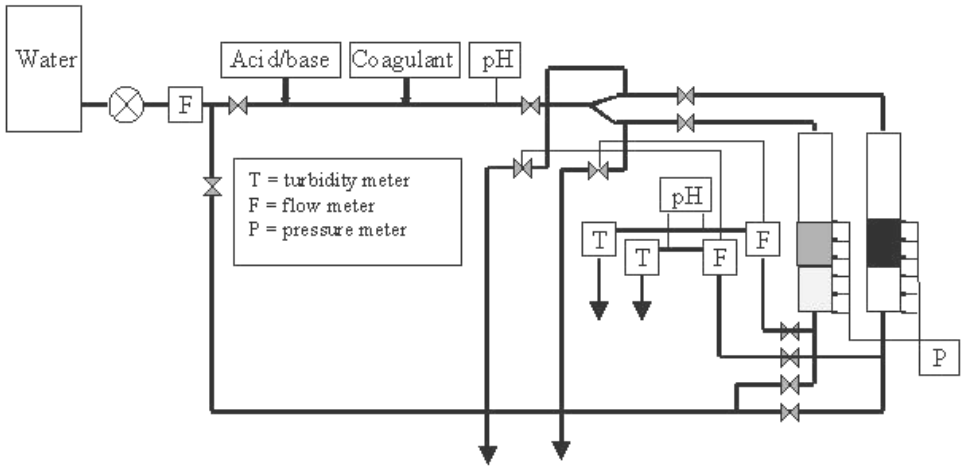

Figure 4.1 The coagulation/contact filtration pilot plant

Raw water was made of tap water added humic concentrate and/or bentonite clay (se below for characterisation). The humic concentrate was in-line mixed to the tap water before the raw water tank. When bentonite was added to the raw water it was introduced in the raw water tank, and kept suspended by the tap water inlet flow. The raw water pH was measured on-line in the raw water tank. Raw water was then pumped by a centrifugal pump, and the flow was measured by a rotameter type flowmeter. During filtration operation a constant flow of 600 l/h was then passed on. Acid in the form of diluted HCl was added for pH control in a in-line mixer just prior to coagulant addition. The coagulant was added in-line in a pipe constriction type mixer with a head loss of about 0,2 m. Humic concentrate, bentonite solution, acid and coagulant were all pumped

from cans by diaphragm-piston pumps. Correct coagulant doses were obtained by keeping a high constant water flow (600 l/h) and by control of the volume added from the graded coagulant measuring cylinder. After coagulation the flow was split, and one side-stream was withdrawn from each of the two main streams. The main streams were led to the top of each filter column by approximately 2,5 m of 25 mm tubing. The 4 meter high filter columns were made of transparent plexiglas, and the filters operated in down flow mode by gravitational force. Inlet pipes ended in the water volume above the filter media. Pressure transmitters were mounted down the side of each column to monitor head losses in the filters. The filtrate was drawn from each filter in the bottom of each column and led trough electronic flowmeters up to overflow boxes. Filtrate pH was measured on-line in the overflow boxes. From the overflow boxes, water was led to on-line turbidity meters and excess water was led to sample ports. At backwash conditions tap water was withdrawn from the flow prior to acid addition, and backwash water velocity was controlled by the same flowmeter that controlled the flow for coagulation.

The sampling points were at the outlet of each overflow box for the filtrate, and from one of the withdrawn side-streams after coagulation for coagulated water. Raw water was drawn from the main flow just after the pump and led to a on-line turbidimeter before a raw water sampling point.

Constant flow conditions in the filters were obtained by a flow control system. On one of the side-streams withdrawn from the two main-streams after coagulation, a control valve was mounted. The control valve operated on signals from the electronic flowmeter mounted on the filtrate stream of the filter. Signals from the other electronic flowmeter controlled an electronic motor that could raise or lower the inlet pipe to the other filter. Both flowmeters was given a set point according to the filtration rate prior to an experiment. This set-up provided stable and correct filtration rates in both filters.

A data logger connected to a computer provided on-line monitoring and data downloading. Signals from the electronic flowmeters, pH-transmitters, turbidimeters and pressure-transmitters were sent to the logger and forwarded to the computer. Data for each filtration run was saved on the computer for later preparation.

A list of the on-line measuring equipment can be seen in Table 4.1.

Table 4.1 On-line measuring equipment for the pilot filter plant.

Parameter	Instrument used
Flow	ABB Instrumentation, Magmaster electromagnetic flowmeter
pH	Amagruss electrode, Prominent Dulcotest transmitter
Turbidity	Hach 1720D low range turbidimeter
Pressure	ABB Instrumentation, 51A sensor, 50T transmitter

4.1.1 The filters used

Two filter columns with internal diameters of 123 mm were used in the experiments. Support layers at the bottom consisted of 10 cm of 5-10 mm gravel, 10 cm of 3-5 mm gravel and on top, in contact with the filter media, 10 cm of 1-3 mm gravel. The reference filter A/S, consisted of a top layer of anthracite and a bottom layer of sand. The top layer was 0,6 m deep with grain sizes of 0,8-1,6 mm, and the bottom layer was 0,35 m deep with grain sizes of 0,4-0,8 mm. This is a conventional filter for drinking water treatment. The Filtralite filter was a combination of a top layer of normal density material (NC), and a bottom layer of high density material (HC). Both layers were 0,47 m deep and the 1,6-2,5 mm NC grains were put on top of the 0,8-1,6 mm HC grains (see section 3 for characterisation of the media).

The filter grains used in F/F were coarser than in a conventional water treatment filter for this type of application. Grain sizes for the Filtralite filter were chosen as presented to avoid mixing of the two layers. The settling velocity curves as a function of grain size are steeper for small grain sizes than for larger grains of the same material. If the grain sizes in the Filtralite filter were equal to those in the anthracite/sand filter, this would cause intermixing problems. One of the challenges was to make use of the increased pore space in the filter bed. According to filtration theory however, small particles are more effectively removed in a filter with small grain sizes. An increase in grain size can be compensated for, to some extent, by increasing the depth of the filter layer (Ives 1965), (Moran et al. 1993). On the basis of this theory and by comparing with the filter bed used by Eikebrokk (1999) for the same application, the Filtralite filter bed was designed. The total filter depth was chosen to be the same as for the reference filter in order to see if it was possible to compensate for larger grain sizes by modifying the pre-treatment, without increasing the depth of the

filter bed. However, the bottom layer depth was slightly increased to optimise the filter bed within the mentioned limits.

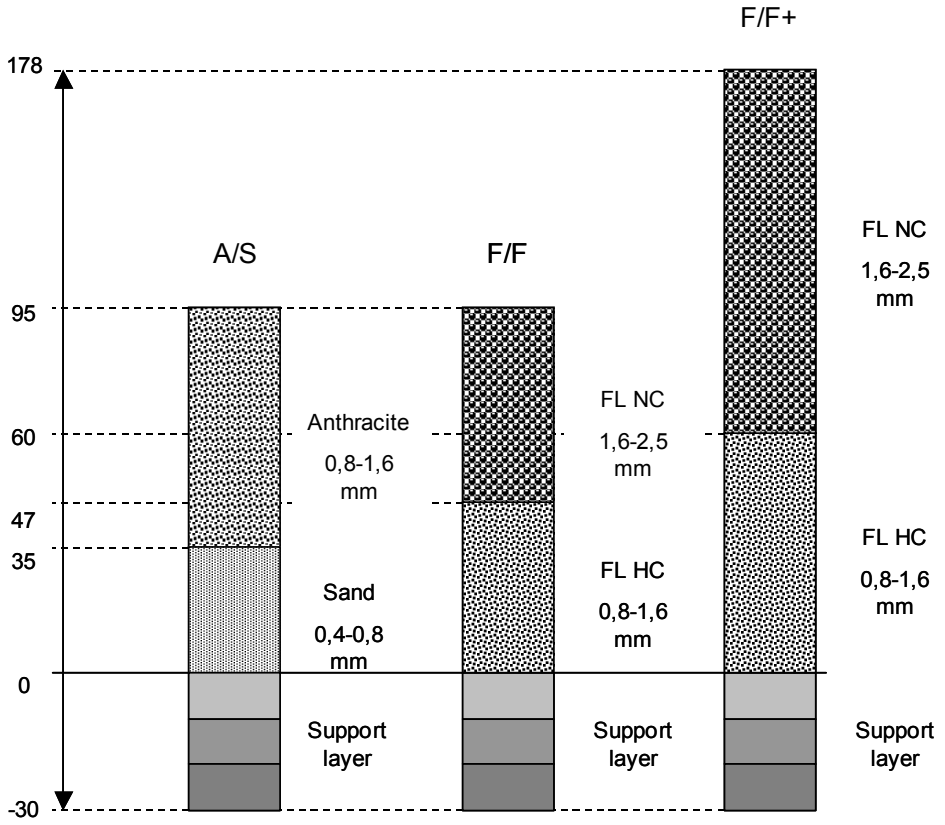

Figure 4.2 Illustration of the different filter beds tested. (Heights in cm)

In the deeper Filtralite filter (F/F+), depths were selected from the relationship of L/d (depth/grain diameter). This relationship has been used where a coarser filter media is replacing a finer media, to find the needed bed depth to produce equal filtrate quality. The experiments of Ives and Sholji (1965) support the use of this relationship, however, other researchers have suggested that the ratio should rather be L/d^a, with $a > 1$. For dual and multi media filters the sum of L/d_e for each layer in the bed is calculated (Kawamura, 1991). This was done for the anthracite/sand filter bed, and necessary depths for the coarser Filtralite filter was found. The depths needed to produce equally good filtrate quality was calculated to be 118 cm of top layer Filtralite NC (1,6-2,5 mm) on top 60 cm of Filtralite HC (0,8-1,6 mm).

4.2 Raw water characteristics

The main component of the different raw waters tested was tap water from the city of Trondheim. The municipal water treatment plant (VIVA) in Trondheim take water from lake Jonsvatnet and filters it trough a calcium carbonate filter for pH and corrosion control in the distribution system. The plant is not designed for particle removal or removal of humic substances.

Two levels of raw water colour was used in this study, RW15, which is tap water with a colour level of about 13 mg Pt./l, and RW50, which is tap water added about 0,06 volume % of humic concentrate, giving a colour of 50 mg Pt./l. The humic concentrate was regenerant from an anion-exchange plant for humics removal in Meraaker near Trondheim. Data on both raw waters are listed in Table 4.2.

Table 4.2 Raw water characteristics

Parameter	**RW15**	**RW50**
Colour (mg Pt./l)	13 (± 1)	50 (± 5)
TOC (mg/l)	2,5 (± 0,3)	5,5 (± 0,5)
Turbidity (NTU)	< 0,25	< 0,25
pH	8-8,5	8-8,5
Temperature (°C)	7-11	7-11
Alkalinity (mmol/l)	1,0	1,0
Calcium (mg/l)	20	20
Aluminium (mg/l)	0,06	0,06
Iron (mg/l)	0,06	0,06

The two humic raw waters were tested for molecular weight according to a HPLC (High Performance Liquid Chromatography) procedure, and the results are presented in Figure 4.3 as each fraction's content of TOC (total organic carbon). Both RW15 (tap water only) and RW50, consist mostly of TOC with molecular weights between 5000 and 20 000 Daltons. The humic concentrate that was added when RW50 was produced had more molecules in the 2000-5000 size range, where no TOC was detected for RW15. The main contribution of TOC from the humic concentrate was in the 10 000-20 000 MW range. From Table 4.2 it can be seen that the ratio of colour to TOC is higher for RW50 than for RW15. This usually indicates a shift towards larger NOM molecules.

Eikebrokk (1999) presented a comparison of the same raw water used in this study, raw water made of not carbonated tap water with humic concentrate and

8 reference NOM water samples (Ratnaweera et. al., 1999). The results showed that for RW15 and RW50 the colour to DOC relationship was not affected by the carbonisation of the tap water, and both followed the linear relationship as was seen for the 9 reference samples.

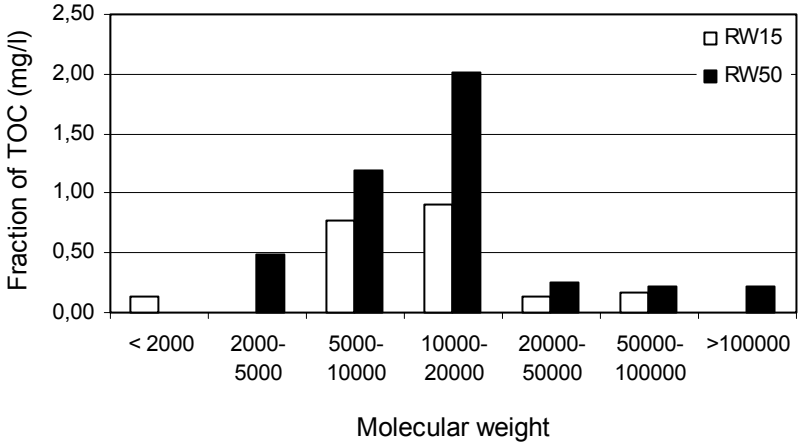

Figure 4.3 Molecular weight distribution for RW15 and RW50 expressed as TOC (mg/l) contribution from each fraction (Eikebrokk, 2001).

A bentonite clay suspension was added to the raw water in some experiments to produce raw water turbidities of 3 NTU (RW15/3 and RW50/3) or 6 NTU (RW15/6 and RW50/6). The bentonite solution with a concentration of 15 g/l was made of bentonite clay suspended in tap water. Size distribution for fresh bentonite (some minutes after suspension in water) and old bentonite (about 1 month after suspension in water) are presented in Figure 4.4. From the figure it can be seen that the old bentonite clay generally has a larger particle size than the fresh one. The d_{50} for fresh bentonite is 0,21 μm, and for old 0,27 μm on particle number % basis. The bentonite suspension used in the experiments was never older than 1 week, therefore the changes in particle size for the bentonite clay was considered insignificant for the treatability of the raw water. The raw water with a turbidity of 3 NTU was added about 9 mg/l of bentonite. Zeta-potential for RW15/3 and RW50/3 was measured to -16 mV and -16,6 mV respectively. This indicates that the potential of the clay particles are insignificantly influenced by the amount of humic substances. There was probably little adsorption of NOM on the bentonite. This was supported by the measured values of true colour (filtered trough 0,45 μm) for RW50/3 which was unaffected by the introduction of bentonite. Specht et al. (2000) found that adsorption of NOM on clay minerals (kaolinite and montmorillonite) had little effect on the electrophoretic mobility of the particles. At pH below 6 a

significant amount of NOM adsorbed to the clay particles (mostly kaolinite), but still with small changes in the electrophoretic mobility.

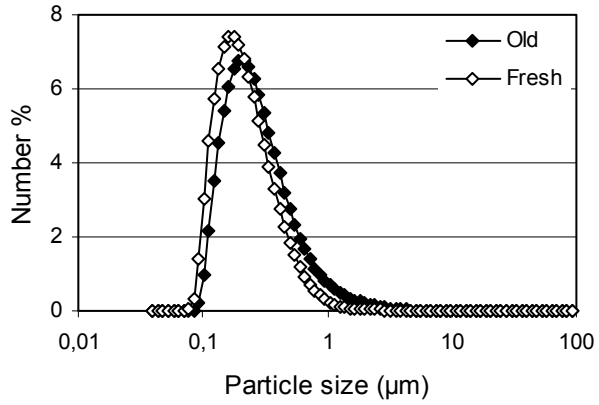

Figure 4.4 Size distribution of bentonite clay suspension. Fresh (some minutes after suspension) and old (one month after suspension)

4.3 Sampling and analysis

Samples of raw water, coagulated water and filtered water from both filters were taken for each filtration run. The samples were collected in glass bottles directly from the pilot filter plant, and stored in a refrigerator before analysis. In Table 4.3 the samples and corresponding analysis are shown.

Table 4.3 Laboratory analysis performed on different water samples

Parameter	**Raw water**	**Coagulated water**	**Filtered water**
PH	X		X
Turbidity (NTU)	X		X
True colour (mg Pt./l)	X		X
TOC (mg/l)	X		X
Metal residual (mg Me/l)	X		X
Suspended solids (mg/l)		X	
Zeta potential (mV)		X	

The laboratory analyses were performed by the author except for the TOC measurements which were performed by laboratory personal at the Dept. of Hydraulic and Environmental Engineering, NTNU, and the metal residual

analysis which were carried out at The Norwegian Institute for Nature Research (NINA). A list of the equipment used is presented in Table 4.4 below.

Table 4.4 List of analysis and the instruments used

Parameter	**Sample pre-treatment**	**Instrument used**
pH	None	Electrode and a Radiometer ION 83 pH-meter
Turbidity (NTU)	None	HACH 2100N turbidimeter
True colour (mg Pt./l)	Filtration through 0,45 µm membrane filter	Hitachi spectrophotometer U-3000
TOC (mg/l)	None	Dohrmann DC190 or Dohrmann Apollo 9000
Metal residual (mg Me/l)	Acidification with H_2SO_4	ICP-MS (Inter Coupled Plasma-Mass Spectroscopy)
Suspended solids (mg/l)	None	0,45 µm cellulose nitrate membrane filter
Zeta potential (mV)	None	Coulter Delsa 440 SX
Particle size distribution (µm)	None	Coulter LS 230

5 COAGULATION OPTIMISATION

5.1 The need for coagulation optimisation

To obtain good quality water in contact filtration one has to ensure that the coagulation process is carried out at optimum conditions for the specific coagulant used. For a given coagulant, the variable parameters are generally pH and coagulant dose.

In Norway, as in many other parts of the world, the major challenge of water treatment is the removal of humic substances. The traditional way of optimising for turbidity removal may result in high concentrations of dissolved organic matter and the risk of forming disinfection by-products (DBP's) in treated water. Enhanced coagulation, implying pH and coagulant-dose control for optimised TOC removal, is incorporated in the US EPA Disinfectants and Disinfection Byproducts Rule (US EPA, 1998). It states that water systems that use surface water or ground water under the direct influence of surface water and use conventional filtration treatment are required to remove specified percentages of organic material (measured as TOC) that may react with disinfectants to form DBP's. The percentage removal requirement depends on the content of TOC and alkalinity in the raw water. This rule is an indication of a shift in focus for coagulation optimisation in USA from turbidity removal to organic matter removal.

Norwegian raw water is usually surface water with low turbidity and relatively high colour levels (Ødegaard et al., 1999). Source water temperature varies with season and is normally between 2 and 15 °C. The traditional coagulation/direct filtration treatment plants in Norway involve pH control, coagulation (usually with a metal salt), filtration, disinfection pH-, alkalinity- and calcium-adjustment (corrosion control).

One of the main problems in coagulation/filtration plants optimised for humic substances removal are the short filter run lengths obtained, specially when a metal salt is used as the only coagulant without any filter aids. Eikebrokk (1999) claims that residual metal in the treated water is usually determining the minimum coagulant dose requirements when treating humic waters. As seen in Figure 2.2, the pH and dose of a metal salt coagulant decides the solubility of

the metal. The coagulation mechanisms are also dependent on pH and coagulant dose, and influence the filterability of the humic-coagulant flocs.

5.2 Coagulants used in this study

The coagulants used in this study ranged from the widely used products for this type of application (like aluminium sulphate), to chitosan, a fairly unconventional product within water treatment practise showing promising results.

5.2.1 Aluminium sulphate (Alum)

Alum is the most widely used coagulant for water treatment in the world. The commercial product used here was granulated (ALG) and is produced by Kemira Chemicals A/S. The chemical formula is $Al_2(SO_4)_3 \cdot 17H_2O$, and the dry granules contained 9,0 weight % aluminium. The coagulant solution was prepared by dissolving 2 kg of ALG in tap water to a final volume of 10 litres. This provided a solution with a concentration of about 17 % and a corresponding pH of about 3. **ALS** is used as an abbreviation for this coagulant in the following text.

5.2.2 Iron chloride sulphate

The iron chloride sulphate concentrate (JKL from Kemira Chemicals A/S) has an iron content of 11,6 weight %, and the chemical formula is $FeClSO_4$. The solution used in the experiments was diluted 1:10 for easy dosing. (Dilution recommended by the producer). **FEC** is used as abbreviation for this coagulant in the text.

5.2.3 Poly aluminium chloride

Poly aluminium chloride (PAX-16 from Kemira Chemicals A/S) was also used in the experiments. This product contains 8,05 weight % of aluminium, and the formula is $Al(OH)Cl_2$. The basicity was 35 % (r = 1,05), which is quite low. This low basicity product was used because it was easy to get hold of and is used by several water treatment plants. The PAX-16 solution was diluted 1:5 prior to dosing. **PAC** is used as abbreviation for this coagulant in the text.

5.2.4 Chitosan

Chitosan is produced from chitin, which is the (water insoluble) structure polymer of the skeleton of insects and crustaceans. Chitin can be considered as modified cellulose, and is the second most occurring polymer in nature. Deacetylated chitin to less than about 15 % acetylated units is called chitosan,

with the acetylated units distributed randomly along the polymer chain. Protonation of amino groups give chitosan the cationic charge, and for this to happen the pH has to be less than about 6. The charge density of chitosan increases with decreasing pH below 6. Chitosan is intoxic, and the cationic properties make it suitable as a primary coagulant. In Figure 5.1 the structure of chitin and chitosan are shown.

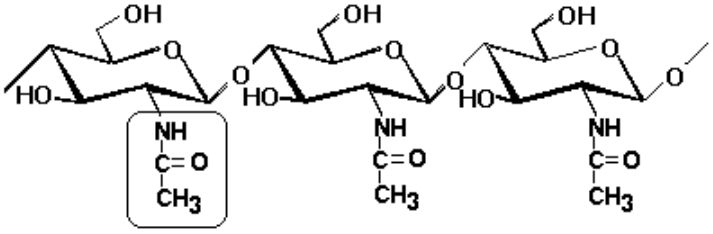

Chitin

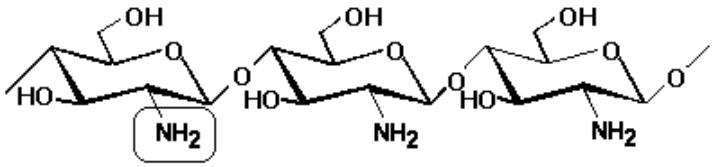

Chitosan

Figure 5.1 Structure of chitin and chitosan.

The chitosan used was ChitoClear from Primex Ingredients ASA. This chitosan is made from fresh shrimp shells with a 93 % degree of deacetylation. (7 % acetylated units). The fine graded chitosan powder was dissolved in tap water with hydrochloric acid to prepare the dosing solution with a concentration of 10 g/l. The abbreviation **CHI** is used for this coagulant in the following text.

5.3 Experimental set up

The coagulation optimisation experiments were conducted on different types of raw water and with the four different coagulants mentioned above. The coagulant doses and pH of coagulation was varied for each filter run. The doses and pH ranges tested were selected on the basis of experiments performed earlier (Eikebrokk, 1999). Water samples for analyses were taken for each filter run when the filtrate from the filters showed a stable turbidity (about 2 hours after start up). In Table 5.1 the dose and pH conditions for the optimisation experiments on RW15 and RW50 are shown. All optimisation experiments on RW15 and RW50 were performed at a filtration rate of 7,5 m/h.

Table 5.1 Conditions for dose and pH optimising experiments on coloured raw water. Doses in mg Me/l or mg CHI/l.

RW15			
ALS	FEC	PAC	CHI
pH:5,3-6,2	pH: 3,9-4,6	pH: 5,6-6,4	pH: 5,1-6,3
Dose (mg/l)	Dose (mg/l)	Dose (mg/l)	Dose (mg/l)
0,6 1,0 1,4	1,5 2,0 2,5	0,4 0,8 1,2	1,0 1,5 2,0
RW50			
ALS	FEC	PAC	CHI
pH: 5,0-6,1	pH: 4,2-5,8	pH: 5,2-6,2	pH: 4,7-6,5
Dose (mg/l)	Dose (mg/l)	Dose (mg/l)	Dose (mg/l)
2,3 3,0 3,7	5,5 7,0 8,5	1,9 2,5 3,1	3,0 4,0 5,0

For raw water with bentonite turbidity the coagulation optimisation experiments are listed in Table 5.2. The increased solids load to the filters gave some experiments with immediate breakthrough after ripening, making it difficult to obtain representative results for the filtered water. When ALS was used for coagulation of low coloured, turbid water, the turbidity was 5 NTU and not 3 NTU as for the other experiments. The optimisation experiments with turbid raw water were performed at a filtration rate of 5 m/h.

To perform the coagulation optimisation experiments in the pilot filters is time consuming compared to a conventional jar test procedure. However, in a jar test the optimum conditions for making settleable flocs are found. When the experiments are carried out in the filter columns, with the actual filters as the particle separation process, the filterability of the flocs is optimised. Also, a jar test does not give any information about filter run time lengths, solids storage capacity or head loss.

Table 5.2 Conditions for coagulation optimisation experiments on raw water with colour and turbidity. Doses in mg Me/l or mg CHI/l.

RW15/3			
ALS (RW15/6)	FEC	PAC	CHI
pH: 5,3-6,2	pH: 4,4-5,7		pH: 4,6-6,1
Dose (mg/l)	Dose (mg/l)		Dose (mg/l)
0,5 1,0	1,0 2,0		1,0 1,5 2,0
RW50/3			
ALS	FEC	PAC	CHI
pH: 5,4-6,7	pH: 4,5-6,2	pH: 5,3-6,6	pH: 4,6-6,5
Dose (mg/l)	Dose (mg/l)	Dose (mg/l)	Dose (mg/l)
2,0 3,0 4,0	5,0 7,0	1,5 2,5 3,5	2,0 4,0 6,0

5.4 Results and discussion

Optimum pH and dose conditions for the four different coagulants were evaluated by filtered water turbidity, metal residuals, colour removal and TOC removal. Zeta potential measurements of coagulated water were performed in order to find some explanation for differences in performance.

All the experiments done were carried out in both filters. The results presented are for the Filtralite filter, but in later sections the two filters are compared.

5.4.1 pH effects

The effects of pH at optimum dosage on the filtered water turbidity and residual metal as well as removal of TOC and colour were studied for the different coagulants and raw waters. Optimum dosage in each case was selected as a compromise between the mentioned water quality parameters.

In the following discussion the effluent water quality as a function of pH for the four coagulants is considered for each raw water. Zeta potential of coagulated water for the corresponding experiments is also presented.

RW15

For this low coloured, low turbidity water the optimum doses were found to be 1,0 mg Al/l as ALS, 0,8 mg Al/l as PAC, 2,0 mg Fe/l as FEC and 1,0 mg/l CHI.

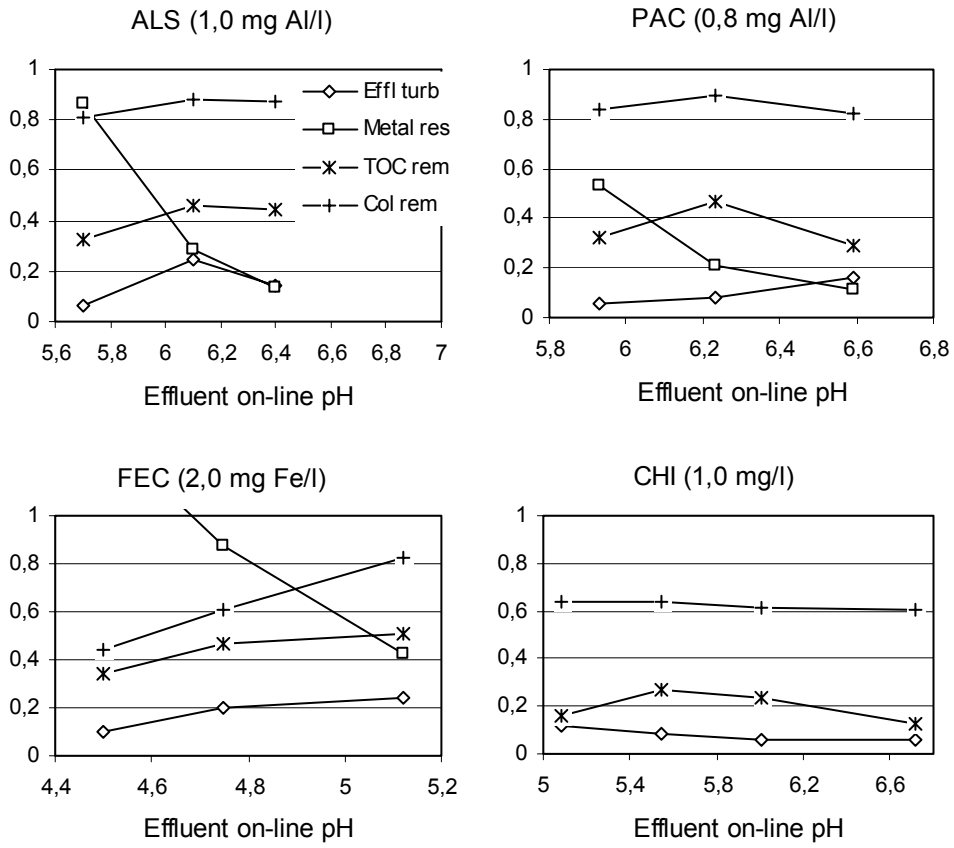

Figure 5.2 Effect of pH on effluent water turbidity (NTU), metal residuals (mg Me/l), removed fraction TOC and removed fraction colour for RW15.

The raw water turbidity for this water was about 0,2 NTU. The aluminium-based coagulants have filtered water turbidities lower or equal to the raw water value. They both show a trend of an increasing turbidity with increasing pH, with the lowest turbidities obtained with PAC. Metal residuals in produced water follow the solubility of the precipitates, and for aluminium the pH of minimum solubility is about 6,5. With PAC coagulation the metal residuals are lower than with ALS coagulation over the whole pH range, reflecting the lower turbidities obtained. Choosing optimum pH for these two coagulants is a question of keeping a low pH in order to reduce effluent turbidity, but high enough to comply with the residual metal limitations.

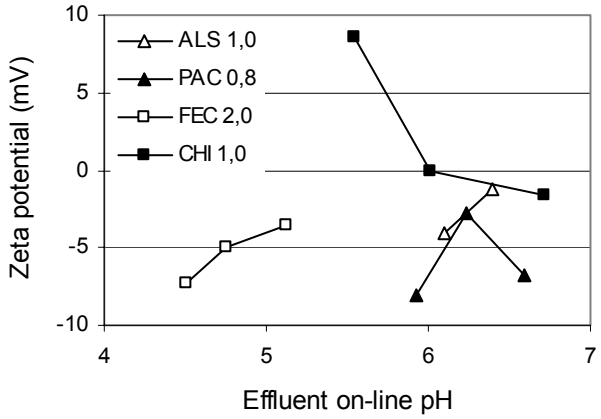

Figure 5.3 Zeta potential of coagulated water as a function of pH for RW15.

For FEC the lowest effluent turbidity is obtained at a pH of about 4,5. At this low pH most of the dosed iron is on soluble form and is able to destabilise the raw water turbidity making it filterable. An increase in pH, increase the iron hydroxide precipitation, and this is probably what shows as turbidity in the effluent. Another solution can be that the hydroxide precipitates are removed, but there is not enough soluble iron left to destabilise the raw water turbidity, which ends up in the effluent. Looking at the corresponding zeta potential measurements, they show a trend of less negative values with increasing pH for FEC. This is in contrast to the normal behaviour of zeta potential as a function of pH, but it can probably be explained by the increasing precipitation of hydroxide giving an increase in positive charge (less negative). CHI is an excellent turbidity remover, and the filtered water turbidity is not as sensitive to pH changes as with the metal-based coagulants. CHI does not create turbidity in the form of metal hydroxide. The zeta potential of CHI coagulated water is decreasing with increasing pH, in agreement with the charge of the CHI polymer. It may also be noted that the differences in zeta potential for CHI does not result in much difference in filtrate turbidity.

TOC removal has a optimum at a pH just above 6 for ALS and PAC, and both are able to remove about 45 % of the raw water TOC. When PAC is used, the TOC removal decreases from 45 % at pH 6,2 to about 30 % at pH 6,6. The reason for this might be the low dose, which narrows the pH range of good removal. A colour removal of about 85 % is achieved with all the metal-based coagulants. FEC show an increasing TOC and colour removal with increasing pH in the whole range of pH tested, but higher pH will increase the effluent

turbidity. At pH 5,1 FEC is removing 50 % of the TOC. When removing organic matter with CHI the removal rates are lower than for the metal-based coagulants. Colour removal is almost not affected when pH varies from 5,1 up to 6,7, and shows a removal of about 60 %. The TOC removal is more pH dependent, with an optimum of 30 % at pH 5,5.

RW50

The optimum doses for the high coloured raw water was found to be 3,0 mg Al/l as ALS, 2,5 mg Al/l as PAC, 7,0 mg Fe/l as FEC and 4,0 mg/l CHI.

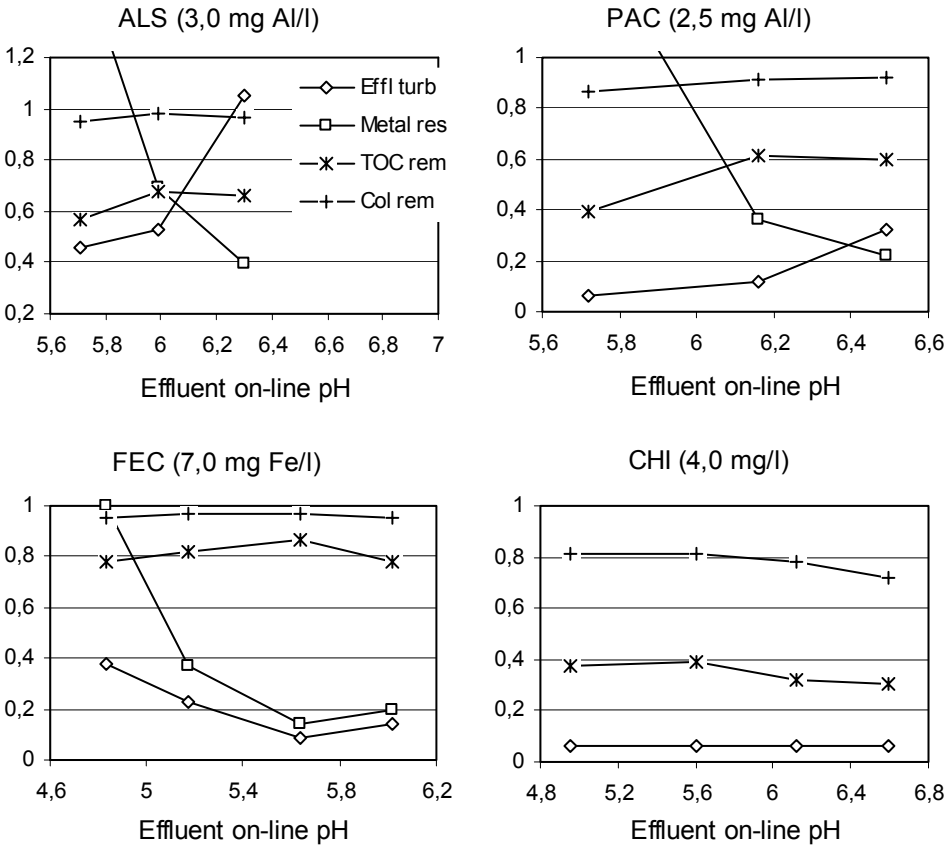

Figure 5.4 Effect of pH on effluent on-line turbidity (NTU), metal residuals (mg/l), removed fraction TOC and removed fraction colour for RW50.

Coagulation with ALS for raw water with high colour levels lead to problems with high turbidity in the filtered water. For the low pH experiment (pH about 5,7) the effluent turbidity is as high as 0,46, which is higher than the raw water turbidity. Increasing pH result in a rapidly increasing turbidity probably caused

by the increasing hydroxide precipitation. These results demonstrate that the poor turbidity removal is due to formation of week hydroxide-humic substances flocs that are broken in the filter pores, penetrating the filter bed. The TOC and true colour removals are almost not affected by the change in pH. The results for PAC show much better effluent turbidities than for ALS, but the same trend of increase with pH increase is seen. The improved filtrate quality is probably due to the fact that the polymeric species from PAC form stronger flocs that are able to resist shear in the filter pores. Van Benschoten and Edzwald found that about 90 % of the aluminium from hydrolysis of poly aluminium chloride was on polymerised form (Van Benschoten and Edzwald, 1990a). The hydrolysis products from PAC has higher charge than from ALS, this allows stronger electrostatic bonding resulting in stronger flocs. The zeta potential for ALS and PAC coagulation show values close to zero. With FEC the zeta potentials of coagulated water are much more negative for all the experiments performed, the effluent turbidity is low however. This might indicate that the zeta potential of the flocs formed is not that important for the filterability. The filtrate turbidity when FEC is used has a well-defined minimum at pH about 5,6. This coagulant has a wider pH range for effective coagulation than ALS, probably due to a lower solubility of iron hydroxide.

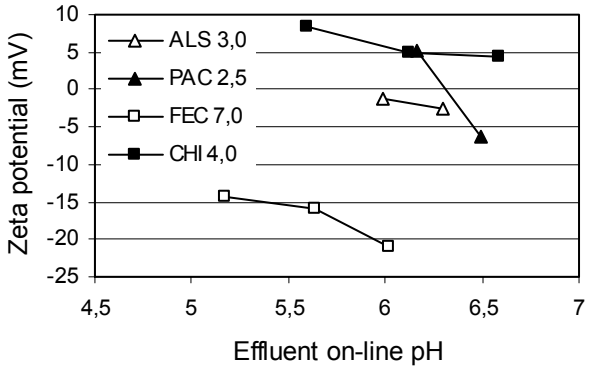

Figure 5.5 Zeta potential of coagulated water as a function of pH for RW50.

The residual metal when ALS and PAC are used follows the solubility of aluminium. For low pH about 5,5 the fraction of soluble Al is high, and good turbidity removal does not ensure low metal residuals. At pH above 6 the precipitation of hydroxide lowers the fraction of soluble Al, but the increased turbidity give a too high total residual aluminium concentration. In the experiments were FEC is used the residual iron also follow the solubility of iron hydroxide, and the turbidity show the same trend as the iron residuals.

There is no hydroxide precipitation when CHI is used as coagulant and therefore less suspended solids and turbidity are formed. The results for CHI show excellent filtrate turbidity bellow 0,1 NTU in the pH range from 4,9 to 6,6. Unlike the case for the metal-based coagulants, the use of CHI is not limited by metal residuals in produced water.

The TOC and colour removals are 40 % and 80 % respectively at optimum pH (about 5,5) when CHI is used, which is lower than for the other coagulants. At a pH of 6,5 the removals of TOC and colour are somewhat lower, 30 % and 70 % respectively. Analysis of the CHI showed that it contains about 60 % TOC, and the relatively low TOC removal can be explained by residual CHI in the effluent. Estimates show that the possible contribution to filtrate TOC from CHI is about 1,0 mg/l, at a dosage of 4,0 mg/l. This residual CHI, which is biodegradable, might contribute to growth in the distribution system.

The metal salts ALS and FEC are the most effective for TOC and colour removal among the coagulants studied. The colour removal for ALS is more than 95 % in the pH range 5,7 to 6,3, with a maximum at pH 6. ALS removes about 70 % of the TOC at this optimum pH, and from the figure it can be seen that TOC removal is more sensitive to pH than colour removal. The same pH sensitivity is seen for FEC, but the TOC removal is generally higher with a maximum of 85 % at pH 5,6. Colour removal is 95 % or more for pH 4,8 to 6,0 when using FEC. PAC has a colour removal of about 90 %, and a maximum TOC removal of 60 % at pH 6,2. The removal of TOC drops to 40 % when the pH is reduced to 5,7.

All the four coagulants seem to have an optimum pH for TOC removal in the ranges tested. For the aluminium based coagulants optimum pH for TOC and colour removal is just above 6. This is not the optimum pH for filtered water turbidity. FEC and CHI have no conflict in optimum pH for organics removal, turbidity and residual metal.

RW15/3

This raw water with bentonite turbidity was coagulated with ALS, FEC and CHI at optimum doses of 1,0 mg Al /l, 2,0 mg Fe/l and 1,0 mg/l CHI respectively. The high solids load to the filters lead to early breakthrough and difficulties with representative sampling of filtered water. For ALS the raw water turbidity was 5 NTU, and results for 0,5 mg Al/l are presented because of the problem mentioned above.

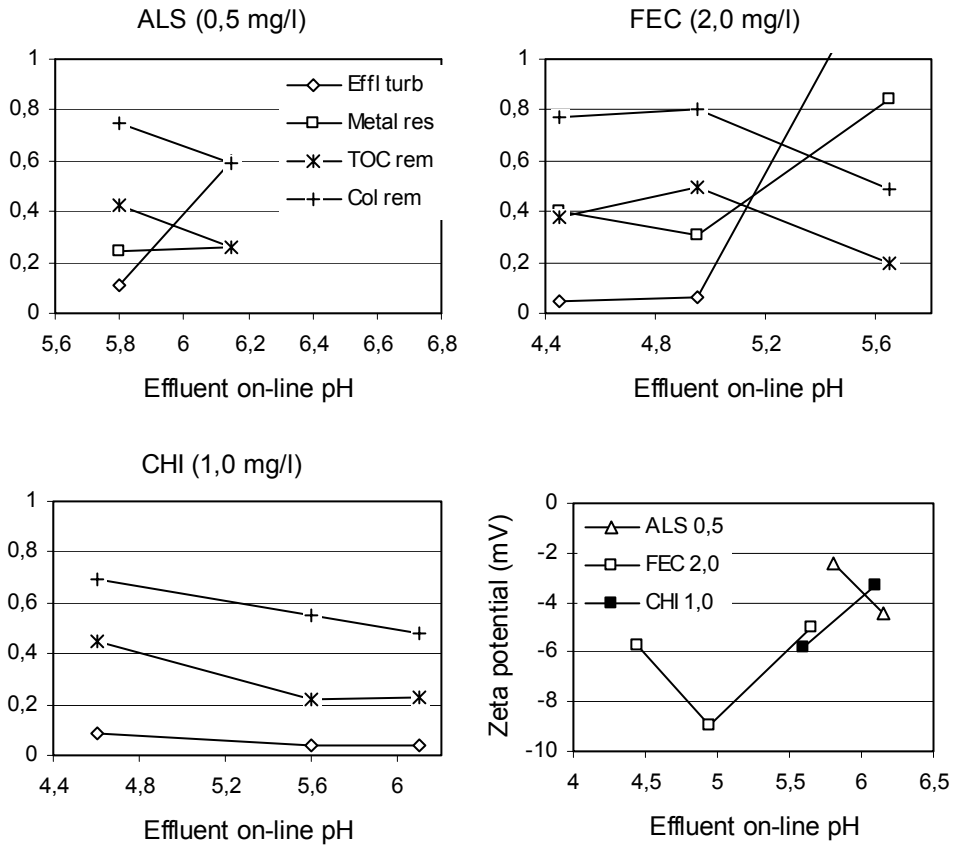

Figure 5.6 Effect of pH on effluent on-line turbidity (NTU), residual metal (mg/l), removed fraction of TOC and removed fraction of colour for RW15/3. Bottom right: Zeta potential of coagulated water for the different coagulants.

It is well known that bentonite clay particles are easy to coagulate, and this is demonstrated in the results for filtrate turbidity, which in many cases is as low as for RW15 for the same coagulant doses. A raw water turbidity of 3 NTU is not high, but the increased solids load is about 10 mg/l. Using ALS and FEC for coagulation of this water show the same trends as for RW15. Filtrate turbidity increase with increased pH in the pH range tested, but the results are more sensitive to changes. This is because there is more turbidity available to penetrate the filter, if coagulation is done at a unfavourable pH. The results for ALS are limited, and the dose is not the optimum one for this raw water. However, good filtrate turbidity (0,11 NTU) is obtained at pH 5,8. The aluminium residuals are relatively high, and are in this case not affected by pH. The reason for this could be that the increased turbidity at pH 6,15 is associated

with aluminium containing bentonite or aluminium hydroxide precipitates (or flocs containing both). At a higher dose and pH just above 6 the effluent turbidity would most certainly have been lower and as a result of that, lower aluminium residual would have been obtained.

In the pH range from 4,4 to 5, FEC remove turbidity very effectively. At higher pH the turbidity increase rapidly and so also the residual metal. The low effluent turbidity at pH 5 is not enough to ensure low metal residuals, indicating that the iron penetrating the filter are on soluble form. CHI is effectively removing the raw water turbidity in the pH range from 4,6 to 6,1 to below 0,1 NTU (bellow 0,05 NTU for pH 5,6 and 6,1). The zeta potential measurements for this raw water show negative values for coagulated water for all the experiments. This is not surprising because the raw water now contains much more negative charge from the bentonite clay.

TOC and colour removals for the metal salts have their optimums at a pH where a rapid increase in hydroxide precipitation is observed, just on the acid side of minimum solubility. The removal of organic matter is high at optimum pH, about 80 % of the colour and 50 % of the TOC are removed in the filter by these coagulants. If the pH is increased from 5 to 5,6 when coagulating with FEC the TOC and colour removal drops to 20 and 50 % respectively. A low pH of 4,6 is more effective than higher pH for the TOC and colour removal when CHI is used, and even higher removals could probably be obtained at lower pH. The removal rates are not much lower than for the metal salts, about 40 % TOC and 70 % colour are removed.

RW50/3

A competition for coagulant between bentonite clay and NOM is expected to be seen for this raw water. The optimum dosages used were 3,0 mg Al/l as ALS, 2,5 mg Al/l as PAC, 7,0 mg Fe/l as FEC and 4,0 mg/l CHI.

From Figure 5.7 it can be seen that effluent turbidity is not the problem for this raw water if the process is kept stable at correct pH. For ALS coagulation the pH of optimum conditions for the filter is about 6, lower pH gives to high metal residuals and higher pH increases the effluent turbidity (0,2 NTU at pH 6). PAC is also for this raw water a more efficient turbidity remover than ALS. In the pH range from 5,5 to 6,3 the effluent turbidity is never higher than 0,07, giving the great opportunity to optimise pH to minimum solubility of aluminium (pH about 6-6,5). FEC is tested over a wider pH range, but there is only one obvious optimum at pH 5,5. The effluent turbidity also has a minimum at a lower pH of about 4,5, but for this experiment the total residual metal value is 3,8 mg/l

because of the high solubility of iron hydroxide at this pH. The zeta potential for FEC coagulated water show about -5 mV for the experiments with pH from 4,5 to 5,5, and it is not possible to explain the differences in turbidity by different zeta potential for the flocs.

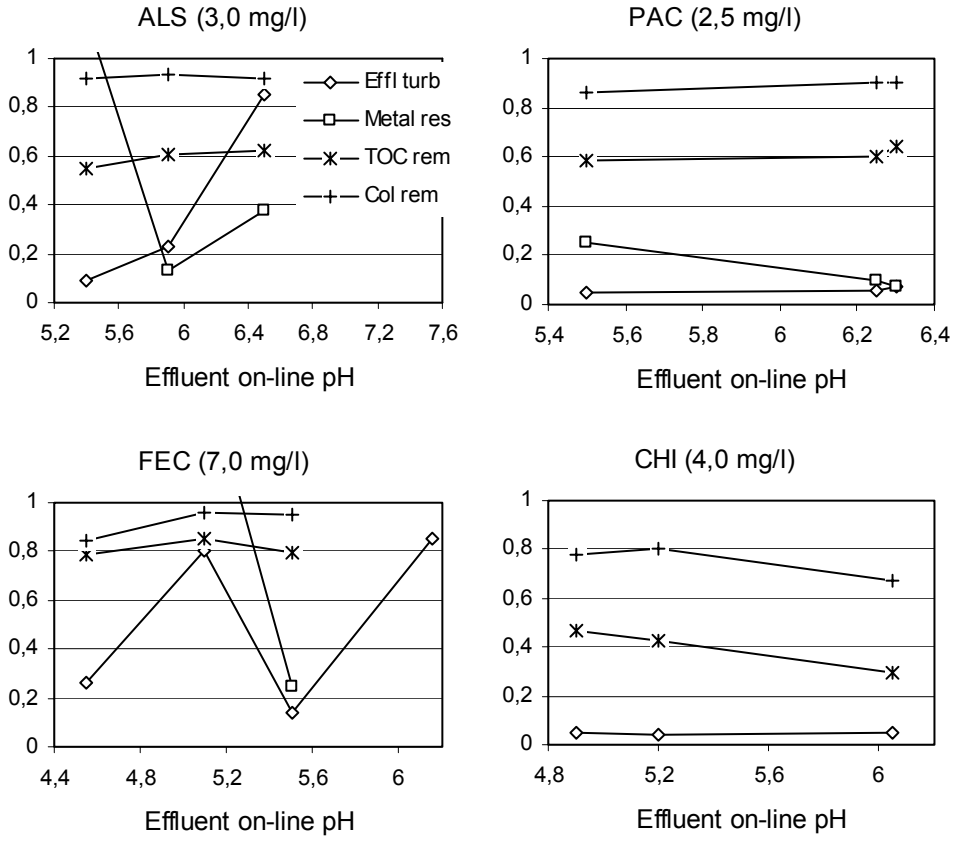

Figure 5.7 Effect of pH on effluent on-line turbidity (NTU), residual metal (mg/l), removed fraction TOC and removed fraction colour for RW50/3.

Effluent water data from CHI coagulation of RW50/3 show excellent turbidity in the pH range from 4,9 to 6,1 (0,05 NTU). To get optimum TOC and colour removal the pH should be in the lower part of this range (40 % TOC and 80 % colour), but at pH about 6 one is still able to remove 30 % of the TOC and 70 % of the colour.

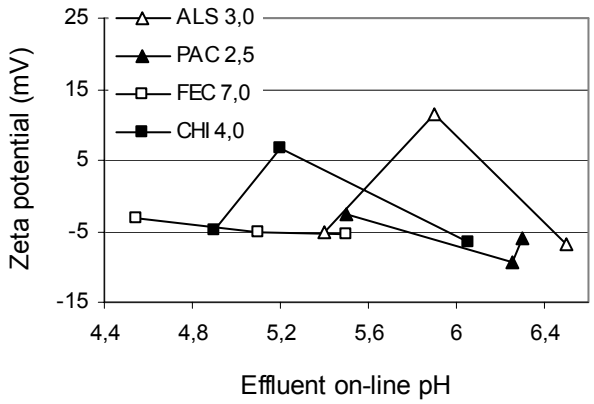

Figure 5.8 Zeta potential of coagulated water for RW50/3.

The TOC removal is best when FEC is used, and for a pH from 4,5 to 5,5 it is about 80 %. ALS and PAC are able to remove 60 % TOC and 90 % colour, while FEC remove more than 95 % of the colour at pH 5 and 5,5. The pH dependency of TOC and colour follow each other in most cases, but it should be noticed that while the colour removal of ALS and FEC are almost the same, the TOC removal is higher for FEC.

5.4.2 Effect of pH on metal residuals

In Norway there is a maximum limit of 0,2 mg Me/l residual metal, which is also the case in the EU and most other countries. As seen from the results presented, metal residuals are often the decisive parameter for coagulation conditions in filtration. The relative high values for residual metal obtained in the experiments, lead to a deeper investigation of metal residuals and metal solubility.

Metal in treated water is a result of soluble metal, and particulate metal that is not filterable at the actual conditions. The soluble metal fractions in RW15 and RW50 coagulated with ALS, PAC and FEC was studied as a function of pH, and the results can be seen in Figure 5.9. The solubility of a metal in water is not only influenced by pH, but also by temperature and the content of organic and inorganic substances.

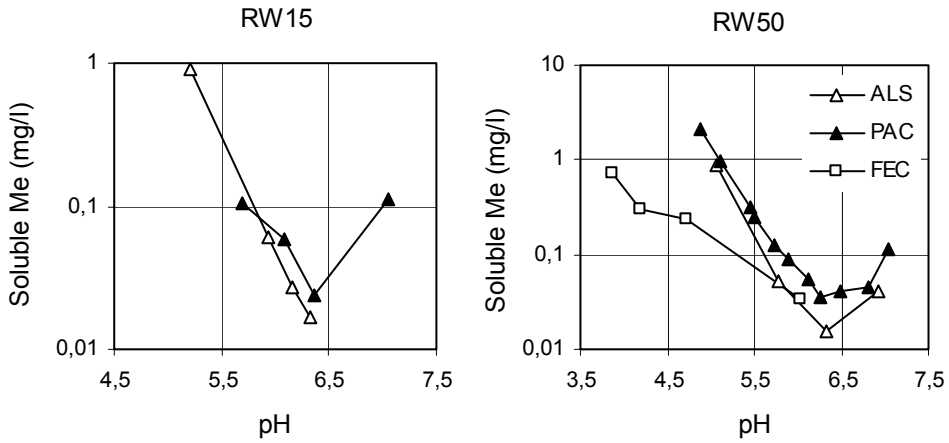

Figure 5.9 Soluble fraction (filtered through 0,2 μm) of aluminium and iron in RW15 (left) and RW50 (right).

The solubility curves in the figure are from filtered samples of coagulated water obtained in the pilot plant. The temperature of the coagulated water was about 10 °C, and the optimum coagulant doses for each raw water and each coagulant were used. Dosages of coagulant always exceeded the solubility limit. Directly after sampling, the water was analysed for pH and filtered through a 0,2 μm membrane filter. The filtered samples were analysed for total aluminium or iron in an ICP-MS as described earlier. Due to relatively easy handling, the 0,2 μm pore size was used to separate soluble from particulate. Experiments performed by Jekel and Heinzmann (1989) showed however that colloidal precipitates could be smaller than this.

The experimental solubility curves show the characteristic minimum in solubility for aluminium hydroxide at a pH of about 6,3. For both raw waters aluminium is more soluble when PAC is used as coagulant. This is probably due to the formation of different soluble aluminium species (polymeric). The solubility of iron hydroxide should theoretically be lower than for aluminium hydroxide, but this is only seen in the very low pH area up to about 5. For a pH of 6 the solubility of iron hydroxide is determined to be 0,034 mg/l by 0,2 μm filtration, about the same as for aluminium hydroxide when ALS is used. The dominant species formed at this low pH (Fe^{3+}, $FeOH^{2+}$, $Fe(OH)_2^{+}$) are positively charged, and able to form complexes with the negatively charged humics. For the aluminium based coagulants it is the same situation but at a higher pH. The forming of soluble complexes with positively charged metal ions and negatively charged humics increase the solubility of the metal. An

excess of coagulant is needed to coagulate the complexes, and achieve low levels of residual metal. Klute (1990) stated that the formation of aluminium complexes with monomeric species happens within microseconds, and for polymeric species within 1 second. Precipitation of aluminium hydroxide is slower, and takes place in the next 1-7 seconds.

The content of organic matter influence the solubility of aluminium (Van Benschoten and Edzwald, 1990b), (Jekel and Heinzmann, 1989). The solubility curves for ALS coagulation of RW15 and RW50 show that aluminium is more soluble in raw water with low content of organic matter on the acid side of minimum solubility (not shown in a separate figure). The TOC content of the two raw waters, about 2,5 and 5,5 mg/l for RW15 and RW50 respectively, show that the colour to TOC ratio is higher for RW50. The experiments have shown that it is possible to remove "all" the colour, but not all the TOC. This non-coloured TOC is more difficult to coagulate than the large humic molecules associated with colour. Higher solubility of aluminium in RW15 is probably due to the fact that the efficiency of coagulation is less for this raw water.

In Figure 5.10 the residual metal concentrations from the coagulation experiments are used together with the curves from the solubility experiments to calculate the fractions of particulate metal in the filtrate. The most obvious observation is that the fractions of particulate metal are very high at low pH, and are in most cases responsible for exceeding the residual metal limit of 0,1 mg/l. The different residual levels for RW15 and RW50 reflect the different levels of dosages used, and the ability of the filter to retain the particles formed. The turbidity for the experiments with aluminium based coagulants show an increasing turbidity with increasing pH in the range tested.

The disagreement between particulate aluminium and turbidity may be due to the performance of turbidity measurements. Turbidity is dependent on particle size, and the maximum contribution is normally from 0,2-0,3 μm particles. Smaller particles than this are able to create turbidity in the effluent, but they are measured as soluble Al (<0,2 μm). Contact filtration does not leave much time for precipitation and floc growth. If the soluble fraction of Al is higher before and in the filter than in the effluent, the soluble Al fractions in Figure 5.10 are too low. This could be the case if the kinetics of precipitation is slow due to cold water. Both Filtralite and anthracite filter media are alkaline, resulting in a pH increase through the filter which might give post-precipitation. The figures show that pH of optimum particulate Al removal is high. When a hydroxide producing metal salt is used for coagulation the residual particulate

metal is a measure of the filterability of the precipitate-humic floc. Optimum filterability of Al flocs seems to be obtained at a pH above 6.

When FEC is used to coagulate RW50 there is a minimum in residual particulate iron for the experiment with effluent pH of 5,64. The pH of minimum solubility is still decreasing with increasing pH beyond 6, but the filterability of the iron-humic precipitates is also decreasing. This increase in particulate iron at pH 6 might also be a result of the increasing hydroxide load to the filter.

The result of these tests show that solubility of the metal is not the main reason for the residual metal problems observed in the Filtralite filter. The main problem is particles > 0,2 µm penetrating the filter bed, and problems related to post-precipitation of hydroxide. Particulate metal has to be removed sufficiently to comply with the residual metal regulations.

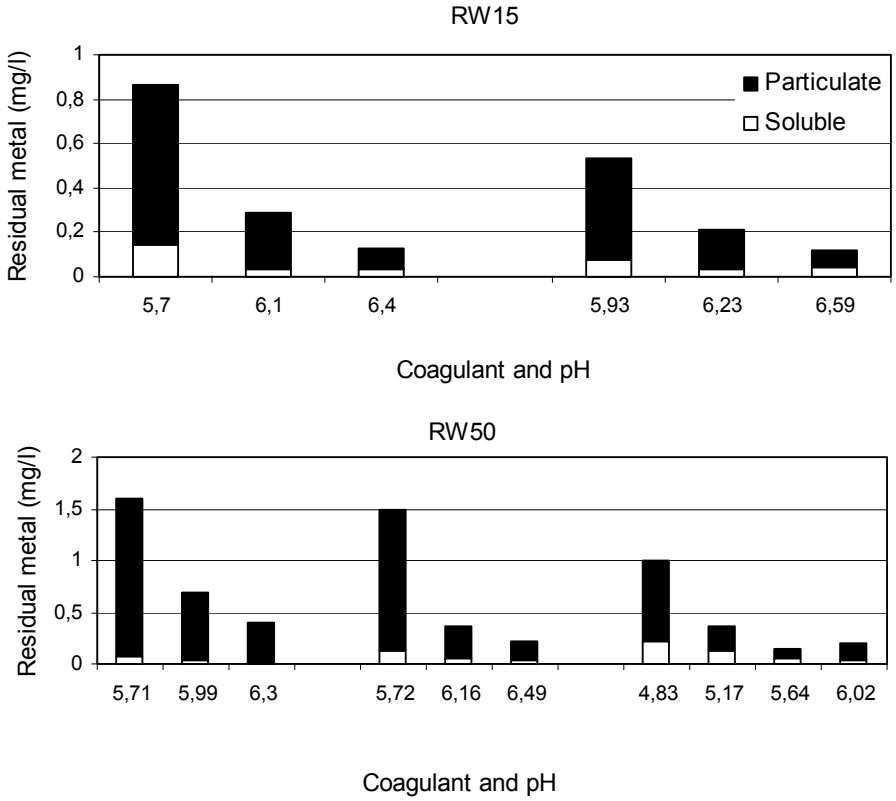

Figure 5.10 Soluble and particulate fractions of residual metal for different pH and coagulants used with RW15 and RW50.

5.4.3 Dose effects

The optimum pH for each coagulant with each raw water was selected, and the effluent water quality was evaluated as a function of the different dosages used at this pH. The effluent pH for comparable doses varies very little from one run to another. pH variations are shown on top of each figure for every coagulant. The parameters chosen to evaluate the results are the same as when pH effect was evaluated, on-line effluent turbidity, residual metal, removed fraction of TOC, removed fraction of true colour and zeta potential of coagulated water. The results are presented in the same way as in the previous section, with each raw water discussed separately.

RW15
Optimum pH for removal in the filter was in the area of 6-6,1 for ALS, 6,2-6,3 for PAC, 5,1-5,2 for FEC and 5,5-5,8 for CHI.

The results show some variations with coagulant dose, but there are generally no big differences. This is probably because the dose ranges for each coagulant are quite narrow. The filtrate turbidity using ALS for coagulation, show the highest value for a dose of 1 mg Al/l. At the same pH the amount of soluble Al is equal for the three doses tested (all doses exceeds the solubility limit at the actual pH). The increasing dose then give increasing aluminium hydroxide formation, which for ALS, has shown to increase the filtrate turbidity due to weak and/or not filterable flocs. Lower effluent turbidity is produced at the highest dose however, but the zeta potential of these flocs show destabilisation, which might indicate better filterability. Increased Al dose as PAC give a lower effluent turbidity, probably because the flocs are bigger and stronger, and more resistant to shear forces in the filter. Aluminium residual increase with increasing dose for this coagulant, and at identical pH the increase must be particulate Al, or for some reason post filter precipitated Al not measured by the on-line turbidimeters.

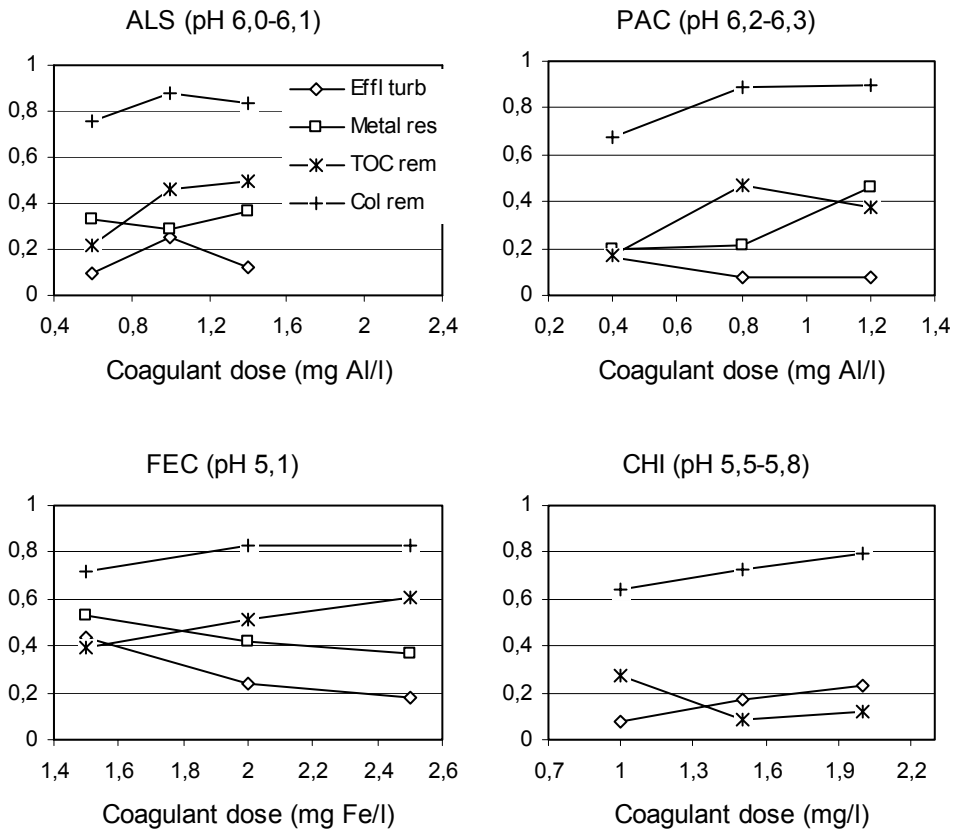

Figure 5.11 Dose effects on filtrate water quality for RW15. On-line effluent turbidity (NTU), residual metal (mg/l), removed fraction of TOC and colour.

The filterability of iron-humic flocs is increasing with dose through the range tested, and the iron residual is decreasing. The relatively high levels of residual iron are due to soluble iron at this low pH. As seen before, the zeta potential of coagulated water when FEC is used is generally negative, but good effluent turbidity can still be obtained. An increasing filtrate turbidity for increased CHI dose may indicate too high doses, and the charge of the flocs support this hypothesis.

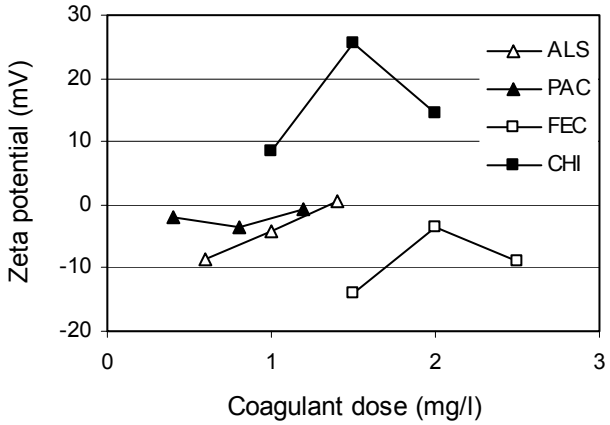

Figure 5.12 Zeta potential of coagulated water as a function of coagulant dose for RW15.

For the metal salts TOC and true colour removal is increasing with increasing doses. For CHI the TOC removal show the opposite trend. Since about 60 % of the CHI is TOC, the low TOC removal could be caused by residual CHI in the filtrate. The true colour removal is not affected by this, and is higher for higher doses. Maximum colour removal seems to be about 90 % for ALS and PAC, and 80 % for FEC and CHI.

RW50

When the raw water contains more colour, higher doses are needed to coagulate the increase of negative charge. Effluent pH for these experiments were between 5,9-6,1 for ALS, 6-6,2 for PAC, 5,2-5,6 for FEC and 5,5-5,7 for CHI.

In Figure 5.14 it can be seen that ALS-flocs created at a low dose have a negative potential, at 3 mg Al/l the flocs have zero charge, and 3,7 mg Al/l restabilise the flocs. Precipitates of Al- and Fe-hydroxide have a zero point of charge at pH 8-8,5 (Tambo and Kamei, 1998), and they are therefore positive in the pH ranges used in this study. For low doses of metal salt, humics adsorb on the positively charged microcrystalline metal hydroxide surface, or they are captured “inside” the hydroxide during precipitation. The excess of humics give the hydroxides a negative charge. An increased dose increases the surface area of precipitates available for adsorbtion by humic substances. For ALS the dose of 3 mg Al/l is sufficient for destabilisation of RW50. A higher dose gives an excess of positive hydroxide leading to restabilisation. Flocculation of the particles in suspension starts when they are neutralised. The aluminium

hydroxide-humic flocs are probably weak and easily broken, which might explain the high effluent turbidity.

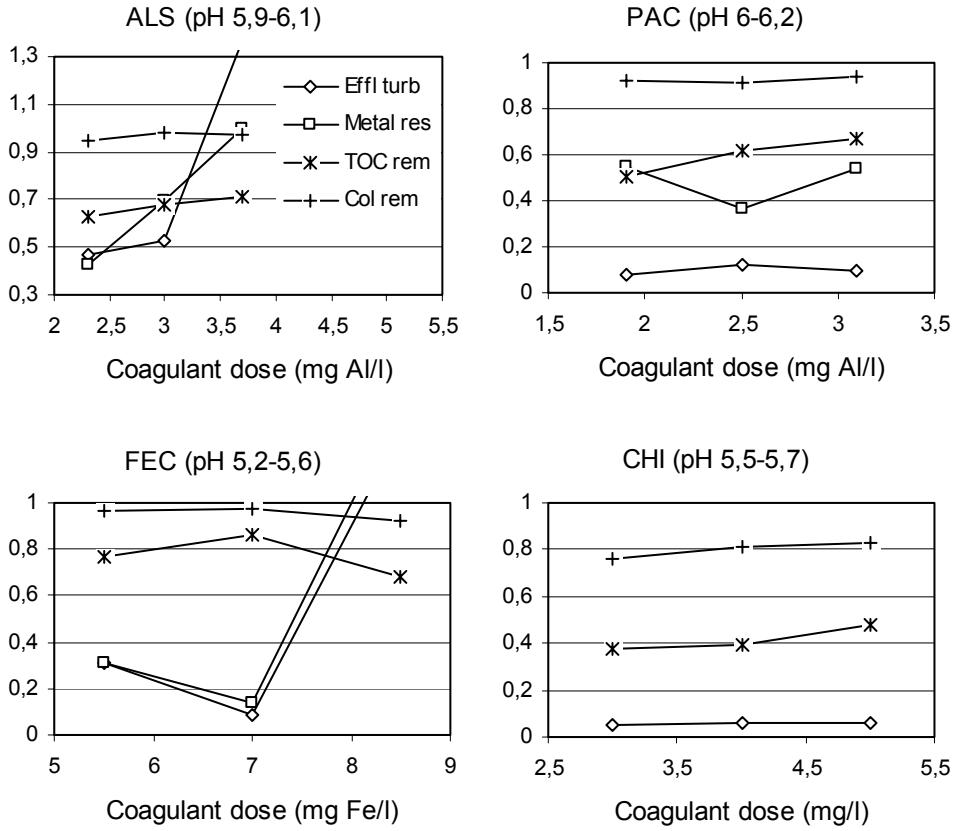

Figure 5.13 Dose effects on filtrate water quality for RW50. On-line efffluent turbidity (NTU), residual metal (mg/l), removed fraction of TOC and true colour.

Aluminium residuals increase with increasing ALS dose, again proving that the flocs (or broken flocs) are difficult to retain in the filter, which is also found by other researchers (Rebhun, 1990). Eikebrokk (1999) found that in a conventional dual media anthracite/sand filter, residual metal content is often higher for low doses than for higher doses. The reason for this can be that the low dose did not exceed the solubility limit, or that the flocs formed at higher doses are more filterable due to their size, strength or charge. This is not seen here with the coarser filter bed when ALS is used because of the weak structure of the flocs. This might also be explained by the more coarse pores of the

Filtralite filter compared to other filter beds for the same application, giving an increased turbidity "leakage".

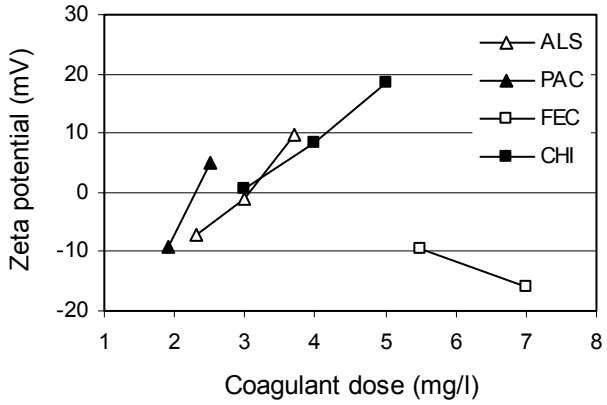

Figure 5.14 Zeta potential of coagulated water as a function of coagulant dose for RW50.

PAC coagulation with this raw water resulted in low effluent turbidity for all three doses tested, but the residual aluminium is not lower than about 0,4 mg/l for a dose of 2,5 mg/l. The pH measured in the effluent water was between 6 and 6,2 for these experiments, indicating soluble Al concentrations below 0,1 mg/l. If pH of coagulation is lower than this and the water experience a pH increase through the filter, precipitation might take place after the filter (and after the on-line turbidity measurement). Due to the short filter run times (terminated by breakthrough) for experiments with RW50 and metal salt coagulation, the time of sampling is crucial to obtain representative results. This might influence some of the results due to samples obtained during the first stages of an early breakthrough.

For FEC the iron residual roughly follow the trend of the effluent turbidity, with acceptable values at a dose of 7 mg Fe/l. From the results for FEC it is obvious that the dramatic increase in turbidity when the dose is increased is a result of iron precipitates penetrating the filter. CHI coagulation shows that polymer-humic flocs are more easily deposited and retained in the filter. The measured zeta potentials for CHI show from 0 to about 20 mV for 3-5 mg/l doses. The high positive charge for the CHI flocs does not influence the effluent turbidity in the same way as for ALS coagulation. CHI produces no hydroxide and therefore less suspended solids are introduced to the filter. From the results it might be interesting to test lower doses of CHI for this raw water.

The very high effluent turbidity at high dose for ALS coagulation does not influence much on removal of TOC and true colour. The excess of aluminium hydroxide in the suspension can explain this. The “slowest” precipitating Al does not contain much humics, and will therefore in the same way as before create turbidity in the effluent, without increasing the effluent TOC. This is not the case for FEC, giving a reduced TOC removal at the highest dose. In this case the increased effluent turbidity, iron hydroxide, carry more TOC and therefore reduce the removal.

RW15/3

The problems of early breakthrough when turbidity was introduced in the raw water have limited the results for this raw water. Even though the filter run times are short, it is still interesting to study the result from a theoretical point of view, especially when knowing that there are tools to extend the run times for instance by the use of a filter aid (polymer). For ALS the pH range of the experiments shown was 6,2-6,4, for FEC 4,8-5 and for CHI 4,6-5.

From Figure 5.15 it can be seen that a dose of 0,5 mg Al/l as ALS is not sufficient to destabilise the turbidity and organic matter for this raw water. The effluent turbidity is considerably reduced at a dosage of 1 mg Al/l, other filtrate water quality parameters was not obtained for this water. An increase in TOC and colour removal is expected for the higher dose. When FEC is used at 1 and 2 mg Fe/l the effluent turbidity is low in both cases, but even higher doses must to be used to obtain low iron residuals. Zeta potential show equal values for 1 and 2 mg Fe/l, and as previous experiments have shown these are also negative.

CHI shows low filtrate turbidity also for this raw water. The lowest filtrate turbidity and the highest TOC and true colour removals are found for the lowest dose of 0,5 mg CHI/l, but the difference in filtrate quality is small between the doses. It should be noticed that CHI is able to remove 50 % TOC from this raw water. Zeta potential measurements for 0,5 mg CHI/l show a negative value, and this is expected because of the amount of negative charge added as bentonite clay. For 1,5 mg CHI/l the zeta potential show a high positive value for the flocs, but the differences in charge does not influence the filtrate water quality. The dose of FEC needed to achieve 50 % TOC removal is 2,0 mg Fe/l, and about 45 % TOC removal is obtained at 1,0 mg Fe/l.

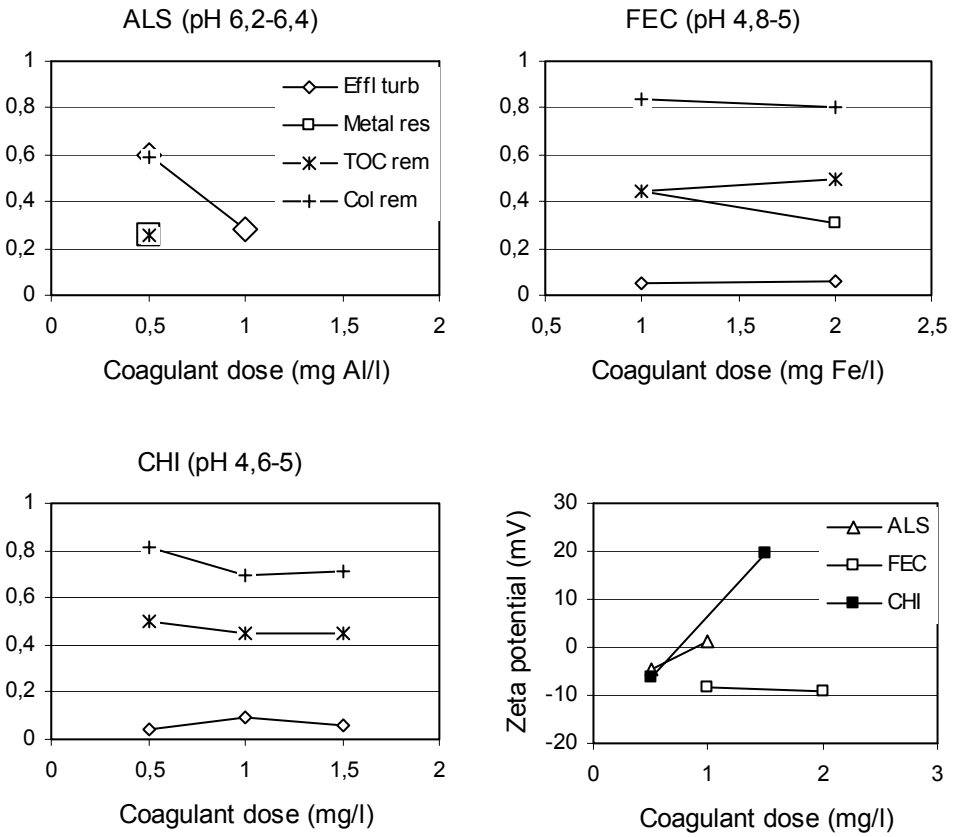

Figure 5.15 Dose effects on filtrate water quality for RW15/3. On-line effluent turbidity (NTU), residual metal (mg/l), removed fraction of TOC true colour. Bottom right: Zeta potential of coagulated water as a function of coagulant dose for RW15/3.

RW50/3

For this raw water with high colour and turbidity it is easier to find the right doses because a too high or too low dose have a significant influence on filtrate water quality. The pH of the experiments presented is 5,8-5,95 for ALS, 6,2-6,25 for PAC, 5,45-5,5 for FEC and 4,6-4,9 for CHI.

The optimum coagulantdose for removal of turbidity and to obtain a low metal residual is 3,0 mg Al/l as ALS. An over- or under-dosing give higher residuals. For this raw water it is actually possible to go below the limit of 0,1 mg Al/l residual metal when ALS is used, with a corresponding effluent turbidity of 0,2 NTU. However, filterable flocs are not created with the raw water turbidity and

NOM at a dosage of 2 mg Al/l as ALS. The high turbidity and metal residual can also be caused by weak flocs that are broken in the filter, and later not deposited.

Using PAC with this raw water one is able to run at a higher pH (closer to minimum solubility of aluminium hydroxide) without increased effluent turbidity. Turbidities below 0,2 NTU is obtained for doses between 1,5 and 3,5 mg Al/l as PAC, and for the two highest doses the turbidity is below 0,1 NTU. The metal residuals are equally low, with a minimum of 0,04 mg/l at 3,5 mg/l dose (0,09 mg/l for a dose of 2,5 mg/l). PAC with its polymeric species is able to create much more filterable flocs than ALS, probably because of increased floc strength. The turbidity in the raw water enhance the turbidity removal at optimum conditions for both ALS and PAC.

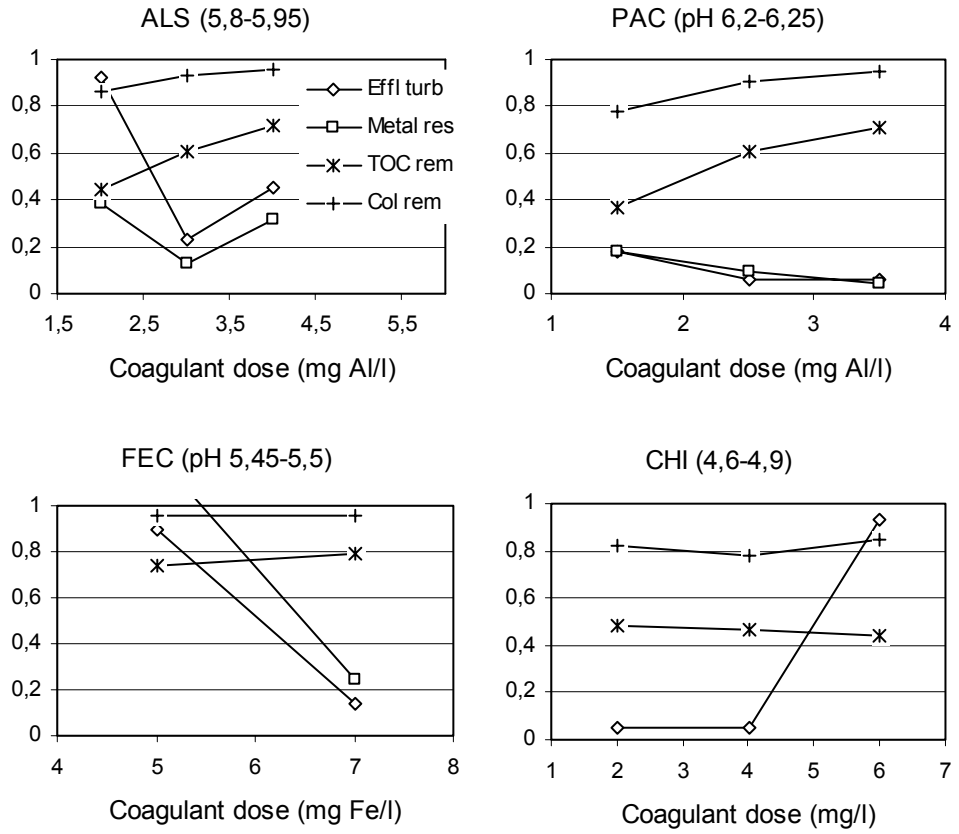

Figure 5.16 Dose effects on filtrate water quality for RW50/3. On-line effluent turbidity (NTU), residual metal (mg/l), removed fraction of TOC true colour.

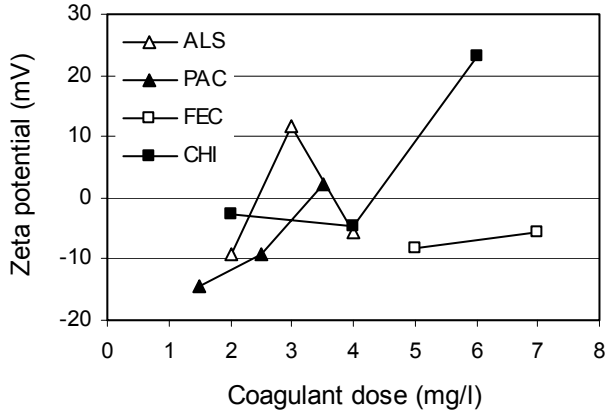

Figure 5.17 Zeta potential of coagulated water as a function of coagulant dose for RW50/3.

A dose of 5,0 mg Fe/l as FEC shows the same symptoms of under-dosing as for ALS coagulation with high effluent turbidity and metal residuals. Increasing the dose to 7,0 mg/l leads to effluent turbidity below 0,2 NTU and residual iron at about 0,2 mg/l. The use of higher doses was not possible because of an early breakthrough. CHI at 2 and 4 mg/l gives excellent effluent turbidity, but at 6 mg/l an overdosing is observed. Overdosing with polymer can occur by adsorption of excess polymer, and the zeta potential for this dose show a relatively high positive value. The TOC removal for 6 mg/l of CHI is about 45 %, and this is just slightly lower than for the lower doses, so there is probably not much residual active polymer in solution.

TOC removal for the aluminium-based coagulants indicates a relatively strong dose dependency. Varying between 40 and 70 % removal for the lowest and highest doses respectively. FEC show a less dose dependent TOC removal for the doses tested, and the true colour removal for this coagulant is about 95 %.

5.4.4 Combined effects of pH and dose

Studying pH and dose dependency one at a time is in many cases not sufficient, and important information can easily be overlooked. In this section some examples of combined pH and dose effects are presented to try to complete the picture of coagulation optimisation for NOM removal by filtration.

Example RW50 with FEC

Experiments with FEC at 5,5 and 7,0 mg Fe/l coagulant dose are presented in Figure 5.18. The most obvious difference between the doses is that the lowest dose has a narrower pH range of effective coagulation. This is in good agreement with results presented earlier (Eikebrokk, 1999) when metal salts are used.

All the effluent water quality parameters show the narrower pH range for the 5,5 mg/l iron dose. Remembering that this is a raw water with about 0,2 NTU and 50 mg Pt./l, the effluent turbidity using 5,5 mg/l iron at pH 6,1 is almost 3. The effluent turbidity at the same pH is 0,14 NTU at 7,0 mg Fe/l. The high turbidity value must come from micro crystalline precipitated iron hydroxide with low filterability, probably with an excess of adsorbed NOM. Increasing the dose to 7,0 mg Fe/l destabilise the system of precipitate and NOM, and the suspension starts to flocculate forming filterable flocs. At low pH the turbidity is low for both doses with optimum conditions at pH about 5,5.

The high effluent turbidity at pH 6,1 for 5,5 mg Fe/l result in a very high metal residual for this experiment. Theoretically the solubility of iron hydroxide should decrease with increasing pH beyond pH 6, indicating that the "excess" residual iron at this pH is particulate. For the lower pH values the solubility of iron controls residual metal, and the residuals are identical for the two doses.

Looking at the results for organic matter removal, the narrower pH range is also observed here. Using a reduced coagulant dose has a stronger influence on the removal of TOC than on the true colour removal at optimum pH. At a pH of 6,1 the true colour removal is only 21 %, while the TOC removal is about 40 % for 5,5 mg Fe/l. This could be due to the high concentration of residual iron (colloidal precipitates smaller than 0,45 μm), which influence the colour measurement.

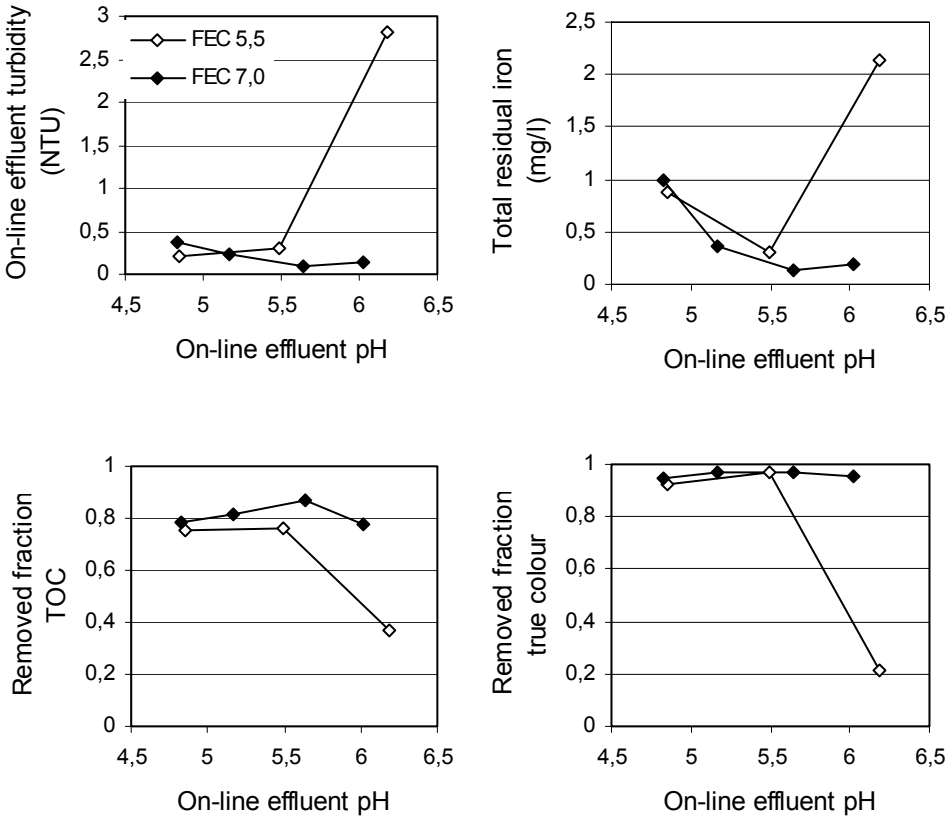

Figure 5.18 Combined pH and dose effects on effluent water quality for RW50 coagulated with 5,5 and 7,0 mg Fe/l as FEC.

Example RW50/3 with CHI

Introduction of turbidity to the raw water increased the performance differences between coagulant doses and its effect on effluent water quality. From the example below it can be seen that it is possible to obtain as good water quality at a reduced CHI dose if pH is reduced. This is possible when using CHI because low pH operation is not limited by residual metal (if raw water metal content is low).

Except for one experiment which probably resulted in overdosing conditions, (high dose and low pH), all the effluent turbidities were below 0,12 NTU for all doses used. This is a result of low suspended solids increase with increase in dose, but it also proves that flocs formed are strong and do not break in the filter pores.

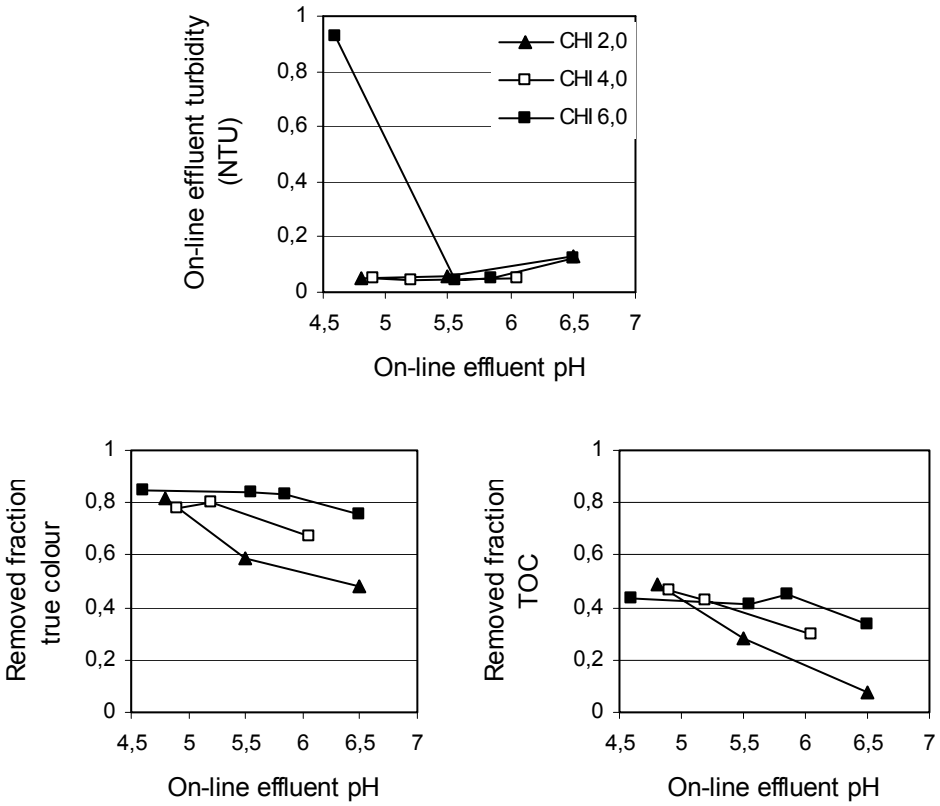

Figure 5.19 Combined pH and dose effects on effluent water quality for RW50/3 coagulated with 2, 4 and 6 mg/l CHI.

At 6 mg/l CHI the true colour removal and TOC removal are more than 80 and 40 % respectively, if pH is between 4,5 and 6. Equal removals can be obtained if pH is below 5,2 for 4 mg/l, and below about 5 for 2 mg/l CHI. The organic matter removal for 2 and 4 mg/l CHI is dramatically reduced at high pH values (10 % TOC removal at pH 6,5). CHI has a charge density, which increases with reduced pH, and this is probably the main reason for the good performance at low pH. As mentioned before CHI contains TOC (about 60 wt %). Thus when a high dose is used the TOC load to the filter is high. Low doses at low pH, i.e. high charge density, are therefore more effective for TOC removal. There is no further increase in TOC removal efficiency for a dose of 6 mg/l when pH is reduced below 6.

The experiment that gave high effluent turbidity did not at the same time give high TOC values. This indicates that the turbidity in the filtrate is bentonite without CHI or just without any CHI containing TOC. The charge density of CHI increases with decreasing pH. Strand (2001) found in her study of chitosan flocculation of bacteria that the amount of adsorbed chitosan on the bacteria was reduced by about 40 % for a pH reduction from 6,5 to 5 when the equilibrium concentration exceeded a few mg/l. The adsorption of highly charged polyelectrolytes onto oppositely charged surfaces is limited by intra- and intermolecular electrostatic repulsion. At low pH the highly charged CHI adsorb to the clay, but further adsorption is restricted by electrostatic repulsion, the amount of CHI on the clay is therefore small. At pH 6.5 lower charge of the CHI reduce the electrostatic barrier and more adsorption on the particles can find place. This might explain why a high effluent turbidity does not reduce the TOC removal for a high CHI dose at low pH.

5.4.5 Raw water organic matter content

Experiments were performed on raw water with two levels of organic matter, RW15 (TOC about 2,5 mg/l) and RW50 (TOC about 5,5 mg/l). As discussed before a fraction of the TOC is not causing colour. This is related to the molecular weight of the humic substances, with the high molecular weight humics responsible for most of the colour. From the raw water characterisation it can be seen that addition of humic concentrate result in a major increase of NOM with MW's between 2 000-20 000, which is a fraction with a major contribution of colour to the water. With a metal salt almost 100 % colour removal can be obtained for RW50, while the maximum TOC removal is about 85 %. The non-coloured TOC fraction is more difficult to coagulate and remove than colour causing TOC, and for RW15 this difficult fraction is higher than for RW50. The experiments presented are the ones considered performed at optimum pH for each raw water.

In Figure 5.20 the TOC removal as a function of specific coagulant dose is compared for the two coloured raw waters.

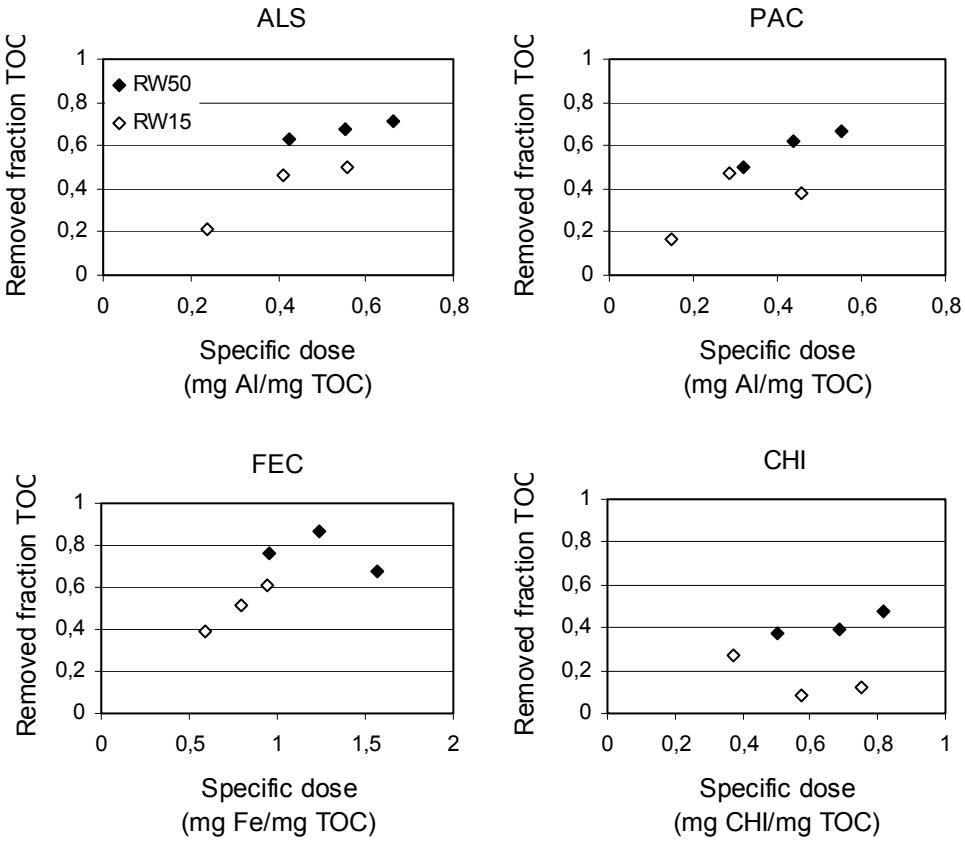

Figure 5.20 Removed fractions of TOC as a function of specific coagulant dose for RW15 and RW50.

The specific dose has generally been lower for RW15 than for RW50, with some overlapping in dose for all the coagulants. TOC removal with ALS coagulation and filtration is more effective for RW50 than for RW15. An increase in removal with dose is seen for both raw waters, which seems to flatten out at about 50 and 70 % for RW15 and RW50 respectively. For the same specific dose of PAC, an equal removal of TOC is obtained. The doses of PAC in mg Al/l used were generally lower than for ALS, because it was observed that filtrate turbidity was lower using PAC. These experiments indicate that TOC removal is dependent of mg/l aluminium added (equal amount of charge), independent of coagulant type. RW15 coagulated with PAC experience an overdosing for the highest dose used.

The results for FEC show that at a specific dose of 1 mg Fe/mg TOC it is possible to remove 60 and 80 % of the TOC in RW15 and RW50 respectively. The decrease in TOC removal for RW50 at the highest dose is probably due to increased effluent turbidity carrying TOC (TOC samples is not filtered). For RW15 coagulated with CHI a dramatic decrease in TOC removal is observed when the dose added exceeds 0,5 mg CHI/mg TOC. A decrease in TOC removal with increasing dose is not seen for RW50. The low TOC removals for RW15 can partly be caused by a somewhat higher effluent turbidity, bringing both raw water TOC and probably TOC from CHI to the effluent.

The TOC removal results presented can to some degree be influenced by a reduced removal of turbidity in the filters, because the TOC samples were not filtered before analysis. True colour is remaining colour after filtration through 0,45 μm membrane filter, and is therefore a measure of how much organic matter that is coagulated regardless of the filterability of the flocs. True colour removal is presented in Figure 5.21 for the same experiments as in Figure 5.20.

ALS and FEC show, as for TOC removal, lower values for true colour removal from RW15 than RW50 at equal specific doses. For PAC maximum removal of true colour is about the same for RW15 and RW50.

Edzwald and co-workers (Edzwald and Van Benschoten, 1990), (Edzwald and Tobiassen, 1999) used specific UV absorbance, SUVA, to see whether a water was high on aquatic humics. SUVA is defined as UV absorbance at 254 nm (m^{-1}) divided by the DOC concentration (mg/l). It can be used as an indicator of the character of the NOM and how effective coagulation of the water is. They found that waters with a high content of humic acids had higher SUVA values than waters with high concentration of fulvic acids. This is due to a higher molecular weight for the humic acids, which is more easily removed by coagulation. SUVA values greater than 4 indicate that the DOC consist mostly of aquatic hydrophobic humics with high molecular weight. DOC controls coagulation, and good removals are expected. Waters with SUVA values between 2 and 4 have a DOC composed of a mixture of humic and non-humic organic matter, which can be both hydrophilic and hydrophobic with a mixture of molecular weights. For this water NOM has influence on coagulation, but DOC removals are lower.

For RW15 and RW50 the SUVA values were found to be 3,7 and 4,9 respectively, indicating that RW50 contains more easy coagulated humics than RW15. This is seen especially when ALS and FEC are used for coagulation, and result in lower removals of true colour for RW15. When PAC and CHI are

used there is almost no difference in true colour removal for the two raw waters. This might have to do with their polymeric properties, involving different coagulation mechanisms.

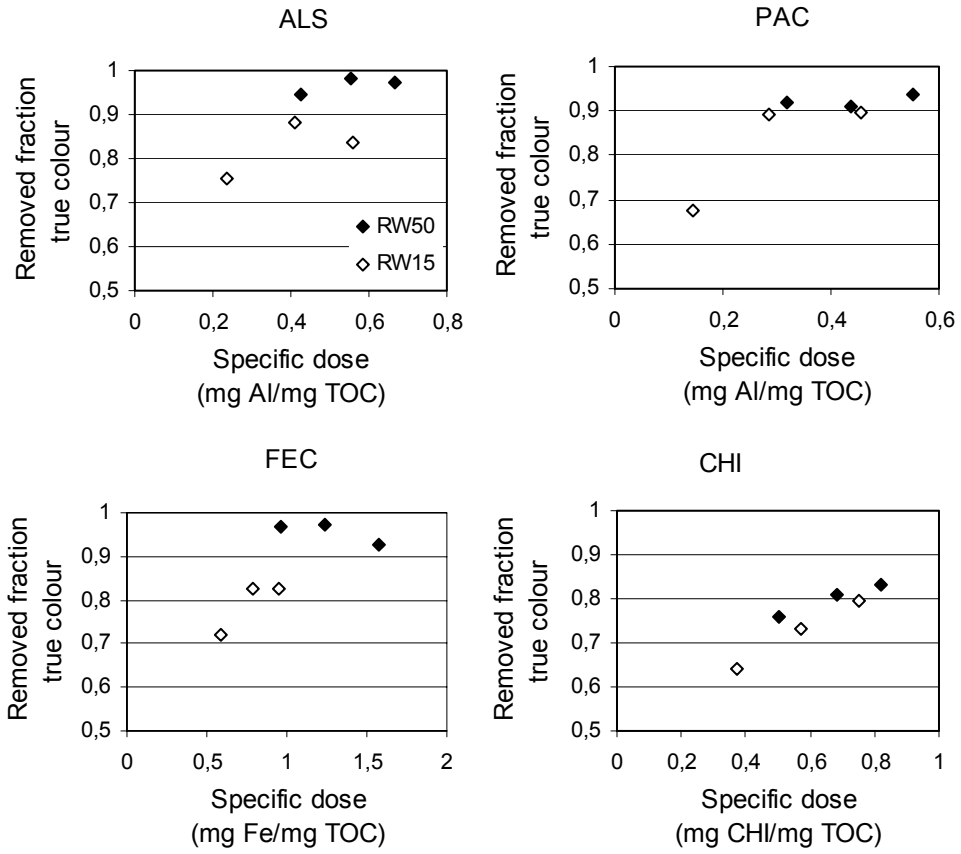

Figure 5.21 Removed fractions of true colour as a function of specific coagulant dose for RW15 and RW50.

5.4.6 Raw water turbidity

Filtration experiments with raw water of two turbidity levels were performed in the pilot filter plant by adding bentonite clay to RW15 and RW50. The purpose of this section is to evaluate the effect of increased turbidity in the raw water on the removal of organic matter. Results for TOC and colour removal from RW15, is presented in Figure 5.22.

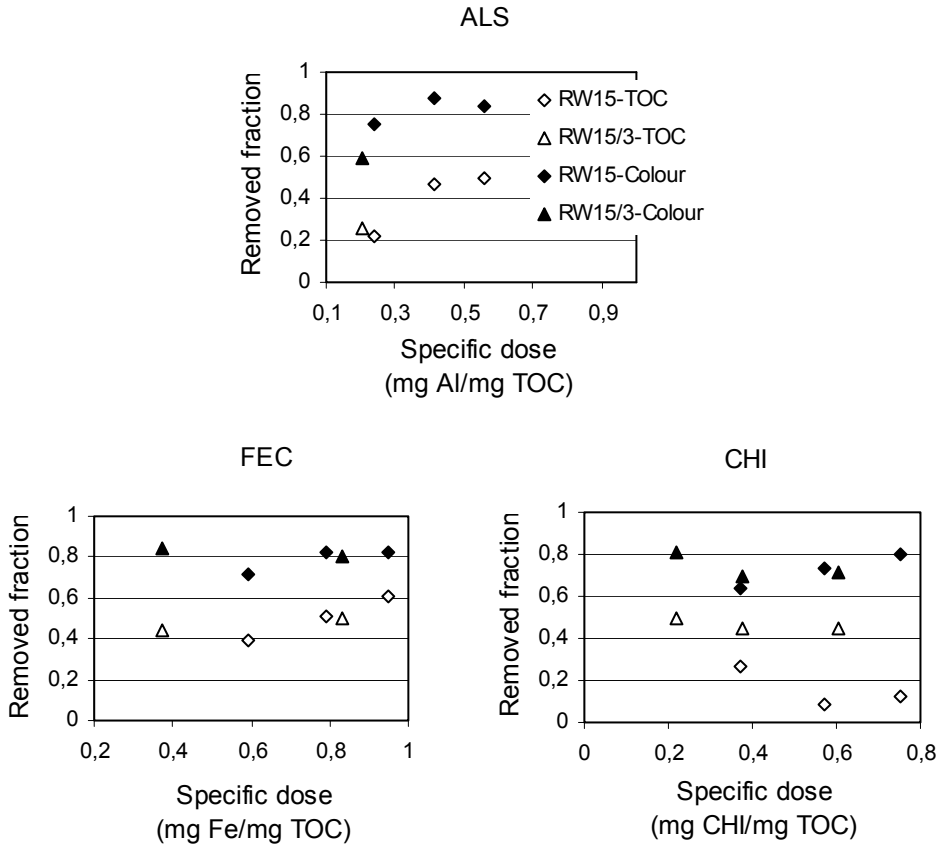

Figure 5.22 Removed fractions of TOC and colour from RW15 and RW15/3.

When the metal salts ALS and FEC are used to coagulate RW15 and RW15/3 (RW15/5 for ALS), removal of TOC and colour is not much influenced by a higher turbidity in the raw water. For FEC it might be that a lower dose is needed to obtain the same removal of both TOC and true colour when there is turbidity in the raw water. This can be a result of adsorption of humics on the clay particles prior to coagulation, or that the clay particles enhance the precipitation of hydroxide giving better NOM removal. RW15 experience a low TOC removal when CHI is used, which is greatly increased for RW15/3. The true colour removal for the same experiments is almost equal for the two raw waters, but also here an indication of better removal at lower dose is seen. It is clear from the results that the increased TOC removal from RW15/3 is not due to an increased removal of colour. The removal of non-colour TOC and/or CHI-TOC must be improved by the addition of clay to the raw water. At a dose of 0,2 mg CHI/mg TOC (0,5 mg CHI/l), a removal of 50 and 80 % of the TOC and

true colour respectively is observed. The relatively low TOC removals for CHI observed for RW15 and RW50 were most likely due to residual TOC from the chitosan. This residual CHI-TOC might associate with raw water turbidity for RW15/3 and RW50/3.

TOC and true colour removal for RW50 and RW50/3 are compared in Figure 5.23. The overall impression is that there are no big differences in organic matter removal when there is turbidity in the raw water for equal specific doses.

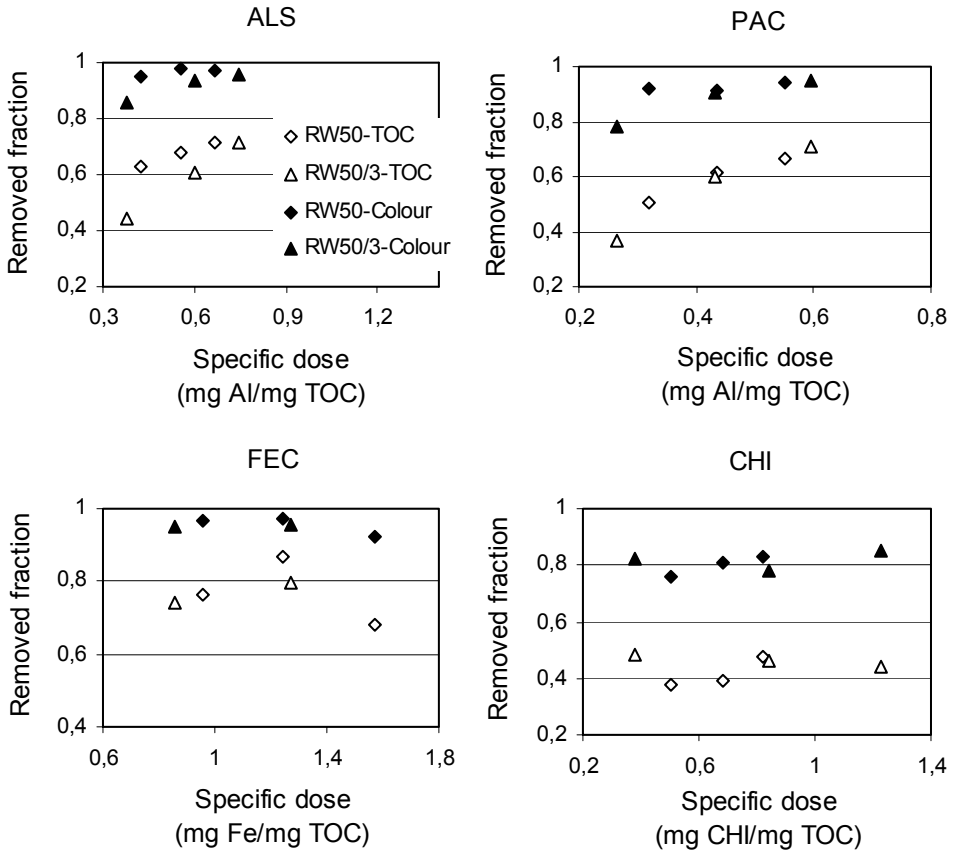

Figure 5.23 Removed fractions of TOC and true colour for RW50 and RW50/3.

Both TOC and true colour removal is marginally decreased at low specific doses of aluminium as ALS for raw water containing clay turbidity. This indicates that the bentonite clay particles use coagulant, which leaves less coagulant available for the removal of organic matter. At the highest specific

doses the removals are almost identical, probably because more filterable flocs (stronger and more dens) are created which allows for higher doses to be used. The results for PAC show an identical removal of TOC and true colour for the two raw waters, except for the lowest dose of about 0,25 mg Al/mg TOC that might deviate from this trend, indicating lower removals for clay containing raw water. From these results and the results comparing removal from raw water with different levels of organic matter, it is observed that coagulation with PAC is less influenced by raw water quality than the other metal-based coagulants.

The experiments run with FEC and RW50/3 show no big deviations from the result with RW50. FEC is very effective in organic matter removal. When comparing the specific doses for FEC with ALS and PAC the molecular weight of Fe must be taken into consideration, which is about twice the weight of Al. Dosing of two times the Fe dose in mg/l as Al gives comparable results (same amount of metal added in moles). CHI coagulation show at least as good removals of TOC and true colour for RW50/3 as for RW50. High removals are seen for low doses with RW50/3 as was the case for RW15/3 compared to RW15. If CHI-TOC is a problem in the effluent it is of course beneficial to reduce the dose to increase TOC removal, and for turbidity containing raw water this is possible. If the improved organics removal is due to increased removal of raw water TOC enhanced by turbidity particles (the simultaneous increase in true colour removal indicate this), it might be a result of adsorption of humics on the positively charged edges of the clay particles. The effects described above are probably coexisting, which is the dominant one depends on the dose added.

5.5 Summary of chapter 5

Optimisation of coagulation conditions were carried out on four different raw waters: RW15, RW50, RW15/3 and RW50/3. Dosages and pH were varied around the expected optimum range for each of the four coagulants: ALS, PAC, FEC and CHI. What is called optimum conditions are that pH and dose that gives the best overall effluent quality, taking removal of both organic matter and turbidity as well as residual metal concentration into account. In Table 5.3 the optimum doses and pH conditions for the four coagulants and raw waters are listed.

Table 5.3 Optimum dose and pH conditions.

Coagulant	ALS		PAC		FEC		CHI	
RW	Dose (mg/l)	pH	Dose (mg/l)	pH	Dose (mg/l)	pH	Dose (mg/l)	pH
RW15	1,0	6,2	0,8	6,2	2,0	5,2	1,0	5,5
RW50	3,0	6,0	2,5	6,2	7,0	5,6	4,0	5,6
RW15/3 (RW15/5 for ALS)	1,0	5,8			2,0	5,0	1,0	4,6
RW50/3	3,0	5,9	2,5	6,3	7,0	5,5	4,0	4,9

The pH conditions presented in Table 5.3 is effluent on-line pH. The pH of coagulation was generally somewhat lower than this.

5.5.1 pH

- As pH increase, the effluent turbidity increase for the aluminium-based coagulants, and the metal residual decrease as pH approach 6,4 (pH of minimum solubility of Al precipitates).
- FEC has generally a lower optimum pH than ALS and PAC, due to the solubility of iron. When FEC is used as coagulant, pH of maximum turbidity removal and minimum metal residuals are in most cases coinciding.
- Removal of organic matter, as TOC and colour, is not as much influenced by pH as effluent turbidity and metal residuals, within the tested pH ranges when a metal salt is used.
- When CHI is used for coagulation, organic matter removal is lower than for the metal salts. However, effluent turbidity is low within the whole pH-range, and there are no metal residuals.
- Non-optimal pH conditions are more critical for raw waters that produce high loads of suspended solids to the filters.
- Optimum pH is not much affected by a higher level of turbidity in the raw water for the metal salts. A reduction in optimum pH is observed when CHI is used for coagulation of RW50/3 compared to RW50.
- Minimum solubility (substance < 0,2 μm) of Al precipitates was found experimentally to be at a pH of about 6,4 for ALS and PAC.
- The levels of Fe solubility when FEC was used were about the same as for Al solubility, indicating a high fraction of particulate Fe with a size less than 0,2 μm (theoretical solubility of Fe is much less than for Al).

In Table 5.4 pH values to obtain Al or Fe solubility less than 0,2 mg/l is shown.

Table 5.4 pH-range to obtain soluble Al or Fe fractions less than 0,2 mg/l. (Predicted values in italic)

RW	**RW15**	**RW50**
Coagulant		
ALS (Aluminium)	5,6-*7,3*	5,4-*7,3*
PAC (Aluminium)	*5,5-7,2*	5,5-*7,2*
FEC (Iron)		4,9-

Some of the values in the table are predicted values due to that all the experimental values obtained were below 0,2 mg/l.

5.5.2 Dose

- For the metal-based coagulants, dose optimisation is a question of increasing the dose to create filterable flocs (which result in low metal residuals), up to the point where the filter is no longer able to remove all the suspended solids produced by coagulant addition (limited by an increase in effluent turbidity).
- Removal of TOC and colour is not as dose dependent as effluent turbidity and residual metal, and organic matter removal is normally not the deciding factor for dose optimisation.
- A lower dose (in mg Al/l) is needed when PAC is used instead of ALS to achieve the same removals.
- CHI shows almost equal results for all doses tested, however, a too high dose used with RW50/3 shows indication of overdosing.
- The level of organic matter in the raw water, and not the turbidity, dictated the optimum coagulant doses used. This demonstrates the high coagulant demand for organic matter, and that the increased raw water turbidity level tested (3 NTU) was moderate.
- Generally lower removals at equal specific doses were observed for RW15 than for RW50.
- An increased turbidity level in the raw water reduced the specific dose needed to achieve the same removals of organic matter, especially when CHI was used as coagulant. The turbidity in the raw water enhanced the removal of residual CHI leaking through the filter.

6 FILTRATION EXPERIMENTS

6.1 Filter run cycles

A typical filter run cycle in terms of filtrate quality consists of an initial ripening period, a water production period with relatively good and constant water quality and a breakthrough period. This is shown in Figure 6.1 together with the linear increase in total head loss with time.

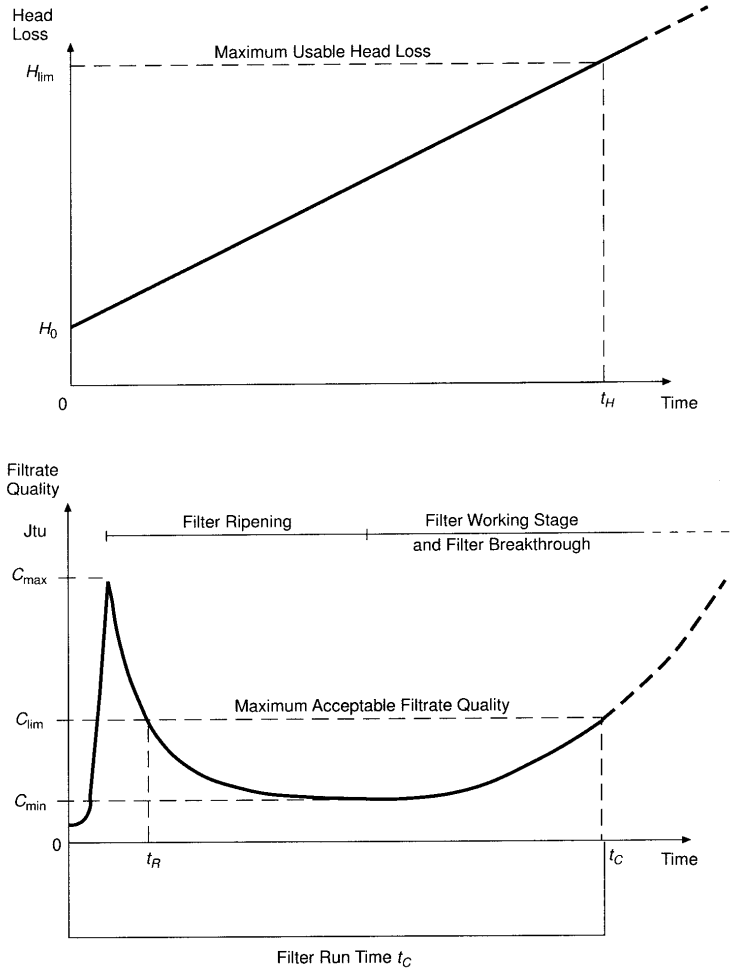

Figure 6.1 Typical patterns of filter total head loss development and effluent water quality. (From McEwan (Ed.),1998).

The first minutes after start up of a filter the water quality will deteriorate, due to remnants from the preceding backwash (Amirtharajah, 1988). The deterioration is probably also caused by raw water impurities, because the filter is clean and have a relatively low filter efficiency. The final stage of the ripening period is characterised by a rapid effluent water quality improvement. The production period often has a slight bathtub-formed quality curve, because at first the filter efficiency normally improves, and later as the deposits clog the filter pores, it deteriorates. In this major period of the run, the water quality is good. Filtration runs are often terminated by a breakthrough when the effluent water quality rapidly deteriorates. The breakthrough is a result of detachment of previously deposited particles and raw water particles not able to deposit.

As deposits clog the filter pores the head loss increase preferably linearly with time (see details at the end of section 2.3.4). If the total available head loss limit is reached the filtration run has to be terminated. Optimisation of filter run times is a question of reaching H_{lim} (total available head loss) and C_{lim} (breakthrough concentration) simultaneously ($t_H = t_C$).

The most common problem in contact filtration of humic waters using a metal salt for coagulation is early breakthrough, caused by weak flocs and probably weak, voluminous deposits. In these cases t_C is reached long before t_H, indicating that the potential storage capacity of the filter is being under-utilised. One way of increasing t_C is to use a filter aid in addition to a metal salt for coagulation, to strengthen the flocs and the adhesion between flocs and filter grains, and to increase filterability.

6.2 Pilot filter run experiments

Experiments were run in the pilot filter plant described earlier with different raw waters and different coagulants. Doses and pH conditions were kept as close as possible to the optimum conditions for each coagulant found earlier.

Some experiments were performed with a modified experimental set-up. It was observed that the addition of polymer as filter aid had little or no effect when it was added just after coagulant addition. Because of this water was lead to an empty column of about 40 cm inner diameter and 1,2 m length after coagulant addition for the experiments using polymer. The detention time (reaction time) in the column was about 4 minutes, and the relatively large inner diameter did not give much flocculation. After this column the filter aid was added just prior to the filter columns. The non-ionic synthetic polymer Magnafloc LT 20 was used as filter aid.

F/F is the Filtralite filter and A/S is the reference anthracite/sand filter (see Figure 4.2). Results for filter runs with the deeper F/F filter bed (F/F+) are also presented. The A/S filter was operated in parallel during most of these runs, but no modifications of the filter bed were done for this filter.

6.2.1 Evaluation of results

The experiments in the pilot plant were evaluated on the basis of water quality as well as a number of operational parameters. The water quality parameters are mentioned earlier, and below follow a discussion of the other evaluation parameters used in this study.

Filter run time
Filter run time is the period of time that the filters produce good quality water. A filter run is terminated either by breakthrough, which in this study is limited by on-line filtrate turbidity values above 0,3 NTU, or by the limiting head loss of 1,8 m. By setting a limit on effluent water quality, a slow ripening (with turbidity higher than 0,3 NTU) of the filter also influence the filter run time. Since turbidity was measured on-line from both filters in all the experiments it is a good water quality evaluation parameter for comparison of results.

Solids storage capacity
Since the filter run time gives no information regarding how much deposits that the filter is able to store in each case, it is necessary to also consider solids storage capacity. In cases of breakthrough termination of the filter run, this parameter tells how much suspended solids (or any other water quality parameter) that can be stored within the filter bed for that particular raw water and pre-treatment. SS (mg/l, filtered through 0,45 μm) in coagulated water was used as the influent water solids content, and by assuming that a water with turbidity below 0,3 NTU did not give any SS in the effluent, the solids storage capacity could be calculated. This is a useful measure of the filterability of flocs and strength of deposits.

Head loss
Head loss is a consequence of deposited particles in the filter pores, decreasing the pore volume available for water flow. It was measured continuously during each filter run and for each filter. By comparing head loss results one is able to get more insight into how each pre-treatment and operational parameter influences the filtration process. The total head loss development with time in the filter is described by Equation (2.39). The k value, which is a constant for

each case, is describing how much head loss (cm) that is created by one gram of solids (g/m^2 filter surface area) entering the filter. Comparing k values between filters or between different pre-treatments for one filter gives information on the distribution of deposits within the bed and how deposits are situated in the filter pores. High k values indicate more blocking of pores for the same amount of solids, or solids can be stored in sections of the bed where they cause a relatively high head loss.

Head loss gradient distribution
Pressure was also recorded continuously at different positions in the filter bed, and each filter column was equipped with a total of 10 pressure transducers. The head loss curves produced from the pressure measurements express the distribution in depth of filter deposits. It can be used to find which parts of the filter bed that is effective in filtration. (See also section 2.3.4).

In the following discussion the distribution of head loss in the filter bed is expressed as cm (cm water column) head loss per cm filter bed depth (head loss gradient). The values are shown for each layer between the pressure transducers, and represent only the increase in head loss caused by deposits. For each layer in the bed the slopes of the Michau-curves (see Figure 2.11), subtracted the initial values at time zero represent the head loss gradient. By doing this only the increase in head loss as a result of deposits are shown. For filter F/F and F/F+ the head loss build up is generally small, and in order to obtain more accurate values it was necessary to use longer filter depth intervals between the readings for some of the experiments. In some figures the gradients have a small negative value, this is because of inaccuracy in the calibration of the pressure transducers, and these values are not shown.

6.3 Results and discussion

In this part of the thesis results for all three filters are compared (F/F: Filtralite, A/S: anthracite/sand and F/F+: deeper Filtralite). The different grain sizes and filter bed depths used for the experiments is a good basis for understanding of different filtration effects. To try to separate some effects and making this thesis easier to read, each raw water is discussed separately. In later sections some parameters are looked at more closely.

6.3.1 Filter bed properties

The filter beds used in this study are presented in section 4.1.1. Most of the filter runs are carried out in parallel with the Filtralite and the anthracite/sand filters. The effect of grain size on filter performance can then be studied by

comparing results from F/F and A/S. The deep Filtralite filter bed, F/F+, was also run in parallel with the anthracite/sand filter, and valuable information on filter bed depth effects is obtained.

RW15

Relatively long filter runs were achieved with this low colour and low turbidity raw water. Breakthrough (BT) or head loss (HL) limitations terminated the filter runs. For the filter runs terminated by BT the maximum storage capacity is obtained for that particular case. HL limitations means that the filter still can store more deposits from the water, but to take advantage of that one has to increase the available head. The results presented in Figure 6.2 are from experiments carried out at a filtration rate of 12,5 m/h.

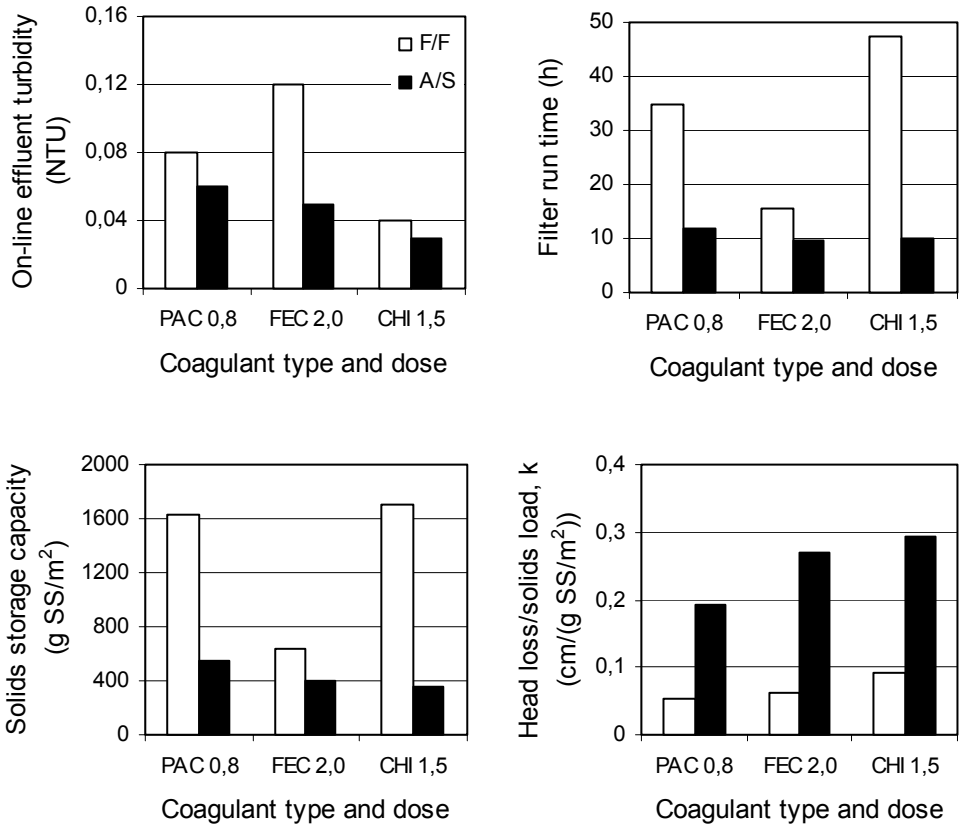

Figure 6.2 Comparison of results obtained in F/F and A/S for RW15 at 12,5 m/h filtration rate. On-line effluent turbidity (NTU), filter run time (h), solids storage capacity (g SS/m^2) and head loss per solids load (cm/(g SS/m^2) when PAC, FEC or CHI are used for coagulation.

Effluent turbidity for the different coagulants show better results for A/S than F/F, because of the smaller grain sizes in filter A/S. The difference is small however for PAC and CHI. PAC and CHI are polymeric coagulants and they produce stronger flocs and deposits than the traditional metal salts, which are not that easily broken in the filter pores. The flocs formed from FEC coagulation are more sensitive to the difference in grain size.

All the runs in Figure 6.2 for the anthracite/sand filter are limited by HL. This means that the storage capacity is not fully utilised for this filter at that specific filtration rate and for the specific conditions tested. CHI used in F/F give the longest filter run of about 47 hours, and PAC also show good results in this filter. The solids load to the filters is dependent of the coagulant used, and by looking at filtration run times compared to storage capacities for CHI and PAC in F/F it is obvious that the suspended solids load from PAC is higher than from CHI. This means that the F/F filter is able to store more solids from PAC coagulated water than CHI in the same period of time. Looking at the head loss build up per gram of solids introduced to the filter (k), it is clear that A/S has a much greater k value than F/F (more head loss per gram of solids). Further more, when this raw water is coagulated with PAC the solids are stored in a way that create little head loss compared to FEC and CHI, where CHI uses the most head loss to store 1 g of solids.

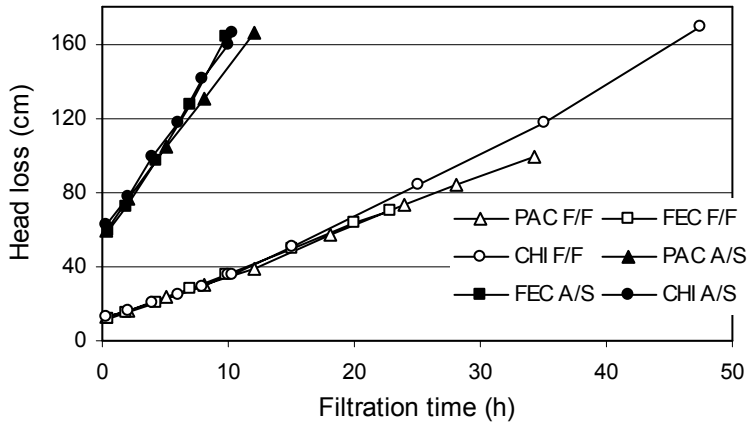

Figure 6.3 Total head loss for F/F and A/S treating RW15.

The total head loss results in Figure 6.3 show that there are huge differences in head loss development between F/F and A/S, but almost no differences between the coagulants. The latter being a result of the difference in head loss per solids loaded. The lower head loss at the end for PAC could be due to a more even

deposition in the depth of the filter, and that CHI show some surface deposition by a upward curving head loss profile.

As the filtration run proceeds in the coarse F/F filter, deposits clog the filter pores more and more, and the shear forces from the water increase. For these relatively long filter runs the filter grains are covered with deposits. In the experiments that are limited by HL, the strength of the deposits "survives" the increasing shear forces. A/S has a very rapid head loss development, but because of the small filter grain size the potential for capture and retention is higher. F/F only experience HL limitations when CHI is used as coagulant, which form strong flocs and create much head loss.

It must be remembered when analysing the results above that the water entering the filters is relatively low in suspended solids, and that the mechanisms controlling the filtration run could be specific for this type of water.

In Figure 6.4 head loss gradient distribution for the two filters are presented. This is head loss after 10 hours of filtration for both filters giving rise to significant differences in values and distribution of head loss in the filter bed.

When analysing Figure 6.4, one has to consider the initial porosity of the different filter media. Even when H_0 is deducted as in the figure presented, the rate of head loss increase to solids deposited in the bed is not equal for the different medias. In other words, 1 mg of suspended solids deposited in the top layer create a lower increase in head loss than 1 mg deposited in the bottom layer of the filter. The head loss distribution in dual media filters is not directly a measure of specific deposits, and therefore this data has to be evaluated with that in mind.

The head loss per cm bed in the top layer of filter A/S is more than 10 times higher than in the top layer of F/F. The main reason for the big difference in head loss cannot be explained from the different initial porosities in the filter media, but rather a much higher deposition of flocs in this layer in A/S. All the coagulants show the same pattern in the A/S filter, with a rapid decrease in efficiency (head loss increase) for the deeper layers. Ending up with almost no deposition in the lowest layer of the anthracite. Assuming that the grain size (porosity) is equal from top to bottom of the anthracite (minor stratification within each layer will occur), the increase in head loss per mg suspended matter deposited should be the same. (This is also the case for the sand layer, and the two different Filtralite layers separately).

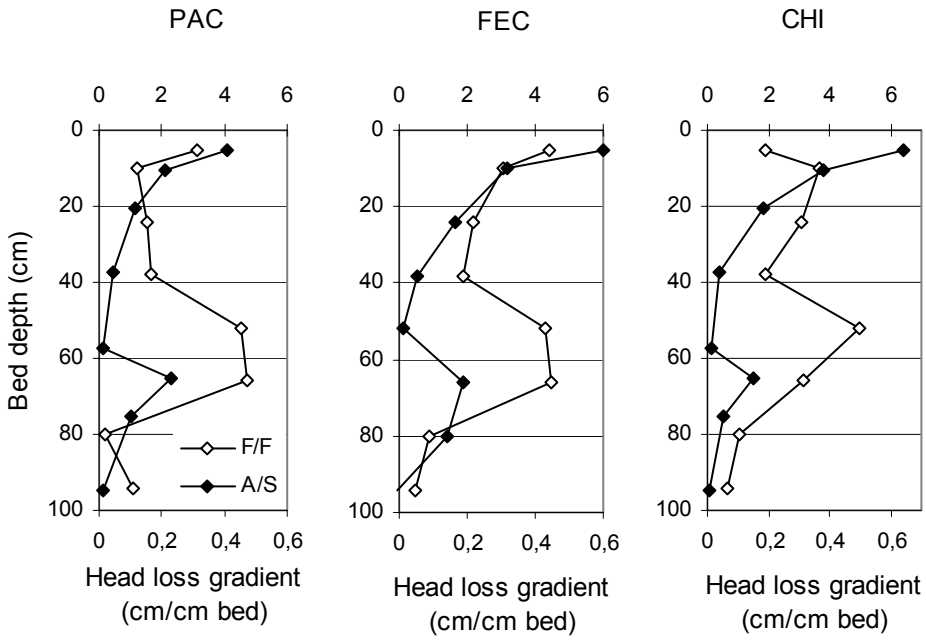

Figure 6.4 Head loss gradient distribution for the filtration runs with PAC, FEC and CHI at 12,5 m/h and RW15 for F/F and A/S after 10 hours operation. F/F use bottom axis and A/S use top axis.

The results show that almost no deposition takes place in the bottom section of the anthracite, and the depth of this layer could probably have been reduced. As the concentration of suspended solids in the water decrease when moving down the filter, the solids load to the sand layer is much reduced compared to the anthracite layer. Lower head loss increases in the top sand section than in the first section of anthracite indicate much lower deposition in the sand. Also for the sand there is a rapid decrease in filter efficiency for deeper sections, and a close to zero head loss increase is observed in the bottom of the sand.

In the coarse F/F filter the general impression is that deposits is much more evenly distributed in the depth of the filter bed. Knowing that in most of these experiments the two filters performed almost identical with regards to water quality, the amount of deposited solids must be about the same in F/F and A/S, with a much lower head loss increase in F/F.

The top layer of F/F is coarse and therefore a large part of the flocs penetrate this layer and proceeds into the bottom layer. In the top of the bottom layer in F/F, more head loss builds up than in the top of the upper layer. This indicates

that the amount of solids deposition for the first centimetres of a new layer is more equal in F/F than in A/S. The bottom layer in F/F has the same grain sizes as the top layer of A/S, the much lower head loss gradient is due to a lower particle load to this layer in F/F. The head loss gradient in the bottom layer of F/F is almost the same for the first two measurement points (at 52 and 66 cm filter depth). This could be because the top layer is 47 cm deep and the reading between 38 and 52 cm is influenced by the lower efficiency of the top layer.

Between the coagulants tested, PAC seems to be the one that is most suitable for A/S. The flocs created is less efficiently removed in the anthracite than the other two coagulants, but more efficiently removed in the top sand layer. If the difference in removal in a layer is primarily related to the size of the flocs created (probably a combination of size, strength and charge) then CHI produce the largest flocs, followed by FEC and PAC. The same trend for the different coagulants is seen in the top layer of F/F (except for the first depth interval with CHI).

RW50

With RW50 full filter runs were performed in F/F, A/S and F/F+ (deep). The results from these experiments will tell something about what happens inside the filter when the solids load increase.

The results in Figure 6.5 show that filter grain size and depth are more important for coagulated filter inlet water with higher content of suspended matter. Turbidity is much lower from A/S than from F/F for the metal salts, especially when ALS is used. F/F+ is able to remove turbidity down to 0,25 NTU when ALS is used, which is about half of the value for F/F. Filtration of ALS-flocs is much more influenced by filter grain size than flocs created with the other coagulants. The reason for this might be that the filter pores in A/S provide the flocculation that is needed when ALS is used. The shear in the filter pores is at all times higher in A/S than in F/F. A/S provides high G values but shorter detention time in the filter. This probably results in small and stronger flocs (than what can be created in F/F), which are properly removed by the small grain sizes. In F/F the pore system provide low G values for a little longer detention time than A/S. Flocs who experience this treatment will be large and fragile, and probably broken further down in the filter bed, where they experience more shear force.

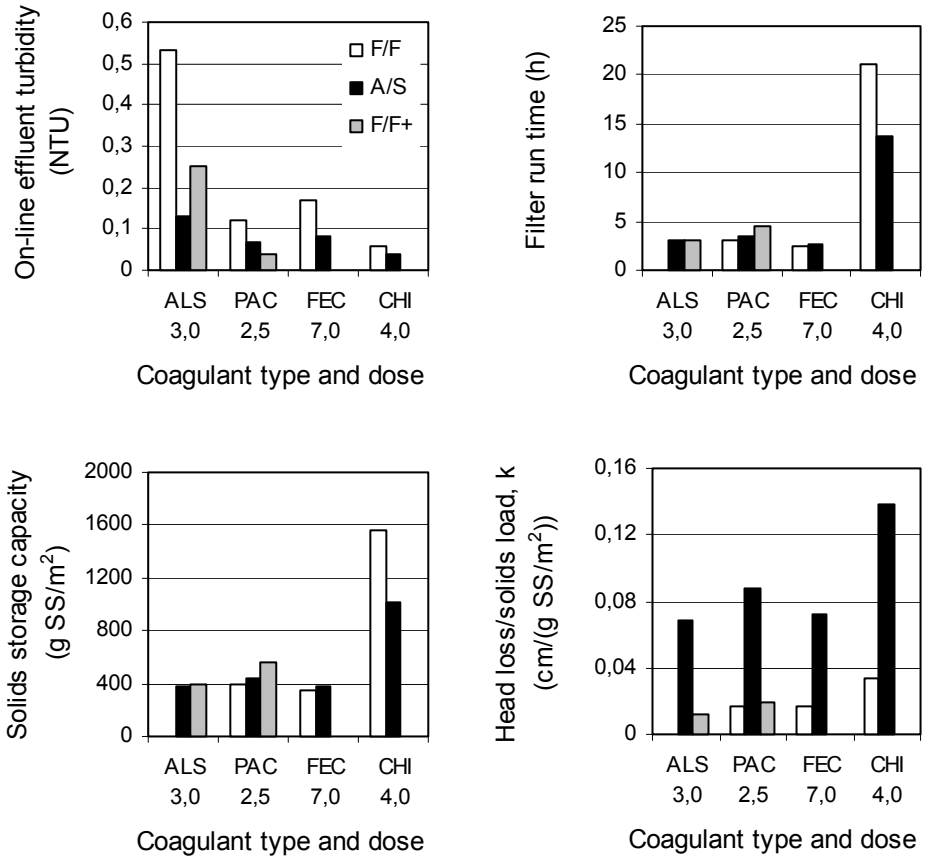

Figure 6.5 Comparison of results obtained in F/F, A/S and F/F+ for RW50 at 7,5 m/h filtration rate. On-line effluent turbidity (NTU), filter run time (h), solids storage capacity (g SS/m^2) and head loss per solids load (cm/(g SS/m^2) when ALS, PAC, FEC or CHI are used for coagulation.

PAC and CHI coagulation provides almost as low turbidity from F/F as from A/S, and these coagulants give the longest filter run times and storage capacities. This indicate that good filterability of flocs correspond with an efficient deposition, due to the stronger flocs formed. The solids load to the filters is also lower when PAC and CHI are used compared to ALS and FEC. It is also seen that even though the effluent turbidity is higher for F/F when PAC and FEC are used, the run lengths for F/F and A/S, which both are limited by BT, are equal. For CHI the experiment for A/S is terminated by HL, and therefore the run time is shorter for A/S. The observation of this almost simultaneous BT for F/F and A/S which are very different filter beds might lead to the conclusion that BT is a process that propagates down the filter layer by

layer from the top. When this "saturation" reaches the bottom layer of the filter there is a breakthrough (see Figure 2.10). Therefore, the depth of a filter has significant influence on the filter run lengths. The run lengths for F/F+ are longer than for F/F and A/S, because the bed is deeper and more storage capacity is available.

Head loss increase is much higher for filter A/S than F/F and F/F+, and between the coagulants CHI create most head loss per solids entering the filter. The filter runs with highest head loss increase is the ones with lowest effluent turbidity for each filter. It is beneficial for the floc removal and the storage capacity of filter F/F to have a high k value (head loss/solids load). This is because the efficiency of this coarse filter is low at the beginning of a filter run, and a high k value indicates rapid efficiency improvement for this filter.

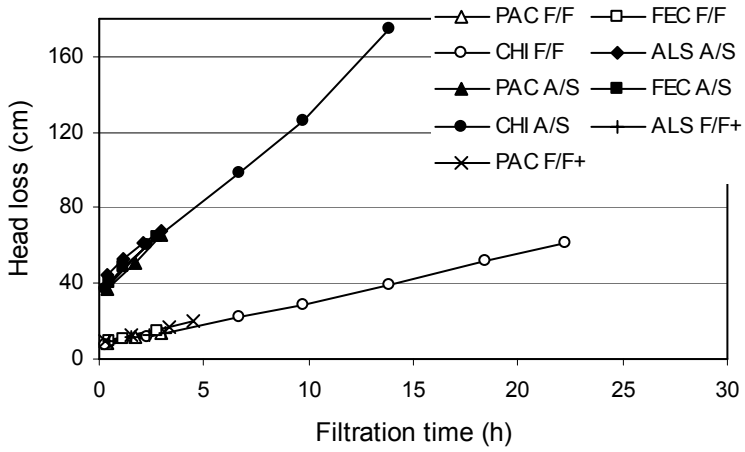

Figure 6.6 Total head loss as a function of filter run time for the experiments with RW50.

The total head loss development with filtration run time is almost identical for all runs in F/F and F/F+, and for all runs in A/S. There are small differences in H_0 for some of the runs in A/S, but no significant differences are seen. The head loss difference from F/F to the deeper F/F+ is small. When PAC is used F/F+ produce lower effluent turbidity than A/S at a considerably lower head loss.

The head loss gradient distributions for these experiments are collected at different filtration run times for the different filters, but at equal run times for each coagulant. This is done because of the big differences in run time and the fact that longer filter runs, with more head loss build up, produce more accurate results.

Results for the deep Filtralite filter, F/F+, are obtained with ALS and PAC as coagulants, and the bed depth axis is adjusted because of this.

The head loss gradient values are in the order of 10 times as high for the anthracite/sand filter as for the two Filtralite filters independent of coagulant type and filter run length. In the A/S filter the pattern of high head losses in the upper part of the two filter media types with a rapid decline in the following layers is seen. The maximum value for the anthracite layer is higher than for sand. This indicates a much higher deposition in the anthracite than in the sand. When ALS is used the decrease in head loss gradient for lower sections of the filter, is especially rapid. The deposition efficiency is very high in the first centimetres of the bed, which might be due to large flocs or rapid precipitation of hydroxide on filter grain surfaces.

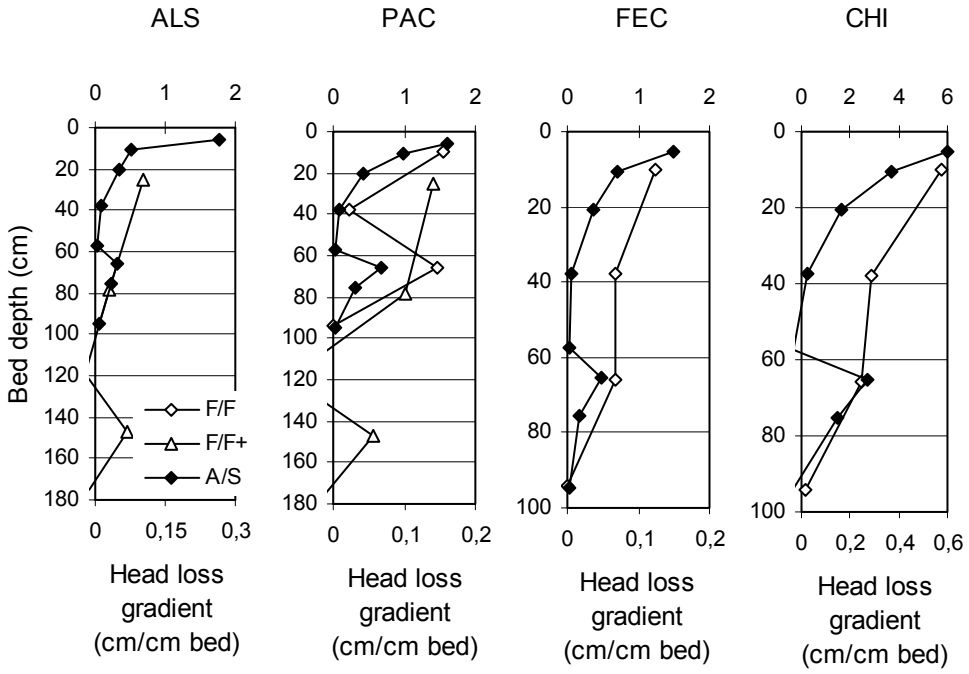

Figure 6.7 Head loss gradient distribution for runs with RW50 in cm head loss/cm bed depth for each layer. After 3 hours of filtration with ALS and PAC, 2,6 hours with FEC and 10 hours with CHI. F/F and F/F+ use bottom axis, A/S use top axis.

Since filter F/F is less effective in the upper layer compared to A/S, the head loss is more evenly distributed, because more suspended solids reach deeper down in the bed. PAC coagulated water gives a high head loss gradient in the top section of the two Filtralite layers and low in the following layers, while FEC and CHI distribute deposits more evenly. However, the head loss in the bottom section of F/F is close to zero in all the runs shown. F/F+ produce less head loss as a function of deposited matter in the filter compared to F/F, due to less blocking of pores when solids are allowed to penetrate deeper down in the filter bed.

RW15/3

This raw water with higher turbidity and low colour is generally easy to coagulate and more filterable flocs are formed. Ebie and Amano (1993) found that the amount of deposits that could be stored in the filter in a direct sand filtration process, was much higher for raw water containing clay turbidity (kaolin) with or without humics than for raw water with only humics.

For this raw water the effluent turbidity is below 0,15 NTU for all the experiments. It is clear that the clay particles enhance the removal of flocs in all the three filters, which probably is caused by an increased density of flocs that are more easily removed by sedimentation on filter grain surfaces. The removal efficiency of these flocs is therefore not as much influenced by the grain size in the filter bed as humic flocs are. The removal of turbidity is almost as good in F/F as in A/S when ALS is used and better with PAC as coagulant.

The deep F/F+ filter proves that it is possible to compensate for larger grain size by increasing the depth. This filter produce lower effluent turbidity than both F/F and A/S when the raw water contains turbidity, and as seen in Figure 6.8 filter runs are longer. The length of filter runs with ALS or PAC coagulated water in F/F and A/S were very short. This was surprising because other researchers have reported longer runs and higher storage capacities when filtering mineral particles compared to humic substances (Ebie and Amano, 1993), (Rebhun et al., 1984). Why filter runs were short in F/F and A/S for this raw water might have to do with the strength of the deposits. If breakthrough is a result of deposits breaking off when exposed to increasing shear forces in the pores, introducing turbidity to the raw water does not seem alter the strength. (Smaller head loss gradients at breakthrough than for RW50, see Figure 6.10). Breakthrough can also be a result of less deposition due to higher pore velocities when pores are narrow from solids deposition. This raw water does also have some organic matter in it that probably weakens the flocs formed.

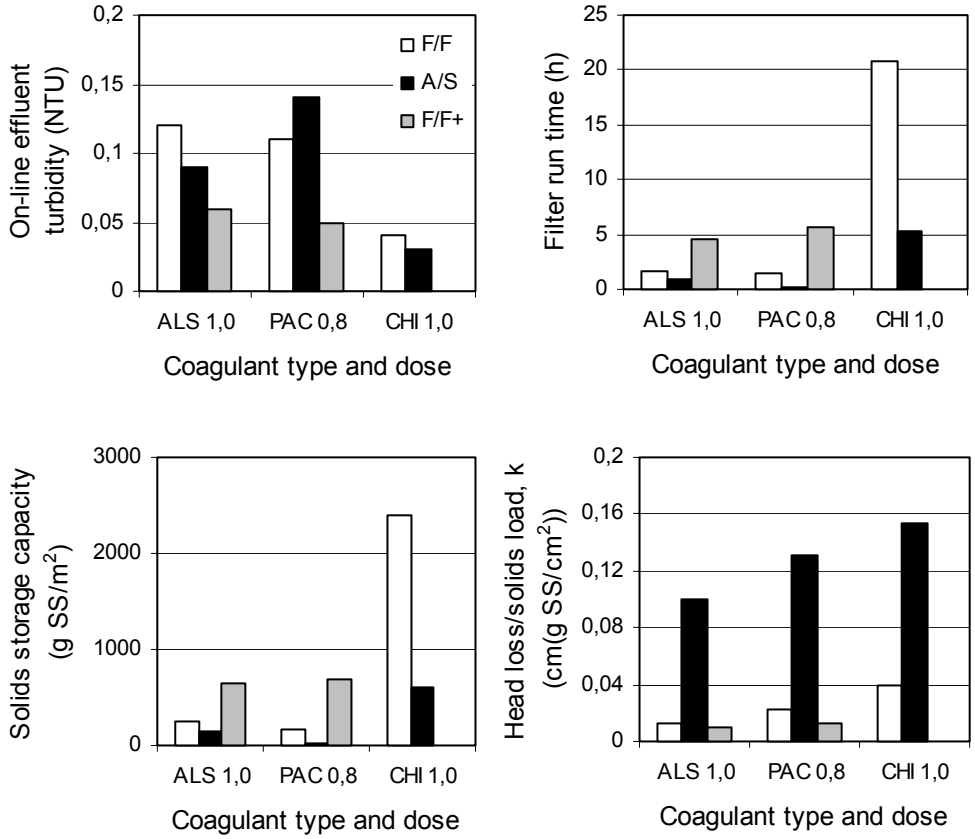

Figure 6.8 Comparison of results for filter F/F, A/S and F/F+with RW15/3 at a filtration rate of 10 m/h. On-line effluent turbidity (NTU), filter run time (h), solids storage capacity (g SS/m^2) and head loss per solids load (cm/(g SS/m^2) when ALS, PAC or CHI are used for coagulation.

There is a small difference in run lengths for F/F and A/S using ALS and PAC, in favour of F/F, indicating that the large pores in the Filtralite filter are better utilized. For the deeper filter run lengths are longer, and the increase compared to F/F and A/S is larger for this raw water than for humic raw water. Both when ALS and PAC is used run lengths in F/F+ are more than twice as long as in F/F and A/S. Because of the deeper and relatively coarse filter bed solids are deposited over a larger bed depth, and narrowing of pores caused by deposits is slow and so are the increase in head loss.

CHI coagulation of this water gives excellent effluent turbidity and filter run lengths of more than 20 hours in filter F/F. In A/S the run is terminated by head loss, not utilizing the full potential of the storage capacity. From the figure it

can be seen that head loss per solids entering the filters is as before highest when CHI is used. Head loss per solids load is about 10 times as high in A/S as in F/F when ALS is used, but only 3 times as high using CHI. Long filter runs are "dependent" of deposits that are able to create much head loss in filter F/F and F/F+. CHI is capable of creating relatively more head loss in F/F than in A/S as compared to ALS.

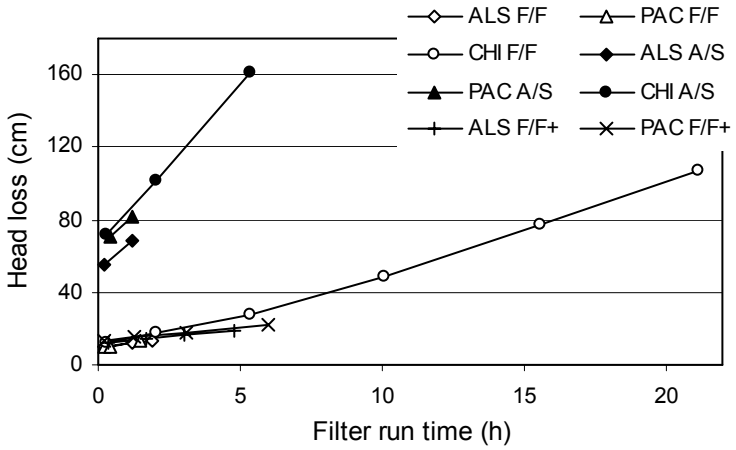

Figure 6.9 Total head loss as a function of run time for experiments with RW15/3.

Total head loss results for A/S show some difference in initial head loss, H_0. The increase in H_0 was due to some intermixing of fine sand with anthracite. To fix this about 10 cm of the intermixing region was removed, and some new sand was put into the column as well as anthracite. Before the anthracite was introduced to the column, the sand layer was fluidised for about 30 minutes and the finest material on the top was removed and replaced by new sand.

The relatively high H_0 in A/S for the run with CHI, which was limited by head loss, probably resulted in a short run time. The run time for this filter would have been longer with the refurbished A/S filter. However, the slopes of the curves are equal for the three runs in A/S, indicating that slope is not much affected by H_0. In F/F the runs have almost the same head loss development until breakthrough, as seen for the other raw waters. F/F+ show a little higher H_0 than F/F, but a slower development with time of filtration. This is because the same amount of solids is deposited over a larger bed depth resulting in a reduced blocking of pores.

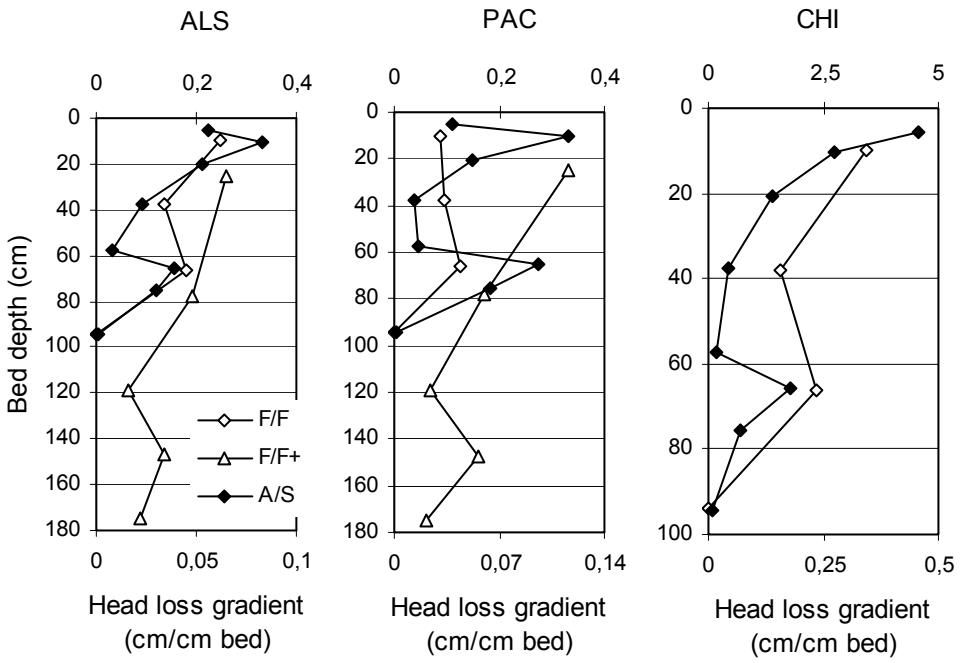

Figure 6.10 Head loss gradient distribution for runs with RW15/3. Values collected near breakthrough for ALS and PAC runs, and after 5 hours of filtration for CHI runs. F/F and F/F+ use bottom axis, A/S use top axis.

Head loss gradients for the three filters are presented in Figure 6.10. For filter A/S there is a low gradient in the top centimetres of the bed when ALS and PAC are used to coagulate the raw water. The particles in the raw water might need the flocculation provided by the filter pores to be more filterable, and are captured further down in the filter. It might also be caused by the relatively low coagulant doses used for this raw water. In A/S when PAC is used, the efficiency of the anthracite is lower than for ALS coagulation resulting in higher head loss gradients in the sand layer. A rapid decrease in gradient for lower sections is seen for all coagulants in A/S.

The gradients are in the order of 4 times higher for A/S than F/F and F/F+ for the aluminium based coagulants. When CHI is used the head loss gradients are, as seen for the other raw waters, about 10 times higher in A/S than in the other two filters. The high head loss gradients experienced when CHI is used indicates that the deposits are stronger (or that deposition takes place at higher pore velocities) than for the metal-based coagulants. The head loss gradients for ALS and PAC that are created before breakthrough occurs are similar in A/S

and F/F/F/F+, respectively. Breakthrough in A/S occurs at much higher head loss gradients than for F/F and F/F+, indicating that not only strength of deposits controls the time of BT. Deposits stored in A/S can withstand much more shear force from the higher pore velocities than what is the case for F/F and F/F+. This indicates that the deposits in A/S are stored in a way that makes them stronger, possibly with a more dens structure.

RW50/3

With this raw water there is relatively much suspended solids produced upon coagulation, and the filter runs are correspondingly short. All the runs shown were limited by breakthrough, which makes it easier to compare results obtained in A/S with the ones from F/F and F/F+.

The results obtained with FEC show higher turbidity and shorter filter run time than the other experiments with this raw water, and there is not much difference between the filters F/F and A/S. The results for the FEC experiment in A/S might be influenced by the initially higher H_0, which is seen in Figure 6.12. When ALS and PAC is used in filter A/S and F/F+, the effluent water quality is good and the run lengths are better than with FEC. It can be seen that the run length in F/F+ is about twice as long as in A/S, indicating a relationship between the depth of the filter and run length. The k value (head loss/solids load) show, as expected high values for A/S compared to F/F and F/F+. As mentioned all these experiments are terminated by breakthrough, which means that the solids storage capacities shown are maximum values for this raw water and pre-treatment conditions.

CHI makes flocs, which are the most filterable, and creates most head loss before breakthrough in both F/F and A/S. Run time for F/F is almost 9 hours, and for A/S about 6 hours. This shows that one is able to utilise the larger pore space in the F/F filter for depositing solids, at a much lower head loss and equal effluent turbidity.

From Figure 6.12 the difference in H_0 for A/S can be seen, which is a result of replacement of some of the finest sand. To which extent this influence the head loss development and other parameters is not easy to evaluate, but the slope of the curves with the "old" A/S is not significantly different from the slopes obtained with the refurbished filter bed.

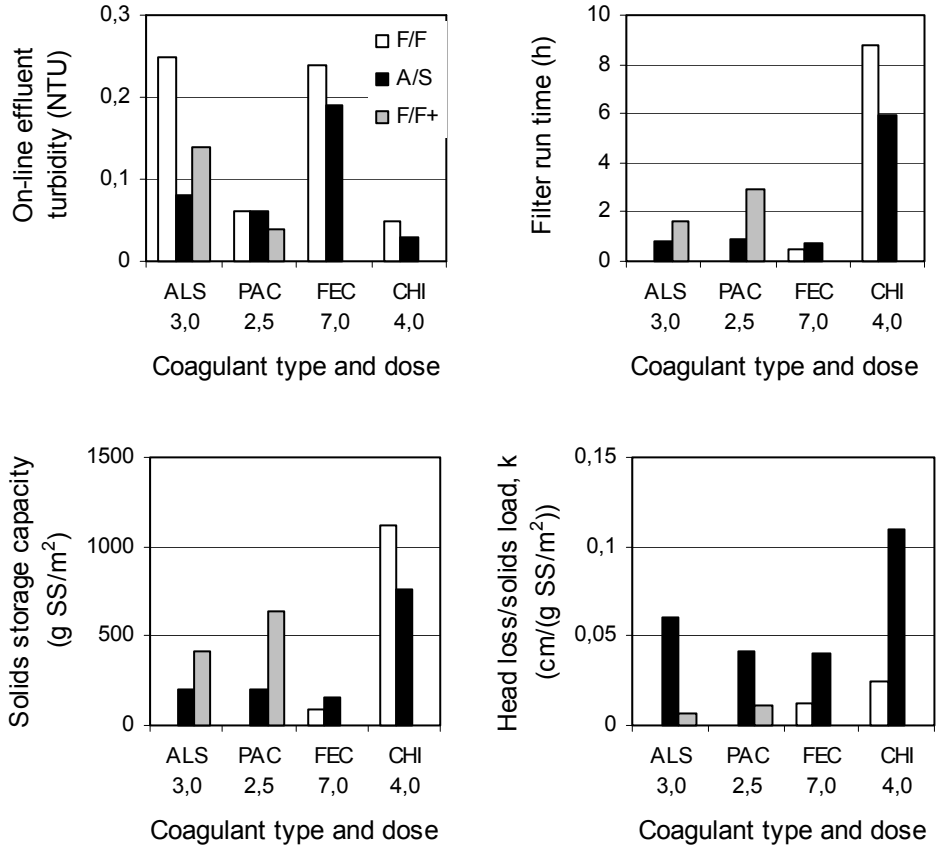

Figure 6.11 Comparison of results for filter F/F, A/S and F/F+ with RW50/3 at a filtration rate of 7,5 m/h. On-line effluent turbidity (NTU), filter run time (h), solids storage capacity (g SS/m^2) and head loss per solids load (cm/(g SS/m^2) when ALS, PAC, FEC or CHI were used for coagulation.

The head loss development with time for filter A/S when PAC and FEC are used is smaller than when ALS and CHI is used. This is a result of less suspended solids in the coagulated water entering the filters. A lower dose of Al is used for PAC than for ALS with this raw water, therefore less precipitate is formed using PAC. The slope for FEC might be influenced by less solids deposition, giving higher effluent turbidity.

In F/F and F/F+ the slope of all the head loss curves is almost identical. The longest run obtained was whit CHI as coagulant for both filters. A linear head loss development with time indicates that there is no surface deposition in the two filters using CHI.

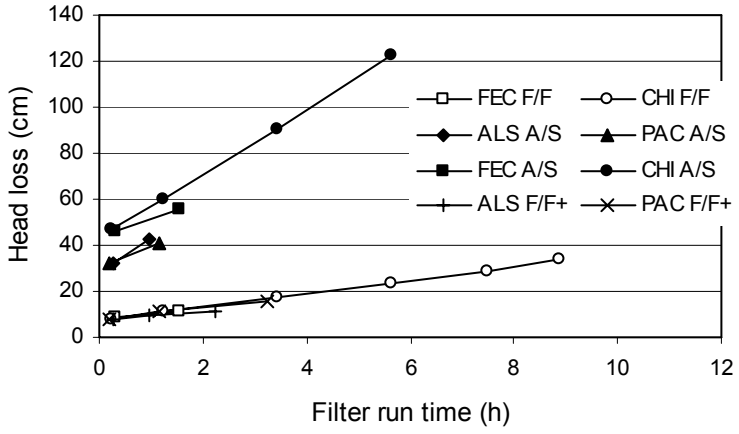

Figure 6.12 Total head loss as a function of run time for the experiments shown with RW50/3.

In Figure 6.13 all head loss gradients shown are values from the point of time in the filter run when the breakthrough limit (0,3 NTU) is exceeded. The results for CHI show as for the other raw waters, much higher gradient values than the other coagulants. Breakthrough occurs when the gradient in the upper most section is 3,46 and 0,56 cm/cm for A/S and F/F respectively. Compared to experiments with ALS and PAC, the gradient in the top sand section of A/S is relatively higher when CHI is used. This might be an indication of the size of the CHI coagulated flocs being smaller than for the metal coagulants, penetrating deeper down in the filter bed. Adsorption of hydroxide flocs to the filter media is also a probable cause for the higher head loss gradient values in the top of the anthracite layer than in the top sand layer using ALS and PAC.

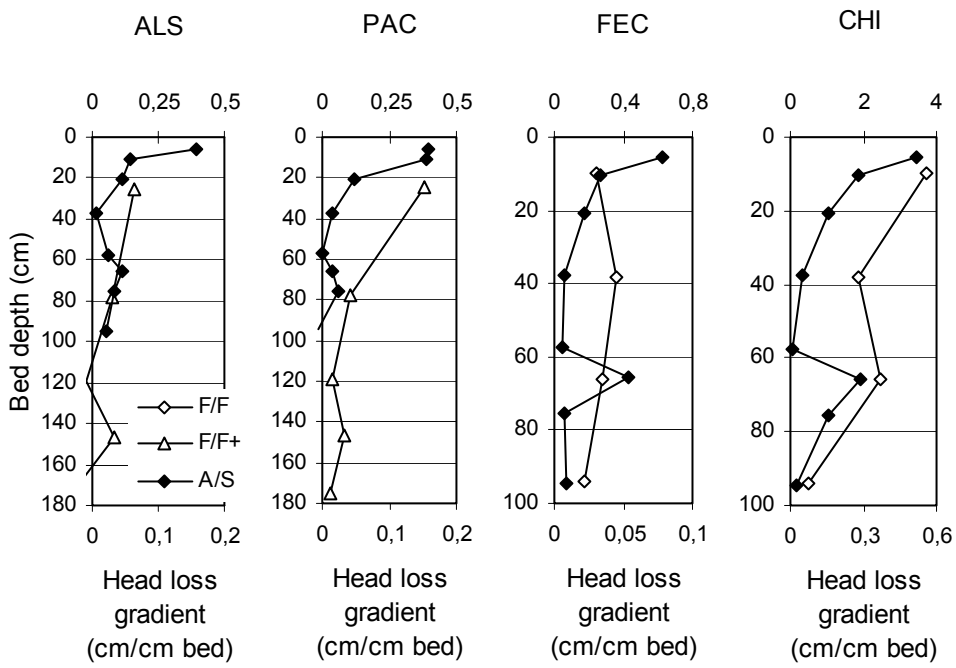

Figure 6.13 Head loss gradient distribution for runs with RW50/3. Values collected at breakthrough for all the experiments shown. F/F and F/F+ use bottom axis, A/S use top axis.

Bed depth and grain size

The results shown have proven that it is possible to compensate for a larger grain size by increasing bed depth. Dependent on the pre-treatment, effluent water quality was slightly better or worse in the deep coarse filter compared to the shallow fine-grained filter. Moran et al. (1993a) studied the effects of bed depth and grain size in depth filtration, and found that when comparing different media size at equal depths, the larger media removed generally less particles than the fine media. Small particles, about 1-2 μm, experienced relatively less removal than bigger particles in the large media. When the two filter media was compared for equal media surface area, i.e. increased depth of large media, the removal efficiency was as good for the large media as for the fine media for all particle sizes. This indicates that using an equivalent media surface area in a deeper filter bed can offset an increase in media size.

Boller and Kavanaugh (1994) introduced a deposit density model to explain the head loss increase for different filtration situations. They used data from several investigations and found good agreement with their model predictions. Their

main hypothesis was that the density of deposited solids control the head loss increase in deep bed filters. Different suspensions have different abilities to store and pack solids in the filter pores, resulting in large differences in deposit density and head loss increase. They used the head loss gradient ratio (I/I_0) as a function of the particle volume deposit (l/l bed), to show among other things that the head loss development is more rapid in coarse grained filters for equal specific deposits. This was explained by the higher number of particles captured in each of the fewer but larger pores of the coarse media, leading to a looser structure of the deposits, and a relatively higher head loss.

6.3.2 Filtration rate

Filtration rate influence the water quality produced and the length of the filter runs as well as head loss development in the filters. To which degree the different filters are able to handle an increase in filtration rate are very much dependent on the design of the filter bed. The results presented are from experiments performed at equal pre-treatment conditions for each coagulant.

RW15
This is a raw water with little suspended solids in the influent water to the filters, and the effluent turbidity is generally low. When the metal salt FEC is used the highest increase in effluent turbidity with increasing filtration rate is observed for both F/F and A/S. F/F is more sensitive than A/S to a higher filtration rate using FEC for coagulation. When CHI is used the effluent turbidity is only slightly higher at 20 m/h than at 7,5 m/h, and the increase is higher for A/S. PAC results show that with this coagulant it is possible to increase the filtration rate from 7,5 to 12,5 without any significant worsening of the effluent water. This show that FEC create flocs with RW15 that are less filterable than the ones created with PAC and CHI. The result of less filterable flocs is more obvious at higher filtration rates and for the more coarse F/F filter.

A decrease in run time with increasing filtration rate is seen for all coagulants and both filters. PAC and CHI give long filter runs in F/F, but the reduction in run length with increasing filtration rate is about the same as for the other coagulants (same slope of the curve).

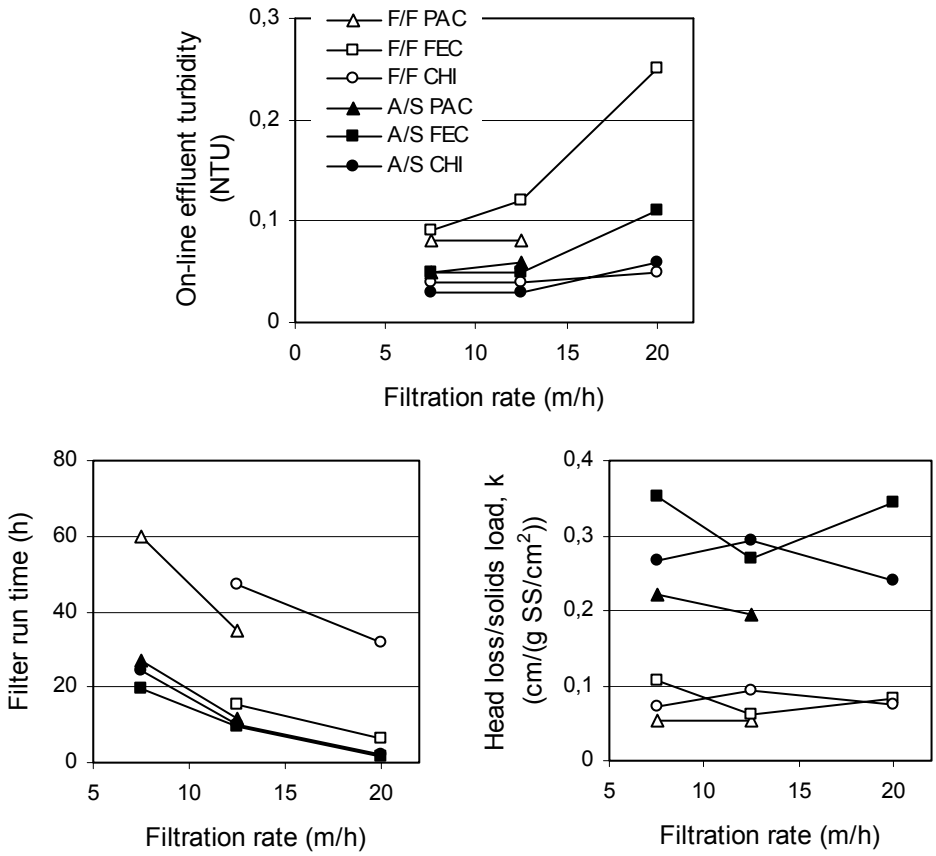

Figure 6.14 Comparison of results at different filtration rates for RW15.

All the runs for A/S have almost the same run length for the same filtration rate, and they are all terminated by head loss. Also shown are the k values (head loss/solids load) for the same experiments, with some differences due to different filtration rates, especially in A/S. It is likely that the different approach velocities giving different pore velocities result in variations in deposit structure. When the pore velocity is increased a floc-particle following a streamline is more difficult to remove. What is considered to be the main filtration mechanisms are generally reduced in efficiency at higher filtration rates. This is seen in the effluent turbidity graph resulting in higher values. The k values for FEC, for which effluent turbidity is clearly influenced by filtration rate, show a minimum at 12,5 m/h for both F/F and A/S. In A/S the k value is about 0,25 at 12,5 m/h and 0,35 for 7,5 and 20 m/h. The lower head loss development per solids load for an increasing filtration rate from 7,5 to 12,5 m/h with FEC is expected, because of the lower removal efficiency. Further increase in filtration rate up to 20 m/h results in an increase in the k value. This

could be caused by a reduced deposition in the more coarse anthracite layer because of the high filtration rate, giving an increased solids load to the fine sand layer. The upper most sand grains are as small as 0,4 mm in size, and an increased solids load might lead to a sand-surface deposition with a rapid head loss increase.

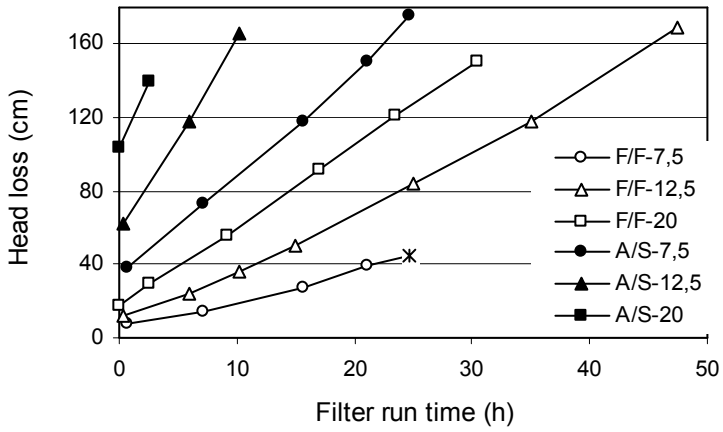

Figure 6.15 Total head loss in F/F and A/S for experiments with 7,5, 12,5 and 20 m/h using CHI as coagulant.

In Figure 6.16 the head loss gradients for the FEC experiments are shown after 100 g SS/m^2 solids load for all three runs. As mentioned above the increasing velocity transport more suspended solids deeper down in the filter bed, increasing the head loss in the sand layer. The high k value at 7,5 m/h is due to deposition in the top anthracite layer, caused by high removal efficiency at this low filtration rate possibly with precipitation of hydroxide on grain surfaces.

Experiments with CHI and PAC show more constant k values with increasing filtration rate, but with an opposite trend and a maximum k value at 12,5 m/h. The reason for the low value at 7,5 m/h using CHI, could be due to a different deposition pattern with flocs deposited on grain surfaces in a way that less pore blocking is created.

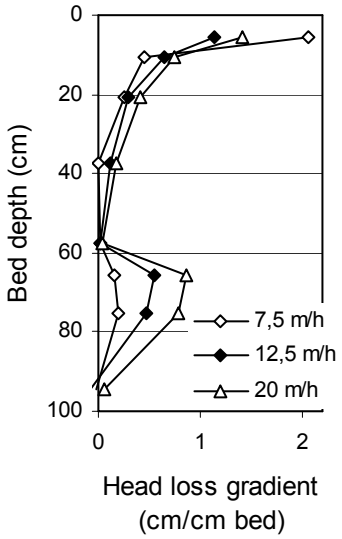

Figure 6.16 Head loss gradients for experiments with FEC at 7,5, 12,5 and 20 m/h filtration rate in filter A/S after 4, 2,4 and 1,5 hours of filtration respectively (100 g SS/m^{2}solids load for all experiments).

The total head loss curves for CHI in Figure 6.15 show steeper curves for higher filtration rates as expected. There is also a difference in H_0, but for F/F the difference is very small. Indications of a dominating top layer deposition can be seen in both filters at low filtration rate as not linear head loss curves. At higher filtration rate, the curves are almost linear and deposited matter is more evenly distributed.

RW50

High colour raw water give generally short filter runs. CHI has proven to be superior to the metal salts in run length and effluent turbidity for this raw water. In the figures below experiments with RW50 at different filtration rates are studied.

As seen in Figure 6.17 the influence of increasing filtration rate is in most cases the same for the three filters and the coagulants used. It is to what extent they are influenced that is different. Between the filters, F/F+ show an effluent turbidity that is perhaps more stable with increasing filtration rate than A/S, with F/F generally showing the highest increase in turbidity. The efficiency of removal deteriorates more with increasing filtration rate for a coarse grained than for a fine-grained filter bed as seen when comparing F/F and A/S. When an

increasing depth is introduced, it is possible to compensate for the large grains, with a result in this case of a less sensitive filter bed.

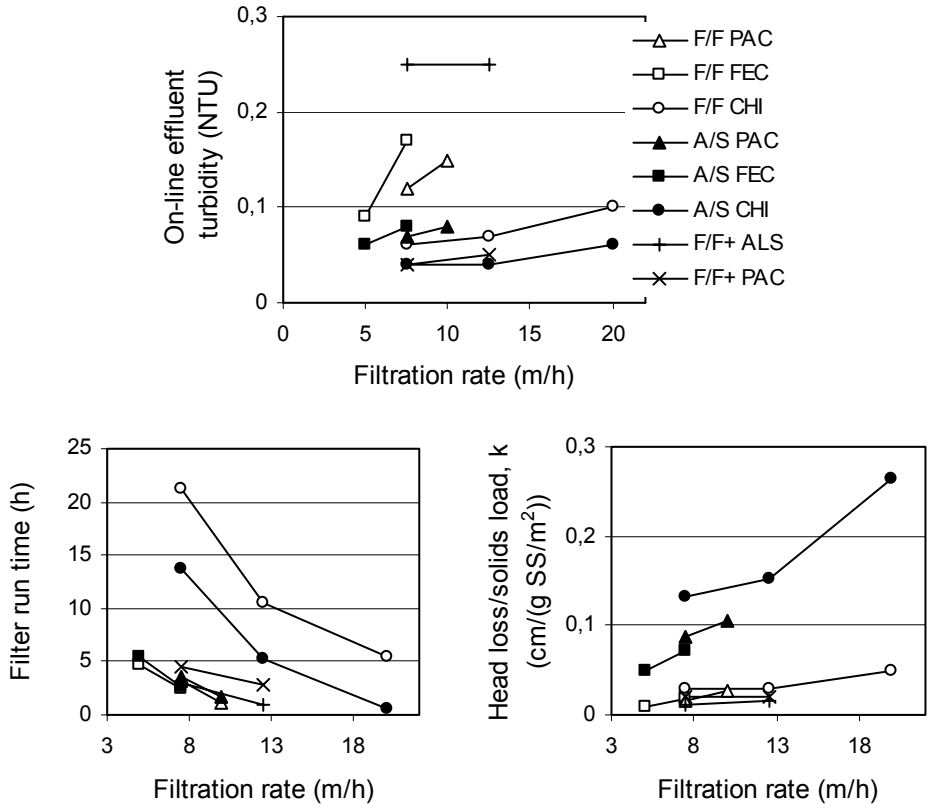

Figure 6.17 Comparison of results obtained with RW50 at different filtration rates in F/F, A/S and F/F+.

When analysing filter performance under different operating conditions, Ives and Sholji (1965) found that a doubling of the filtration rate created a need for doubling of filter bed depth to achieve equal removals. They also found that when grain sizes were increased from 0,65 mm to 0,93 mm (43 % size increase), the bed depth had to be increased from 24 to 39 inches (63 % depth increase). The conclusion of their study was, as many other researchers also have found, that the filter coefficient (filter efficiency) is inversely proportional to the filtration rate, filter grain size and water viscosity. According to this relationship, when comparing F/F and A/S (equal depths) an increase in filtration rate is more crucial for F/F than for A/S as seen in Figure 6.17. A comparison of A/S and F/F+, (which was originally designed to produce the

same quality effluent), show almost the same behaviour when filtration rate is increased and this is also in agreement with the relationship described.

Between the different coagulants there are large differences in the response to filtration rate increases. When using metal salts, effluent water quality is more influenced by filtration rate increases than when CHI is used for F/F and A/S, as expected. In F/F+ the results when ALS is used show the same effluent turbidity at 7,5 and 12,5 m/h, but relatively high values are experienced with this coagulant. In contact filtration, the increased bed depth, which provides more filter pore flocculation, has a significant effect on water quality and roughness of operation. It can be observed that the run lengths for this raw water are about the same in F/F and A/S, with some increase for the F/F+ filter. However, the decrease in run length with increasing filtration rate is not that distinct for filter F/F+.

The runs with CHI in the A/S filter are all terminated by head loss limitations, while they are terminated by breakthrough in F/F. When comparing k values for CHI coagulation in F/F and A/S, an increasing trend with increasing filtration rate is seen. The head loss build up in A/S is very high compared to F/F, and the difference is largest at 20 m/h. This trend is also seen for the other coagulants. In Figure 6.18 the head loss gradients for F/F and A/S are presented for the experiments using CHI. In F/F results are compared at a total solids load of 932 g SS/m^2 filter surface area, and 124 g SS/m^2 for A/S.

As the filtration rate is increased flocs are deposited further down in the filter. In F/F the gradient in the top layer is identical for all three velocities, but there is a relatively large increase with filtration rate in the upper part of the bottom layer. It was expected that the gradients in the top layer at high filtration rates was lower than at lower velocities, and this is observed in A/S. At the same time the total head loss per solids load of the filter bed increase with filtration rate. This indicate that the same amount of suspended solids create more head loss at high filtration rate, because more deposition take place in parts of the filter bed with lower porosity. The head loss gradients are calculated by subtracting values earlier in both time and filter depth. This means that the values are comparable between experiments in the same filter bed.

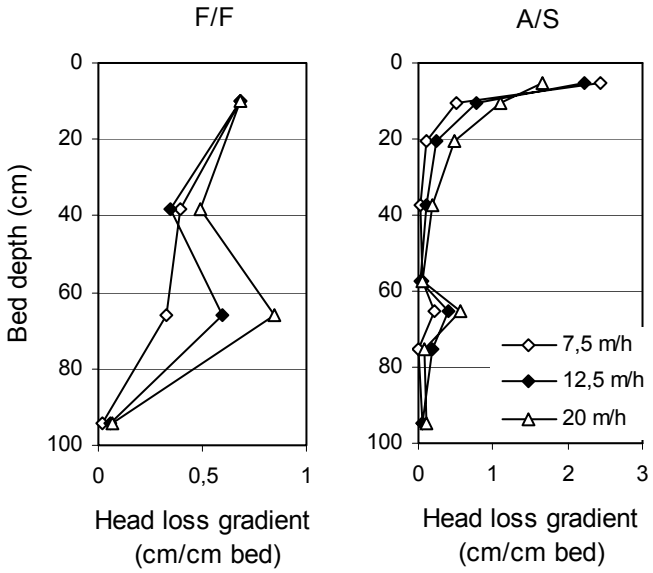

Figure 6.18 Head loss gradients in F/F and A/S using CHI for coagulation, results are compared for equal amounts of solids load in each filter. (931 g SS/m^2 in F/F, 124 g SS/m^2 in A/S)

RW50/3

This raw water with turbidity creates denser flocs that are more influenced by sedimentation on the filter grains than the humic flocs, or more resistant to erosion/detachment forces. An increased filtration rate reduces the effect of sedimentation, but higher floc density increase the effect. It is, from a theoretical point of view, reason to believe that turbidity in the raw water make depth filtration less sensitive to increasing filtration rate.

Effluent water turbidity deteriorates with an increase in filtration rate for all the experiments shown. The degree of influence is much dependent on the coagulant used in A/S, where ALS gives a effluent turbidity of 0,08 and 0,35 NTU at 7,5 and 12,5 m/h respectively. PAC coagulation of this raw water produce flocs that are less sensitive to an increase in filtration rate for both filters, with F/F+ being the less sensitive of the two filters.

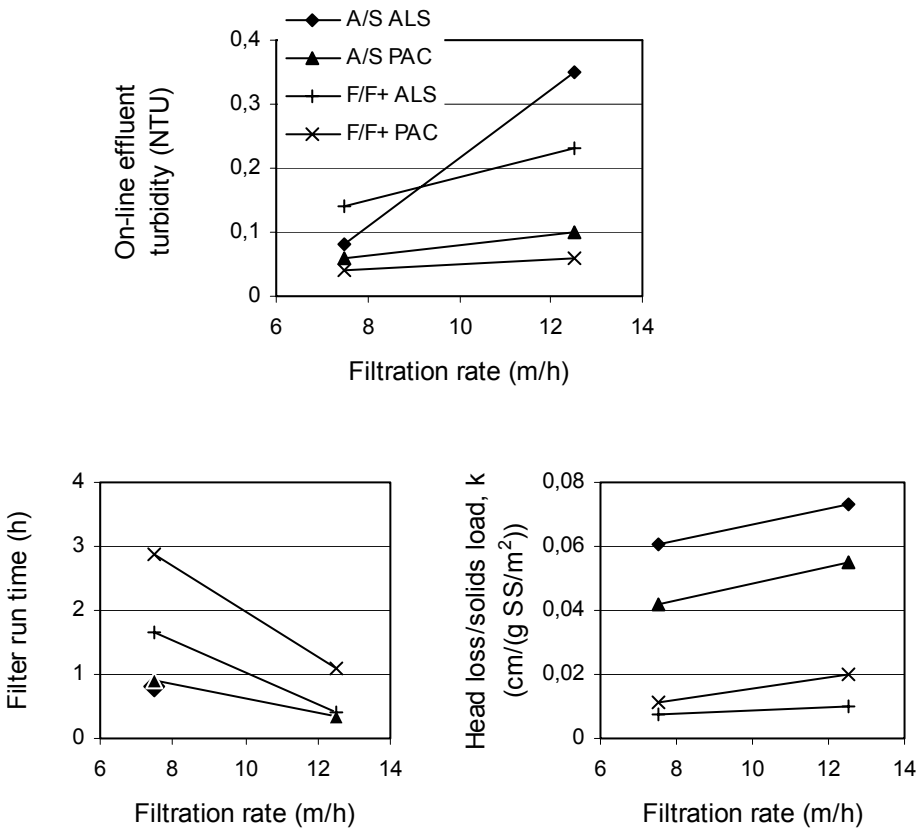

Figure 6.19 Comparison of results obtained with RW50/3 in filter A/S and F/F+ at different filtration rates.

The filter run time is short for this raw water with a relatively high concentration of suspended solids. It can be seen in Figure 6.19 that the experiments with a short run time at 7,5 m/h in A/S experience relatively less shortening of the run time when the filtration rate is increased to 12,5 m/h. This could be caused by the high sensitivity of effluent water turbidity in A/S, giving less deposition at high filtration rates. The longest run time of about 3 hours was obtained in filter F/F+ using PAC, which also produced the lowest effluent turbidity. Because of the grain size difference in the two filters, A/S have a higher k value than F/F+. All experiments show an increase in head loss per solids load with increasing filtration rate, maybe with the exception of ALS used in F/F+, which is almost not influenced. This was also seen for RW50, and is probably a result of more deposition in deeper fine-grained filter layers. Figure 6.20 show the head loss gradients for the experiments with PAC in A/S

at the two filtration rates used, compared when the accumulated solids load to the filters was 121 g SS/m^2.

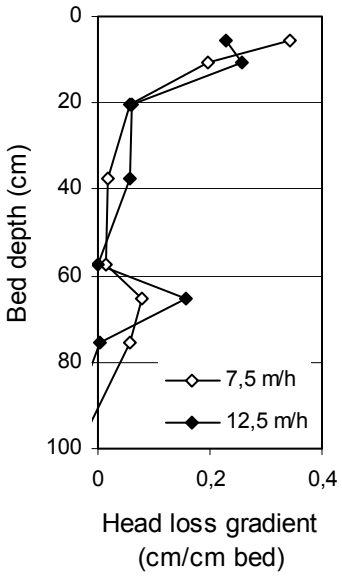

Figure 6.20 Head loss gradients in A/S using PAC with RW50/3. Results are compared at equal amounts of solids load to the filter.

It is seen from the figure that more of the deposited matter is situated in the top sand layer when the filtration rate is 12,5 than at 7,5 m/h. The top section of the anthracite shows a lower gradient than the deeper section at 12,5 m/h. This was observed during the entire filter run, and is also seen for other coagulants especially with turbidity containing raw waters. This might show that a flocculation/reaction time is needed for this raw water, which is not fulfilled at 12,5 m/h.

Moran et al. (1993a) experienced that a higher filtration rate reduced the removal efficiency for all particles in the size range between 1-25 μm. When comparing results obtained at two different filtration rates for a similar hydraulic detention time in the filter bed, initial removal efficiencies were very similar. In this study, when results for A/S and F/F+ are compared, the response (e.g. effluent water quality) is influenced both by grain size and depth differences creating differences in pore velocity, detention time, specific deposit, head loss development among other factors.

Boller and Kavanaugh (1994) found that the head loss gradient ratio (I/I_0) as a function of particle volume deposit (l/l bed) was independent of the filtration rate. This implies that the deposit density was not affected by changes in filtration rate for the range of rates tested (6,7-22,4 m/h).

6.3.3 Ripening and breakthrough

Ripening is defined as the initial period of effluent water quality improvement following filter backwash. It is caused by remnants from the backwash process, transient non-optimum coagulation conditions and because already deposited particles in the filter pores enhance the removal efficiency. At the end of a filter run there is a breakthrough when effluent water quality deteriorates as a result of deposited particles breaking off, or influent particles passing right through the filter.

Researchers have studied these phenomena, and among other things found evidence of detachment of deposited particles being a major factor contributing to breakthrough (Moran et. al., 1993b), (Kau and Lawler, 1995). The detachment was demonstrated to be a continuous process which was dominated by large particles. They also found that the rise in head loss did not appear to be a major factor affecting detachment.

Darby and Lawler (1990) found when studying ripening in depth filtration, that ripening was strongly correlated to the volume of (previously) captured particles. Ripening (with time) was observed for small particle sizes, but not for larger particles. Changes in particle size distribution with time and depth was seen, which was related to the capture of particles and groups of particles (flocs) breaking off.

In the following examples a filtration run from start to end is analysed by means of effluent water quality and head loss distribution (head loss gradient). In Figure 6.21 and Figure 6.22 the hydraulic gradient trend curves for each section in the filters are presented for the entire filtration cycle. The top curves are head loss gradients for the top filter media layer (in black) with values on the left axis, and the bottom curves (in grey) are gradients for the bottom filter media layer with values on the right axis. Also shown is the turbidity from the on-line measurement (right axis). Numbers on the right of the gradient curves are the filter bed depths.

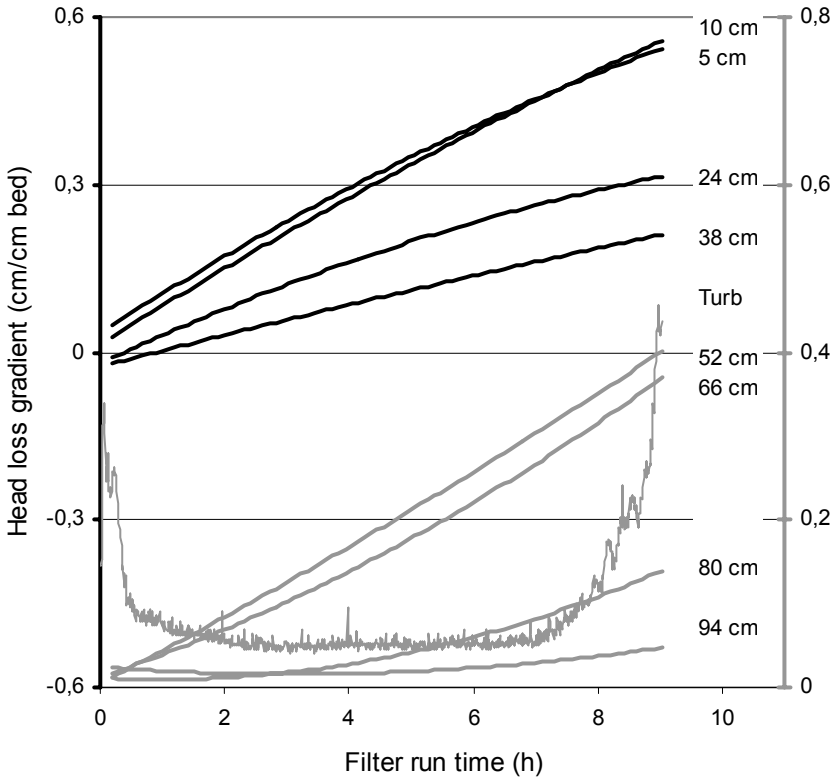

Figure 6.21 Effluent turbidity and head loss gradients for filter F/F as a function of time and filter bed depth. (RW50/3, CHI, 7,5 m/h).

For filter F/F which is a coarse two media filter, the head loss gradients in the top layer increase with time as expected. The upper most 5 cm show a decelerating growth while the following 5 cm show an almost linear growth with time. When evaluating total head loss curves an upward curving trend is an indication of surface deposits due to large flocs causing top layer straining. A decelerating curve indicates either a lower deposition rate or a higher detachment rate, demonstrating that the deposits reach a point of saturation. Further down in the filter the next two sections of the top layer show a decelerating growth, and the top two sections of the bottom layer show accelerating growth. This might demonstrate that when a overlying section of the filter bed is to coarse for effective removal of flocs, underlying sections experience an increased solids load and due to finer grain sizes they show a more exponential growth. The top two sections of the F/F bed, are also "co-

working" sections, with the underlying carrying the increasing load from the overlying section.

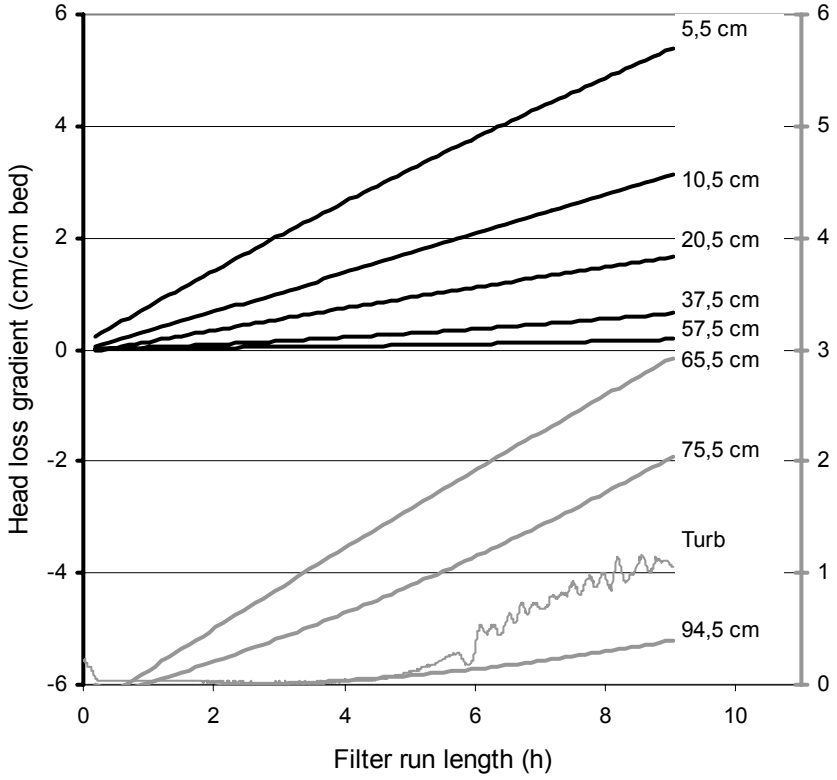

Figure 6.22 Effluent turbidity and head loss gradients in A/S as a function of time and filter bed depth. (RW50/3, CHI, 7,5 m/h).

From Figure 6.21 it can be seen that after the initial ripening peak and until the breakthrough starts after about 7 hours of filtration in F/F, effluent turbidity show a slow improvement for the first hours (ripening) and a slow deterioration the following hours. Looking at the head loss gradient curves for the two bottom sections of the bottom filter layer (80 and 94 cm), there seem to be a connection with the incipient breakthrough of turbidity after about 4 hours, and later the terminating breakthrough at the end of the filter run. These two bottom sections show no increase for the first hours of the filter run, and therefore it is reasonable to believe that there is no deposition of solids in this period. When flocs start to reach the section in the filter bed that is second from the bottom a gradient builds up, and at this point in time the effluent turbidity start to deteriorate. This section still got filter bed beneath it, but this is not true for the

bottom section. As soon as head loss start to increase in the bottom layer, after about 6-7 hours, the terminating breakthrough occurs almost spontaneously. Moran et al. (1993b) stated that detachment is a continuous process throughout the filtration cycle. The final breakthrough in a filter seems to be controlled by solids reaching the bottom most layer of the filter without any possibilities of re-attachment.

This implies that even though the deposits are able to withstand high shear forces in the top sections of a filter, a breakthrough occurs as soon as the "solids front" reaches the bottom layer.

Hunt et al. (1993) found that different sections of a filter bed have a maximum specific deposit (g/l bed), and that the top section reaches its maximum first but sections deeper down in the filter could obtain higher specific deposits. They also found that the hydraulic gradient continued to increase when the deposition in a filter section had reached its maximum. It seems however from their results, that the top sections of the filter bed experience a decelerating growth of the hydraulic gradient with time when the maximum value of specific deposit is reached.

In filter A/S the same trend is seen. When the gradient in the bottom sand section starts to increase, there is a rapid breakthrough in turbidity. It should be noticed that only a minor increase in gradient, indicating low content of flocs, is needed to produce the terminating breakthrough. Also seen from the results in A/S is the very low gradient increase in the bottom section of the anthracite. This demonstrates that the efficiency of this section is minimal, indicating that a shallower layer of anthracite could be used in this case. This can be compared to the results for F/F where all the sections in the top layer show increasing gradients, and perhaps a deeper layer should have been used (as in the F/F+ filter).

The above example showed results obtained with CHI as coagulant and RW50/3. Figure 6.23 and Figure 6.24 shows similar results for experiments where PAC is used with RW50 in filters F/F and A/S respectively.

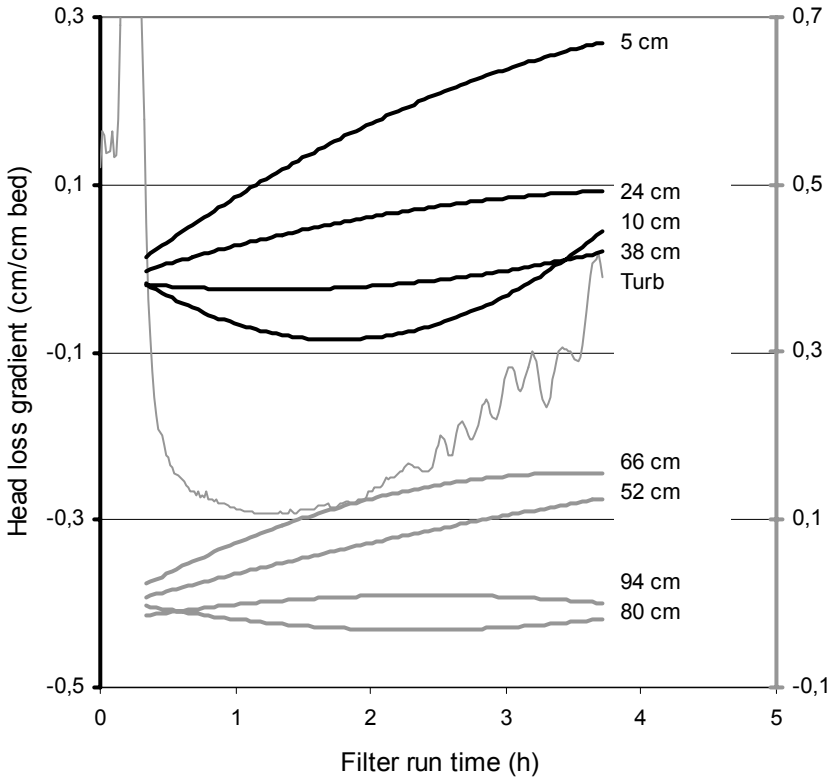

Figure 6.23 Effluent turbidity and head loss gradients in F/F as a function of time and filter bed depth. (RW50, PAC, 7,5 m/h).

This experiment in F/F shows an almost immediate breakthrough of turbidity after the initial ripening peak. The top section of the top layer show a decelerating growth curve while the next section show a decrease in gradient for the first two hours of filtration, then an increase. If the curve for the 10 cm depth is correct, it indicates that head loss (deposits) is "lost" in this section, which must be a result of wider pore openings. This could perhaps be due to deposits that were not properly removed during the previous backwashing or compaction of an adjacent section after start up from a backwash, but this is not fully understood.

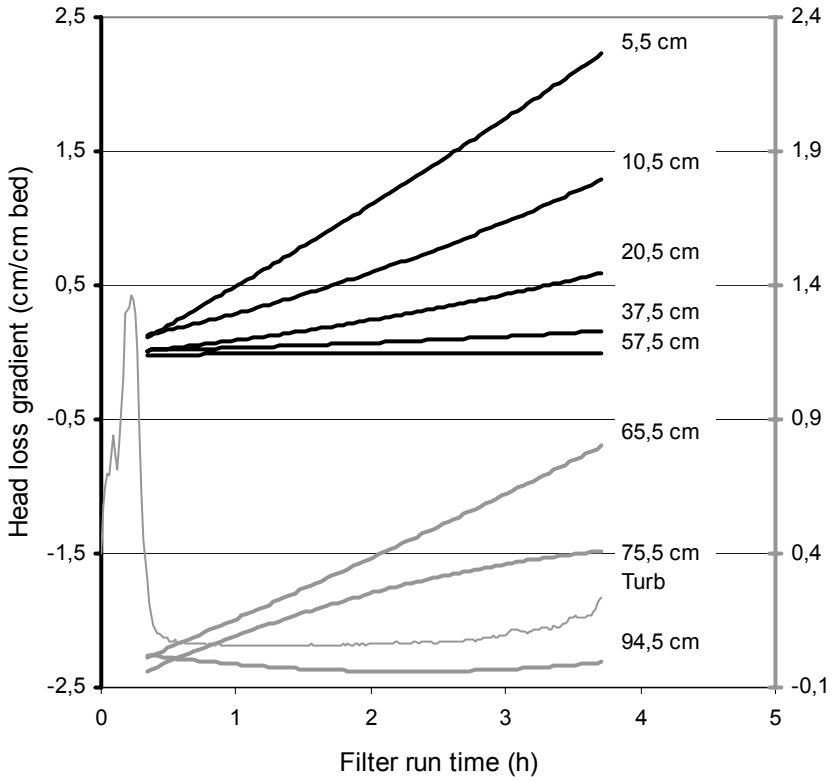

Figure 6.24 Effluent turbidity and head loss gradients in A/S as a function of time and filter bed depth. (RW50, PAC, 7,5 m/h).

The bottom layer of F/F shows gradients that are higher for the second and fourth section than for the first and third section respectively, but all the values are low. The bottom section shows an increase in gradient from the start of the run, and a small decrease at the end of the period. It might be that this run experience breakthrough from the bottom section of the bed before the initial ripening period is finished, leading to too high values of turbidity in the production period of the run. The reduction in gradient at the end of the run for the bottom section of the filter might indicate detachment of deposits.

The results for filter A/S presented in Figure 6.24 show mostly the same trends as in Figure 6.22. The top layer sections of the filter bed give a close to linear relationship between head loss gradient and time of filtration. The bottom section of the top layer experiences no increase in gradient, indicating only minor deposition. It is clear that whatever passes this section has to be removed

by a more effective collector, in this case in the form of smaller sand grains. For the second to the bottom section in the sand layer the gradient show a considerable decreasing growth at the end of the run, indicating that a deposit saturation condition is reached for this section. At the same time the bottom most section has an increasing gradient at the end of the run where the turbidity indicate breakthrough, as seen in the other experiment.

From both examples shown in this chapter, a modification to the Filtralite filter bed (F/F) was justified. Because the grain size was set, the layers in the filter bed needed to be deeper and from that the F/F+ filter was designed. In the anthracite/sand bed the bottom layer of anthracite is not utilised before breakthrough occurs in the bottom sand layer and the run is terminated. The relationship of anthracite to sand with respect to bed depth could be decreased to create a more "balanced" filter bed. It should be noted that in all filter beds, that are not completely mono-sized, there will be a stratification of the media within each layer. The result of this is that the largest grains within each layer accumulate at the bottom of the layer, and the smallest at the top, giving an initial decrease in efficiency from top to bottom. For a mono-sized filter media the difference in head loss gradient between the sections in a filter layer would have been less than in a conventional filter bed.

6.3.4 Effects of different raw waters

Results for different raw waters have been presented separately earlier. In this section examples of experiments using the same pre-treatment but with different raw waters are compared. First, a relationship between run time and solids load is presented, comparable to the relationship presented by Eikebrokk (1998) for a dual media anthracite/sand filter.

In Figure 6.25 the run time for filter F/F as a function of the solids load to the filter is presented for experiments with all the coagulants and raw waters tested. The points in the figure show solids load calculated as C_0 v (suspended solids in influent multiplied by filtration rate) on the x-axis and filter run length on the y-axis. RW15 with a low suspended solids concentration show low values of solids load and generally long filtration runs are obtained. The other three raw waters with higher levels of suspended solids generally give shorter filtration runs. There are no clear differences between the raw waters regarding the ability of the filter to handle high solids loads; they seem to follow the same trend. The significant differences in run time are between the coagulants. If chitosan is used, independent of raw water, longer filtration runs are obtained than if a metal salt is used. The two trend lines in Figure 6.25 are calculated

from the experiments with CHI used with all four raw waters, and the metal based coagulants with all four raw waters. The difference in run length between experiments using CHI and the metal-based coagulants is bigger for low values of solids load, and at about 50 g SS/m^2/h a run with CHI is about 40 hours as opposed to 10 hours using a metal salt. The two larger diamonds in Figure 6.25 show results for RW15 with PAC as coagulant. These data points are not following the same trend as the other metal salts, but show a more chitosan-like trend. The reason for this can be that the low dosage of Al added to RW15 as PAC (0,8 mg/l) creates little aluminium hydroxide. PAC is also known to form polymeric species when added to water. Therefore these runs are more like the runs with CHI.

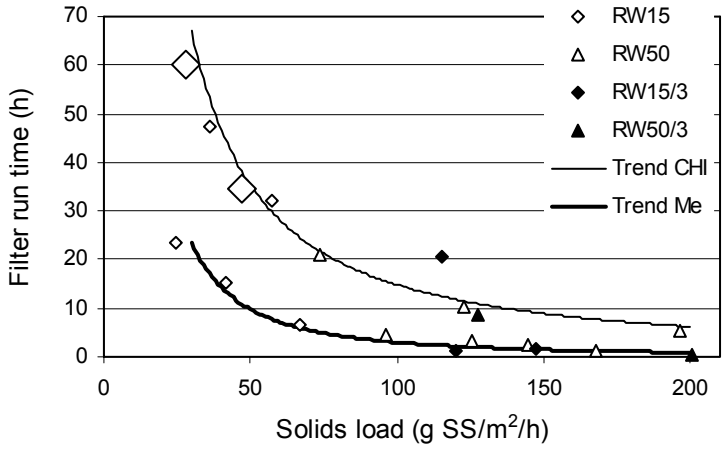

Figure 6.25 Filter run time as a function of solids load to filter F/F for experiments with different raw waters.(RW15 with PAC: big diamonds).

The figure shows that the filtration run time in F/F at identical solids load is independent of raw water quality for CHI coagulation and metal salt coagulation separately, for the raw waters tested in this study. Relationships like this can be used to find guideline values for run time for given raw water and coagulant.

To see the effect of increasing raw water turbidity, some experiments were carried out with a bentonite clay turbidity of 6 NTU in the raw water (RW50/6). In the example below filter performance when treating RW50, RW50/3 and RW50/6 are evaluated both for filter F/F and A/S. The same dosage of 4 mg CHI/l is used in all three experiments.

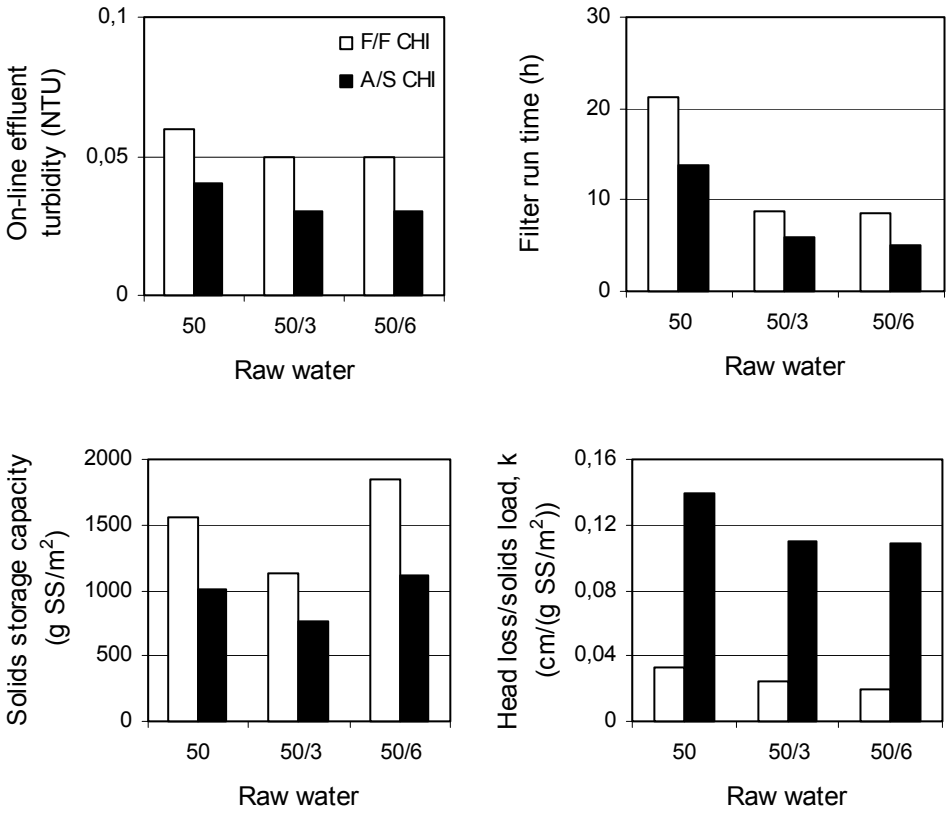

Figure 6.26 Comparison of results obtained in filter F/F and A/S for RW50, RW50/3 and RW50/6. Filtration rate: 7,5 m/h.

When using CHI as coagulant the effluent turbidity produced is low for all raw waters and both filters. Slightly higher turbidity values is seen for RW50, colour only, than for the experiments with higher levels of raw water turbidity. The flocs formed are more easily removed by sedimentation on grain surfaces when clay particles increase their density. The difference in effluent turbidity between the two filters is constant for all the three raw waters.

Longer filtration runs are obtained for RW50 than for the other raw waters. Increasing raw water turbidity from 3 NTU to 6 NTU give only a slight decrease in filter run length. All the three runs for filter A/S are terminated by breakthrough, except for the experiment with RW50. Because of this the difference in run length between filter F/F and A/S is bigger for RW50 than for the other raw waters. The bar graph showing storage capacity in the filters

before termination of a run illustrate the difference in filterability of the different raw waters. RW50/3 show the lowest storage capacity while RW50 and RW50/6 give higher values. This trend is seen for both filters, but the storage capacity is higher in F/F than in A/S for all three raw waters. A higher solids storage capacity indicates differences in the way deposits are attached and stored, that prevent breakthrough compared to the other raw waters. Results for RW50/3 and RW50/6 indicate that the difference in storage capacity between F/F and A/S increase with increasing turbidity of the raw water. This is an indication of the large storage potential of the coarse Filtralite filter, which is better utilised for raw waters with relatively high turbidity.

Why RW50/3 show less storage capacity than the other two raw waters is not that clear. It might be that the quality of the flocs formed with this raw water is much influenced by the colour content, giving them poor filterability properties.

Figure 6.27 show the total head loss curves for the experiments discussed. The total head loss development with time demonstrates that head loss builds up more quickly for raw waters with higher content of turbidity. Comparing these curves to the k values from Figure 6.26, it is seen that despite the slower head loss increase with time for RW50, the increase per solids load is higher for this raw water than for turbidity containing raw waters. This is proving that the deposits from humic flocs are either more voluminous or deposited in places where they create more pore blocking than other flocs. It is likely that more dense flocs containing clay particles are mainly deposited on the top of filter grains by sedimentation, while lighter humic flocs are mainly captured by interception on the sides of the grains.

The experiment with RW50/6 in filter A/S is limited by breakthrough just before maximum head loss is reached. For this raw water the filter is showing optimum performance, utilising both the capacity to produce satisfactory filtrate as well as the hydraulic capacity (Ives, 1980). From these results with increasing turbidity in the raw water some of the same trends are seen as for an increasing filtration rate. This is not surprising as both of these parameters will increase the solids load to the filters, and as shown in Figure 6.25 the type of raw water is not significant with respect to solids load capacity of filter F/F.

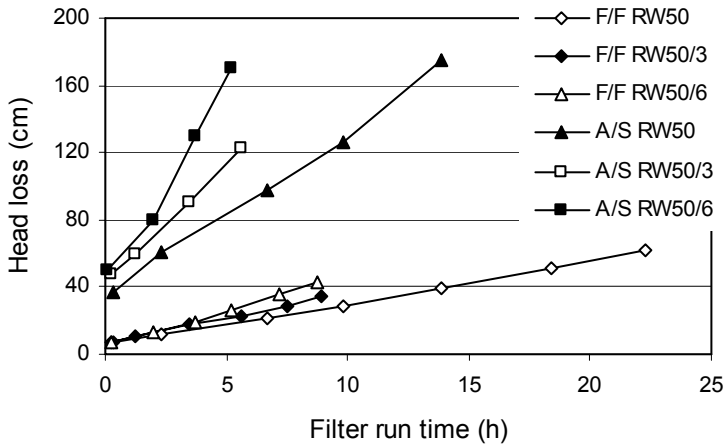

Figure 6.27 Total head loss curves for F/F and A/S with RW50,RW50/3 and RW50/6 using CHI as coagulant.

In Figure 6.28 the head loss gradient distribution in the depth of the filters is shown after 3 hours of filtration and at termination of the run (breakthrough or head loss limitations).

Between the raw waters, RW50 has a significantly higher gradient in the top of the filter at the end of the run than the other two raw waters. This is seen for both filter F/F and A/S, and is the main reason for the higher k values for this raw water. For filter F/F the storage capacity for RW50/6 is slightly higher than for RW50, at the same time the head loss gradient at breakthrough is higher for RW50 in almost all the sections of the filter. For RW50 relatively more solids are stored in the top layer than in the bottom layer. This indicates that for this raw water more solids are captured early in the filter bed. Because the dosage used for all these experiments are identical, there is reason to believe that there are more free positive sites on the polymer chains from coagulation of RW50, than when using the same dosage on a raw water with higher coagulant demand (turbidity also). When flocs of humic substances and chitosan get into the filter, the positive sites on the polymer chains can attach to the filter grains.

Boller and Kavanaugh (1994) suggested that head loss development was related to the number of particles captured, due to a lower density (contains more water) of deposits for higher number of particles. They calculated deposit densities from several investigations of deep bed filtration and showed that discrete particles can reach very high packing densities compared to hydroxide flocs that formed loose deposits with high water content.

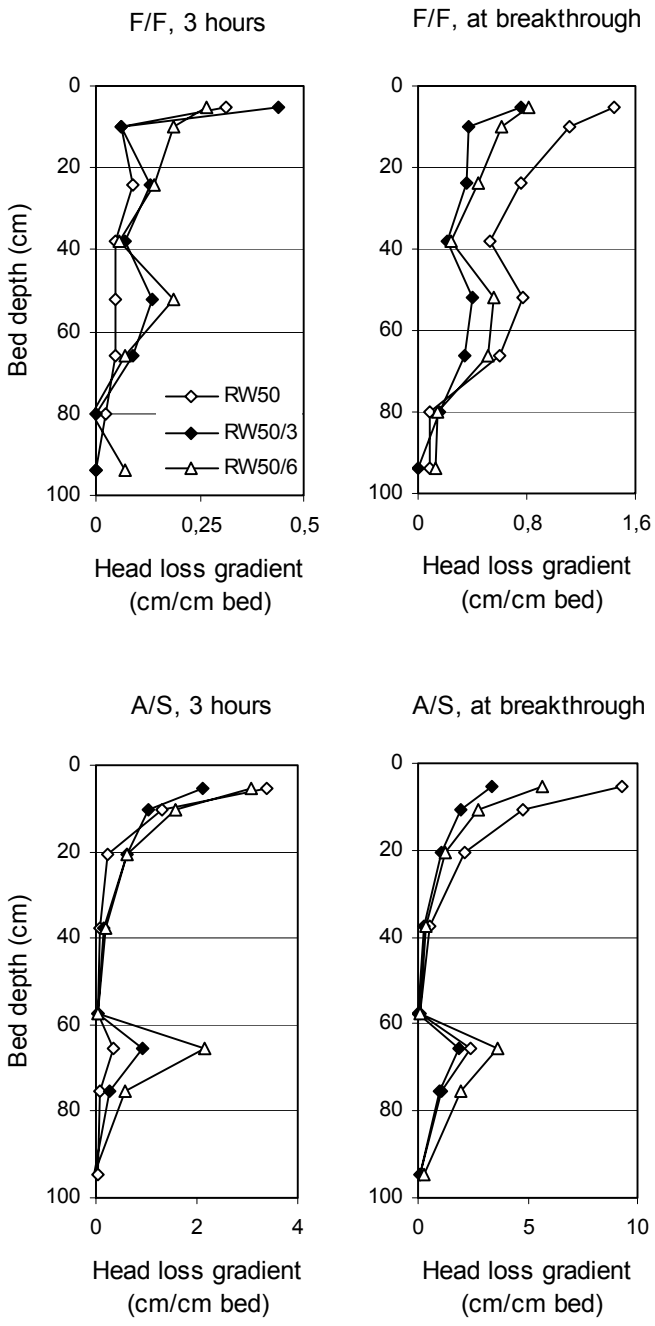

Figure 6.28 Head loss gradients for the experiments with different raw water turbidity. After 3 hours of filtration and at breakthrough (effluent turbidity > 0,3 NTU).

6.3.5 Polymer as filter aid

To overcome the problems related to loose hydroxide-humic flocs and early breakthroughs when using a metal salt to remove humics by coagulation and filtration, experiments using a polymer as filter aid were carried out. A filter aid is very useful in situations where the breakthrough occurs before head loss limitations are reached, to extend the length of the filter run. After coagulation the water was lead to a column of water providing about 4 minutes of coagulant reaction time before the filter aid was added just prior to filtration. The filter aid used was a non-ionic, high molecular weight polymer (Magnafloc LT20). When using a non-ionic polymer, the flocs formed after coagulation must be sufficiently destabilised, i.e. the double layer thickness must be reduced to the extent where close contact can be obtained between the colloids and the polymer. It was observed that addition of filter aid right after coagulation did not have the desired effect on filtration run lengths. The dose of coagulant was in most cases kept at the same level as for the runs without filter aid to get a proper removal of organic matter.

Effects of filter aid in the three filters
The following examples are comparing results for experiments with and without the addition of filter aid in the three filters used in this study.

The experiment without filter aid in F/Fwhen ALS was used as coagulant did not produce effluent turbidity below 0,3 NTU, which is the limit for satisfactory water quality set in this study. When adding 0,05 mg/l of the non-ionic polymer as filter aid however, the effluent turbidity decreased from 0,53 to 0,2 NTU. For the ALS experiment with polymer addition, a remarkably long filter run was obtained in the Filtralite (F/F) filter at the relatively low polymer dose used. In filter A/S, effluent turbidity is low without polymer compared to filter F/F, and only a slight decrease with polymer addition is experienced. The run length in F/F is terminated by breakthrough, and therefore a higher polymer dose can be used to further increase run length. In A/S the experiment with filter aid is limited by head loss, and a reduction in polymer dose could increase run length for this filter.

When PAC is used as coagulant in filter F/F+, it looks like the gain in run length is not that high compared to the runs with ALS as primary coagulant. This might be due to the higher filtration rate used in this experiment. As seen before, PAC coagulated organic matter creates more filterable flocs than when ALS is used. However, the effect of the non-ionic polymer on filter run times is higher in combination with ALS than with PAC.

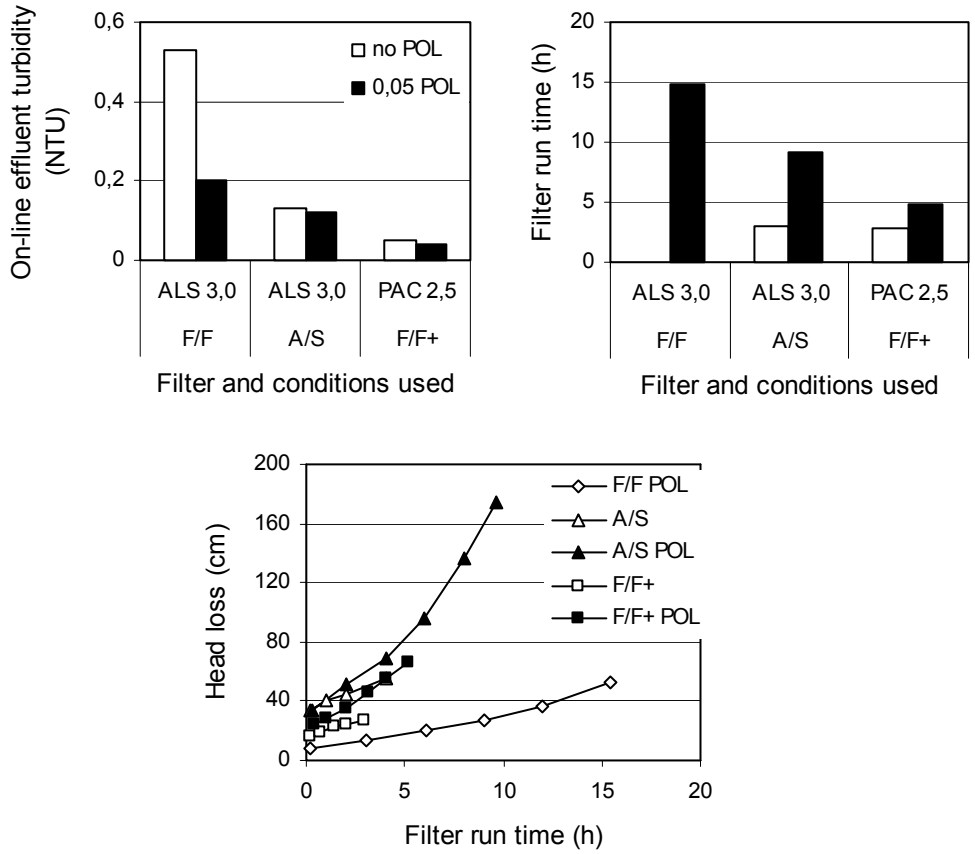

Figure 6.29 Results from experiments with and without polymer as filter aid for filter F/F, A/S and F/F+. (RW50, 7,5 m/h for F/F and A/S, 12,5 m/h for F/F+).

An almost linear trend is seen for the head loss curve of filter F/F, compared to A/S where the curve clearly is exponential. This is taken as an indication that surface layer deposition takes place in the top section of the anthracite because of the larger and stronger particles (and deposits) formed by adding polymer. For the run without polymer in A/S results show that head loss build up is slower, compared to results with polymer, and no indication of surface deposits is seen. The head loss in F/F+ is relatively high because of the higher filtration rate used in this experiment. It can also be seen that H_0 for the run with polymer was higher than for the run without, this is probably a result of initial porosity differences in a part of the filter bed, after the grains have settled from backwashing.

Due to the differences observed in head loss development, head loss gradient curves for the different experiments were studied.

What is seen from the head loss gradients in Figure 6.30 is that filter F/F, which is less effective than the other filters, store deposits much more evenly in the filter bed. After 3 hours of filtration only small gradients are seen for filter F/F, but at breakthrough the gradients for this filter are relatively high.

In filter A/S the experiment without polymer shows indications of deposits in the top of the two filter layers after 3 hours of filtration (breakthrough). After 3 hours of filtration with polymer addition, gradients in the top anthracite section, are the same, but in the top section of the sand layer the run with polymer show higher values. This is where the difference in head loss is for these experiment, showing that relatively more solids are stored in the sand layer when a filter aid is used. At HL limitation the run with polymer show high gradients in the top sections of anthracite and in the upper most section of the sand. If this run had been carried on, there would probably have been more deposits stored deeper down in the sand layer. When the run was HL limited, the deposits "saturation front" had not yet reached deeper layers in the sand and storage capacity was still available.

The experiments in the deeper F/F+ show differences between the gradients after 3 hours of filtration for the runs with and without polymer. The effect of polymer on storage capacity and corresponding head loss gradients in the upper parts of the filter is clearly demonstrated by the results. The gradients at a depth of 120 cm (bottom of top layer) and at 180 cm (bottom of bottom layer) show very little difference between the three situations. This is probably an indication of the limitation of the filter layer to remove flocs of a specific size range. What can be removed with the coarse grains in the top layer is already removed from the suspension at a depth of 120 cm, and likewise for the bottom layer.

When adding polymer as filter aid one is not adding any suspended solids, but the fraction of flocs bigger than 0,45 µm can be higher compared to the situation without polymer. During the filtration experiments it was clearly observed that the polymer made large visible aggregates of the existing Al-humic flocs.

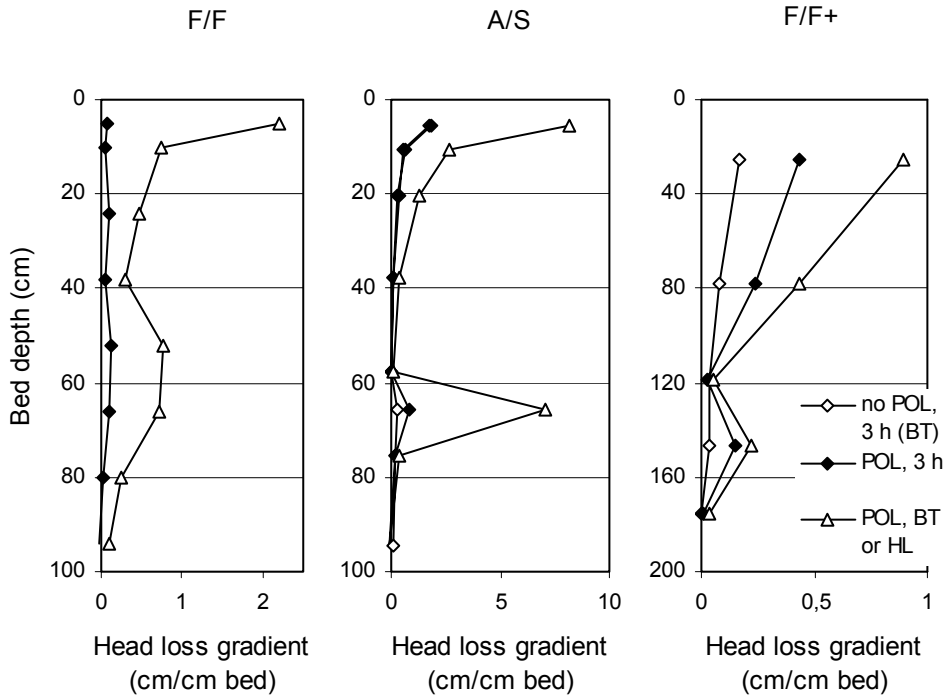

Figure 6.30 Head loss gradient curves for experiments with and without polymer addition shown in Figure 6.29. Legend show run time (h), breakthrough (BT) or head loss (HL) limitations.

Dose effects

The effect of a too high polymer dose was experienced in a run with 2,5 mg Al/l as PAC and 0,2 mg/l polymer. This run had to be terminated before breakthrough or head loss limitations were reached due to surface deposits, and the large mud-balls formed in the top filter sections of both filters had to be gently broken by a plastic pipe during fluidisation. The occurrence of operational problems when using too high polymer doses is also described elsewhere (Eikebrokk, 1982). In Figure 6.31 some results using PAC and FEC as coagulants in combination with the non-ionic polymer as filter aid are shown.

An increased polymer dose reduces effluent turbidity both in combination with PAC and FEC. Lower turbidity is obtained when using PAC as coagulant than when FEC is used. The run lengths obtained when using FEC and filter aid are short, however with a slight increase for the higher polymer dose. These run lengths are however very similar to the ones obtained without the use of filter

aid. The experiment with PAC and 0,05 mg/l of polymer show a run length of about 6,5 hours, longer than for the FEC experiments, and a significant improvement compared to the results without polymer. Due to the circumstances described earlier, the run with 0,2 mg/l of polymer was stopped after 6 hours, and as seen this run shows an exponential increase in head loss. The run with a lower polymer dose has an almost linear head loss development, indicating no surface layer deposition.

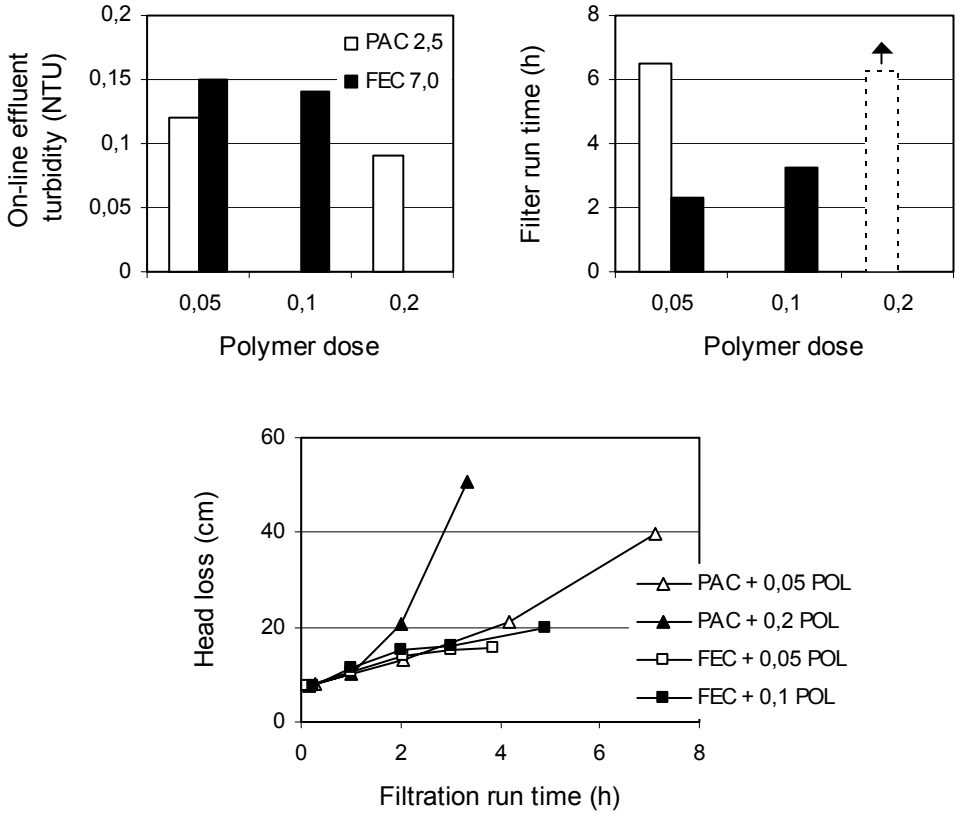

Figure 6.31 Results for experiments with PAC and FEC as coagulants with different doses of filter aid in filter F/F. (RW50, 7,5 m/h).

The head loss curves for the experiments with FEC and filter aid show a decline in slope after about 2 hours. Why the head loss slopes have a breakpoint after about 2 hours is not known. However, the ripening period for these two runs were especially long, and this has probably influenced the development of these two runs.

From the head loss gradient curves in Figure 6.32, it can be seen that there is no increase in head loss in the second section from the top of the filter, and low values in the upper most section using FEC and polymer. Both experiments with FEC show relatively high gradients in the bottom layer of the filter compared to the top layer. The flocs made from the combination of FEC and polymer are probably smaller than the ones made using PAC with polymer (also seen from visual observation in the filter columns). A polymer dose of 0,2 mg/l together with PAC was too high, and the surface layer deposits are clearly seen in Figure 6.32. The gradient in the top section of the filter is as high as what is normally observed in the anthracite/sand filter, and deposition is not seen in any other parts of the filter bed. A reduction of the polymer dose to 0,05 mg/l, reduce the top section gradient, and evidence of increased deposition deeper down in the filter is clearly seen.

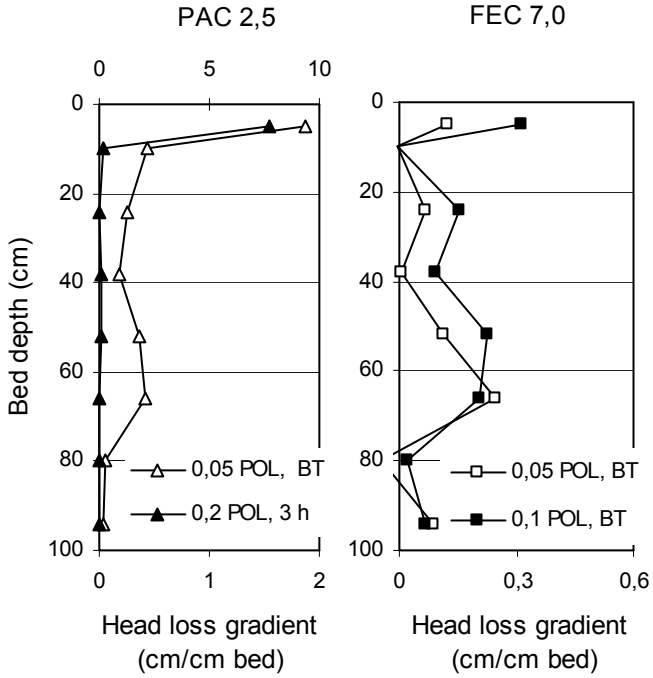

Figure 6.32 Head loss gradients for experiments with PAC or FEC in combination with polymer as filter aid. (PAC + 0,2 mg/l polymer use top axis).

6.4 Summary of chapter 6

Filtration experiments at the established optimum doses and pH conditions were carried out in the pilot plant until limiting conditions in effluent water quality (breakthrough) or head loss, were reached.

6.4.1 Filter bed properties

The three filter bed configurations tested was a fine-grained anthracite/sand filter, a coarser grained Filtralite filter and a deeper Filtralite filter. All the three filter beds were dual media in relation to grain size fractions.

- Generally, the coarser grains in the Filtralite filter did not produce as good water quality as the anthracite/sand filter when compared for equal filter bed depth.
- For coagulated water low in suspended solids the difference in effluent water quality between the two filters was small. This was also the case for all raw waters when chitosan was used as coagulant.
- Head loss build up was, due to the difference in grain size, much higher for the anthracite/sand filter compared to the Filtralite filter. In cases where both filters produced satisfactory water quality, filter run times were considerably longer for the Filtralite filter, because the anthracite/sand filter was limited by head loss.
- When chitosan was used as coagulant, the head loss build up per weight fraction of solids in the influent to the filter was higher than when a metal salt was used. This was beneficial for the coarse Filtralite filter with much head loss available.
- The deposition in the depth of the Filtralite filter was more evenly distributed than in the anthracite/sand filter, where deposits mainly were located in the top sections of the anthracite and sand layers.
- The deeper Filtralite filter bed could compensate for the coarser grain size by producing equal or better water quality when PAC or CHI was used as coagulants.

6.4.2 Filtration rate

- The coarse Filtralite filter was more sensitive, with regards to effluent water quality, to high filtration rates than the anthracite/sand filter when a metal salt was used for coagulation.
- When chitosan was used the influence of filtration rate was generally small for all filters tested.

- An increased filtration rate transport the deposits further down in the filter bed. This gives lower storage capacity in the top of the filter bed for equal conditions, and result in early breakthrough.

6.4.3 Ripening and breakthrough

- Experiments have shown that deposition is a dynamic process that proceeds down the filter bed depth. A solids front progress down the filter bed, and when this front reaches the bottom section of the filter, breakthrough occurs.

6.4.4 Raw water quality effects

- An increased turbidity level in the raw water enhanced the removal of turbidity and residual metal in both filters, however, the performance was more improved in the Filtralite filter compared to the anthracite/sand filter.
- For all the raw waters tested, filter run time as a function of solids load, is independent of raw water quality. Considerable longer filter run times were seen however, when CHI was used for coagulation instead of a metal salt.
- The humic substances in the raw water form voluminous flocs with both CHI and the metal salts tested. These flocs are more easily captured in the top section of the filter than flocs formed from raw waters containing higher levels of turbidity.

6.4.5 Polymer as filter aid

- The available head loss in the coarse Filtralite filter can be fully utilised when a polymer is used as filter aid in addition to a metal salt for coagulation. This also resulted in considerable improvements in effluent water quality.
- Some minute's reaction time for the coagulant was needed before polymer addition.
- Filter aid enhances the growth of flocs and the strength of the deposits in the filter.

7 MATHEMATICAL MODELLING

7.1 Clean bed efficiency

The clean bed efficiency model shown in Chapter 2.3.4 was used to model some of the experiments from this study. This is a mechanistic model based on the three main particle transport mechanisms in filtration: interception, sedimentation and diffusion. It can be used as a tool to study effects of filter bed or suspension modifications on the removal efficiency. In this chapter it is used to predict the removal efficiency for special particle characteristics in a model of the actual filter bed. The calculations are based on spherical filter grains, and only one particle type can be modelled at a time. If the model is used to compare actual removal efficiencies in a filter bed, with raw water containing poly-disperse particles, the calculated particle size must be recognised as a representative particle size of the suspension.

The clean bed removal efficiency must be approximated to the situation just after the high initial ripening peak in turbidity that mainly consists of backwash water remnants.

As seen from Figure 2.9 the difference in predicted removals between F/F and A/S are huge for the situation described. From Figure 2.8 one can see that if equal removals are going to be obtained in the two filters, the suspension must generally contain denser and bigger flocs.

The calculations used in the following model predictions are based on the model of Rajagopalan and Tien (1976) for the single collector efficiency (Equation (2.25)), and the relationship of C/C_0 (Equation (2.24)) presented by Yao et al. (1971). The three filter beds used in the modelling are presented in Figure 7.1, and are models based on the pilot filter beds used in this study. The constants used in the calculations are listed in Table 7.1.

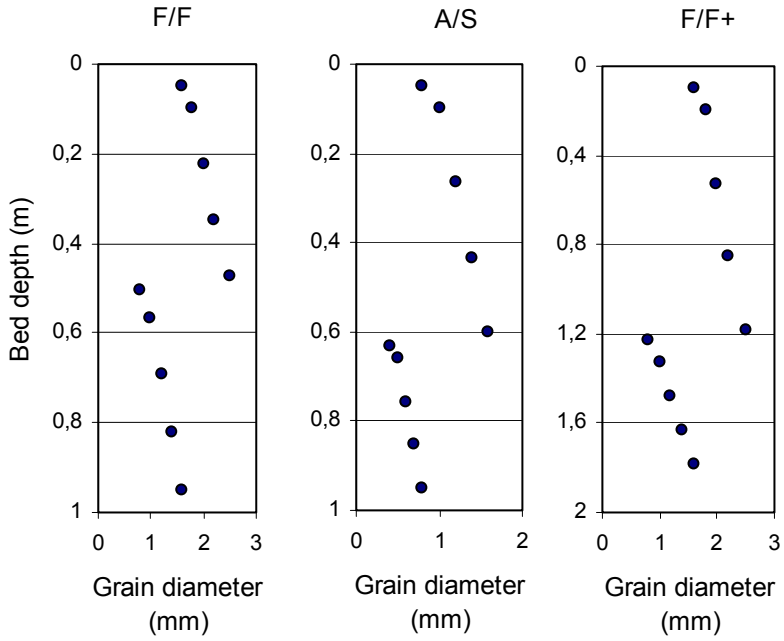

Figure 7.1 Models of the three filter beds used in the following predictions.

Table 7.1 Constants used in the model predictions of clean bed head loss for filter F/F, A/S and F/F+.

	Parameter	**Value**	**Comment**
Filter F/F	Porosity (f_0)	0,7/0,6	Top/bottom layer
Filter A/S	Porosity (f_0)	0,55/0,43	Top/bottom layer
Filter F/F+	Porosity (f_0)	0,7/0,6	Top/bottom layer
Boltzmann's constant	k_B	1,38e-23	[J/K]
Hamaker's constant	k_H	1,0e-20	[J]
Temperature	T	283	Absolute temperature, [K] (equals 10 °C)
Water viscosity	μ	1,31e-3	[N·s/m^2]
Water density	ρ	999,7	[kg/m^3]

When the filter beds are designed and the constants used in the equations are as in the above table, the variables are filtration rate (v), suspended particle size (d_p), suspended particle density (ρ_p) and the collision efficiency factor (α). The collision efficiency factor is defined as the number of successful particle-filter grain contacts divided by the total number of contacts that occur. Therefore this parameter reflects the chemistry of the system, and is equal for one specific suspension and pre-treatment. When comparing results for the three filters treating the same influent, the variables mentioned are equal for all filters.

7.1.1 General effects

In the figures below the C/C_0 relationship in filter effluent water is modelled for the three filters beds, with different filtration rates and particle characteristics. The particle sizes and densities are selected in order to see pronounced effects and the parameter values are taken from the findings of other researchers.

Figure 7.2 shows the results of different filtration rates on the removal of 5 and 50 μm particles with a density of 1050 kg/m^3. This particle density is probably representative for the particles formed from coagulation of humic substances by a metal salt, which is known to form loose and voluminous flocs (Rebhun et al., 1984), (Hossain and Bache, 1991).

Figure 7.2 show that an increase in filtration rate from 5 to 15 m/h does not have a crucial effect on the removal of 50 μm particles. In filter A/S the large particles are almost entirely removed in the top anthracite layer, also at 15 m/h filtration rate. Although the large particles are totally removed in the top layer of filter A/S, the small particles (5 μm) experience very little removal in the top layer. The small particles are much better removed in the sand layer than in the bottom layer of the two Filtralite filters, but the effluent from A/S still contain about 50 % of the influent 5 μm particles. This results for the A/S filter give a picture of large particles deposited in the top layer and small in the bottom layer.

The small particles are very sensitive to filter media grain size, and almost no removal is obtained in the Filtralite filters. These particles are difficult to remove because they are light (not very effective sedimentation), too small for effective removal by interception and too big for effective removal by diffusion. The large particles are almost completely removed in the F/F+ filter at a filtration rate of 5 m/h, while about 10 % penetrates the bed and end up in the effluent at 15 m/h. The distribution of the large particles in F/F+ is much more even than for A/S and head loss build up will be much slower with time for this

bed. In F/F the depth of the bed is not sufficient to remove all the large particles, even at 5 m/h filtration rate.

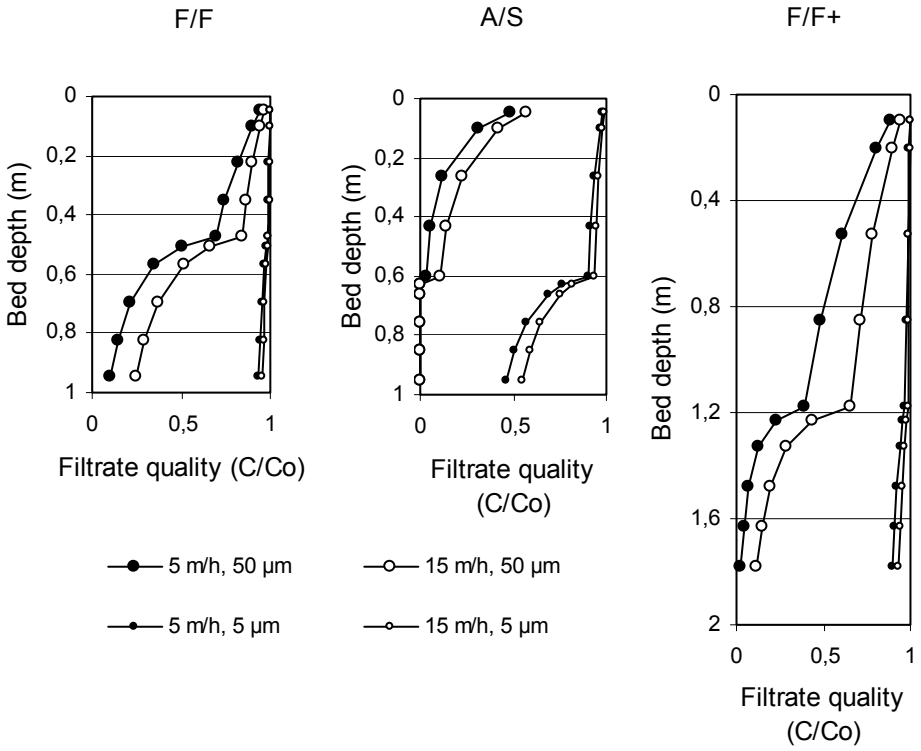

Figure 7.2 Predicted effects of filtration rate and particle size on the removal efficiency in filter F/F, A/S and F/F+. Particle density, ρ_p = 1050 kg/m^3, collision efficiency factor α=1.

The overall impression of the effect of filtration rate is that an increase makes the bed less effective, but this can give a positive effect because particles are deposited more evenly in the filter bed, utilising the depth of the filter.

In Figure 7.3 the effect of higher particle density and lower collision efficiency (from insufficient pre-treatment) is studied. The particle size used is 50 µm at a filtration rate of 15 m/h.

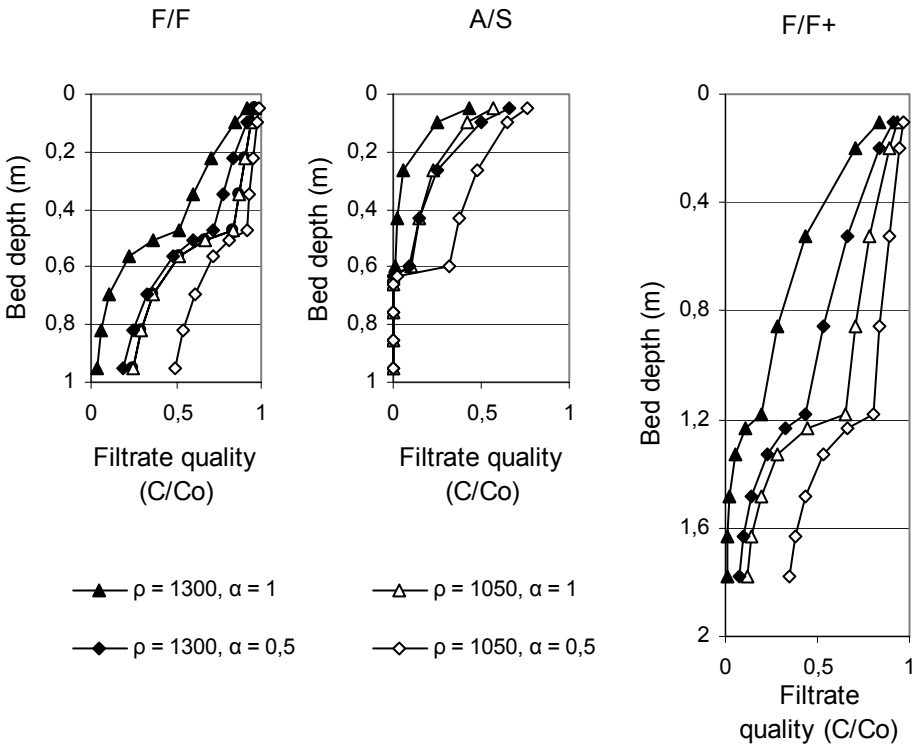

Figure 7.3 Predicted effects of particle density and collision efficiency in filter F/F, A/S and F/F+. Particle size d_p = 50 µm, filtration rate v = 15 m/h.

As can be seen in Figure 7.3 these large particles are still completely removed in the A/S filter when the collision efficiency factor is reduced to 0,5 (α is proportional to $\ln(C/C_0)$). The effect of an insufficient destabilisation (pre-treatment) is more pronounced for low particle densities. Very little of these particles enters the sand layer, but for the fraction who does, they are removed by the small grain sizes of the top sand section. The model predicts that the removal of particles from suspension is faster for the more dense particles when seen from the top of the filter and going downwards.

The effluent water quality is about the same for particles with a density of 1300 kg/m^3 as for the 1050 kg/m^3 particles in F/F and F/F+ respectively, when 50 % of the collisions between particle and grain result in attachment for the more dense particles. The distribution in the filter bed are different however, indicating that large grain sizes is very sensitive to particle density, mainly because they have to depend on sedimentation as the removal mechanism.

For comparison, about 45 cm of top layer Filtralite media (equal in F/F and F/F+, 1,6 mm size) and about 4 cm of top layer anthracite (0,8 mm size) is needed to remove 50 % of the 50 μm, 1300 kg/m^3 particles. This is predicted by the model, and is a result of the difference in grain size.

7.1.2 Prediction of experimental results

Attempts to use experimental values of influent water turbidity to predict effluent water turbidity failed. The idea was to find a characteristic particle size and density for a suspension, which could be used for the three different filters. There were generally a huge difference in predicted effluent quality between A/S and the two coarse Filtralite filters. The model showed a better removal for the A/S filter and poorer removal for the F/F and F/F+ filter for equal suspension conditions, compared to experimental results. The main reason for the lack of fit between model and experimental data is probably that the contact filtration process has similarities with an adsorption process, and cannot be considered as only a particle separation process. There are few opportunities, especially in the raw water with low turbidity, for particle-enhanced precipitation before the water enters the filter. In the filter bed, precipitation can occur on filter grain surfaces. Eikebrokk (2001) suggested that hydroxide precipitate formation happened inside the contact filter, and that the hydroxides acted as effective NOM adsorbers.

7.2 Head loss-specific deposit model

In this study the head loss gradient (cm/cm bed depth) is used to understand differences in deposit distribution in the filter bed depth. The head loss gradient is of coarse dependent on the initial head loss in a filter layer, and direct comparison is only possible between the same filter sections. Most head loss models that are developed for deep bed filters are relating the head loss gradient at a specific deposit volume (l/l bed) to the initial head loss gradient. Boller and Kavanaugh (1995) used the equation below to compare experimental results from several filtration studies of shallow layer filters. Suspensions used in the studies were mono-sized latex and TiO_2 suspensions, and heterogeneous Fe-hydroxide particulates. In all studies particle mass balances where performed, together with particle size and density measurements.

$$\frac{I}{I_0} = \left(1 + p\frac{\sigma_v}{f_0}\right)^x \left(1 - \frac{\sigma_v}{f_0}\right)^y \tag{7.1}$$

Boller and Kavanaugh found a good fit between experimental and predicted data using the constants p = 35, x = 1,5 and y = -1. σ_v is specific volume of deposits (l/l bed) and f_0 is clean bed porosity.

In this study the head loss gradient ratio model described is used to predict deposit volumes, and in combination with measured solids loads, to calculate solids content in deposits.

In the previous evaluation of filtration results the head loss gradient was used with the initial gradient subtracted ($I-I_0$). This does not take into account the initial porosity difference of the different filter media, it only consider the increase in hydraulic gradient due to deposits. The expression for I/I_0 also provides a normalisation for the difference in initial head loss. In fine-grained sections of the filter bed, little deposits are needed to create a considerable head loss, implying that higher head loss gradients are needed in fine-grained sections to store equal amounts of deposits.

7.2.1 Specific deposit

When studying filtration results of iron oxide flocs, Camp (1968) found that the volume of the floc was not substantially reduced after deposition. At the end of a filter run the deposits in the top of the bed are exposed to high shear forces due to the narrowing of pore space, however, this did not result in a considerable loss of water from the deposit. This implies that at any depth and time the deposition volume rate in a filter layer equals the rate of floc volume removed.

The model described was used on each layer of the F/F and A/S filter beds using experimental values of I/I_0 from the filter runs. By doing this the specific deposit volume in each layer, and the total specific volume, of the bed could be calculate. The initial bed porosities were as described in Table 7.1. In Figure 7.4 the head loss gradient ratio (I/I_0) is described as a function of total specific deposit volume for filter F/F and A/S for an experiment where CHI is used to treat RW50. Also shown is specific deposit as a function of filter run time.

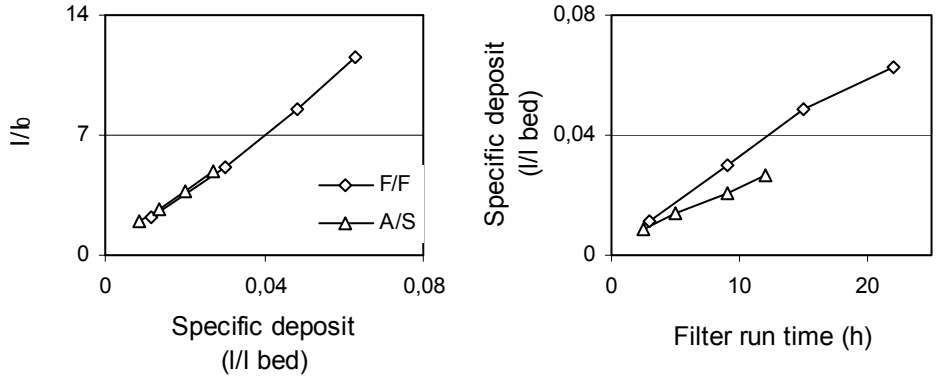

Figure 7.4 Head loss gradient ratio as a function of predicted values of total specific deposit (left), Specific deposits as a function of run time (right), (RW50, 4,0 mg/l of CHI).

The figure shows that the relative head loss increase in filter F/Fand A/S is equal for equal total specific volume deposited, regardless of the difference in filter bed properties. This result indicate that the model is able to predict the deposited volumes in the filter bed in a way that considers initial porosity and differences in deposit distribution in the bed depth. However, looking at the difference between F/F and A/S when specific deposit is seen as a function of run time, they indicate a rather large difference between the two filters. The increase in specific deposit volume is more rapid in filter F/F than in filter A/S, implying that the experimental I/I_0 values indicate that a higher fraction of the pore volume is occupied in F/F than in A/S for the same influent water. If all incoming SS is assumed to be removed, (effluent turbidity from both filter F/F and A/S were below 0,06 NTU), the deposits in A/S must contain more solids, i.e. have a higher density. This can be a result of deposit compaction due to narrow pore space and higher pore velocities, or less entrapped water.

One of the findings of Boller and Kavanaugh was that the larger the number of particulates deposited, the lower the deposit density, and therefore the available pore space is more quickly occupied. This results in a more rapid increase in the hydraulic gradient. They found that the head loss gradient ratio increased more rapid in a coarser filter media than in a fine grained media, and explained this by the higher number of particles captured at each grain in the coarse bed (due to fewer grains) giving looser structure of the deposits.

This can be compared with the curves showing I/I_0 as a function of time, indicating that equal mass of deposits (= equal mass of influent flocs in this case), create a more rapid relative head loss increase in filter F/F than in A/S.

In Figure 7.5 the specific deposit volumes as a function of run time for the experiments with CHI and RW50/3 and ALS with RW50 are shown for both filter F/F and A/S. The head loss gradient ratio as a function of specific deposit volume was similar for the two filters in each experiment, as shown for Chi with RW50 in Figure 7.4.

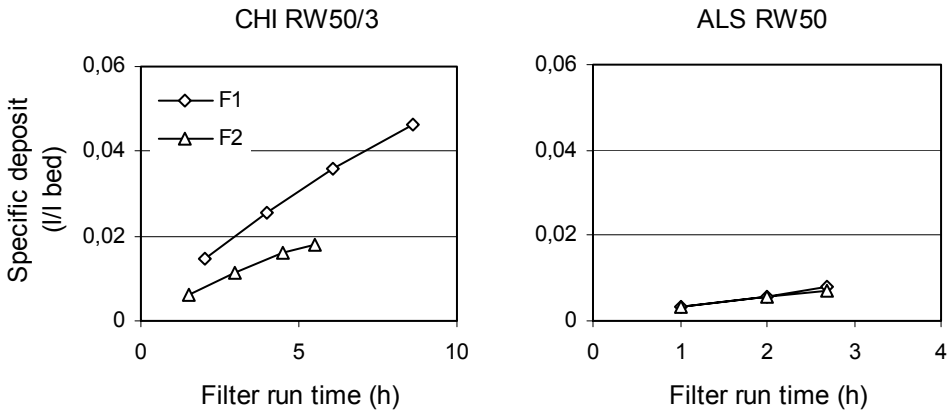

Figure 7.5 Specific deposit volume (l/l bed) as a function of run time for filter F/F and A/S. (RW50/3 with CHI, RW50 with ALS).

The predicted deposit volumes using CHI to treat RW50/3 show a higher deposition in F/F than in A/S with increasing time, as seen in Figure 7.4. This is probably a result of more voluminous deposits with a lower density in F/F. The effluent turbidity was below 0,05 NTU for both filters, indicating an equal removal of suspended solids. The higher volumes deposited in F/F is therefore no indication of a higher removal rate for this filter, but rather a deposit density characterisation. This is based on the assumption that all the SS is removed when the effluent turbidity is below a certain limit. When the effluent turbidity is higher, the amount of suspended solids in the effluent is also higher, and this should show as lower values of deposited volumes.

The experiment using ALS with RW50 show an equal development of specific deposit volume with time for the two filters. The effluent turbidity for filter F/F and A/S (in the period of stabile water quality production) were 1,05 and 0,13 NTU respectively. It is likely that this suspension give rise to differences in deposit density as seen for the other two suspensions. Therefore, an equal

deposition of volume with time indicates lower removal in F/F than in A/S as demonstrated by the effluent turbidity results.

From the results shown it is clear that using deposited volume to study removal efficiency differences between the two filters is not straightforward. What is indicated as a higher volume deposited in F/F than in A/S, cannot be taken as higher removal efficiency for this filter, but mainly as a result of lower deposit density for this filter.

7.2.2 Deposits solids concentration

As predicted by the model the content of suspended solids in the deposits varies with the porosity of the filter bed for the same suspension. The specific deposited volumes calculated are total deposit volume averaged over the whole depth of the filter bed. As previously shown, the amount of deposits differs much between the sections in the bed, and so probably also the solids content of the deposits. The calculations of solids concentration in the deposits are therefore an average for the whole filter bed depth.

Camp (1968) stated that the removal of flocs in a filter is controlled primarily by the principal component of the floc, i.e. water. He found that 85-99 % of the floc volume could be occupied by water for ferric and aluminium oxide flocs. From this it is clear that flocs (and deposits) with high solids content are of great importance for the efficiency of filtration.

In Figure 7.6 the solids load to the filters and the volumes predicted by the model is used to calculate the solids concentration in the deposits. However, this is not the deposit density because the fraction of deposit volume that is occupied by the influent solids, and how much is entrapped water, is not known. The relationship between specific mass and volume deposited can be described by:

$$\gamma = \frac{\sigma_m}{\sigma_v} \tag{7.2}$$

Where σ_m is deposited mass in (g SS/l bed), σ_v is deposited volume in (l/l bed) and γ is solids concentration in deposits (g SS/l deposit). σ_m is calculated from the equation below, on the assumption of total suspended solids removal:

$$\sigma_m = \frac{vC_0t}{1000 \cdot L} \tag{7.3}$$

Where v is filtration rate (m/h), C_0 is influent suspended solids (g/m^3), t is filter run time and L is total bed depth (m). The two equations are used to construct the curves in Figure 7.6.

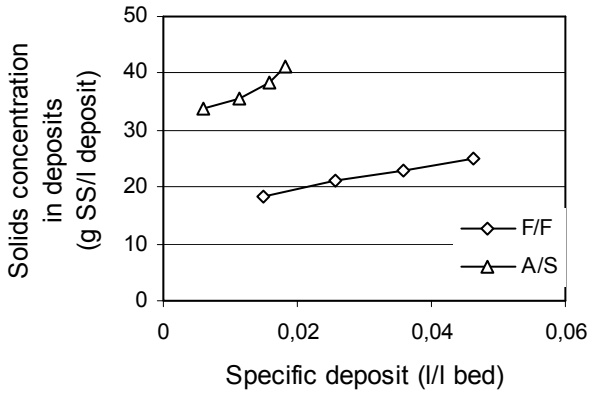

Figure 7.6 Solids concentration of deposits as a function of deposit volume for filter F/F and A/S. (RW50/3, 4,0 mg/l CHI.)

The curves indicate that the concentration of suspended solids in the deposits is increasing with increasing specific deposit volume for both filters. The solids concentration is considerably higher for A/S than for F/F, as was expected. When more and more flocs are deposited, more and more water is captured inside the deposits, however, because the deposit solids concentration increase the deposit density is increasing. The increase in deposit density can be a result of compaction of the deposits, which also is suggested by other researchers (Sembi, 1981).

Contrary to the results presented here, Boller and Kavanaugh (1994), experienced a decreasing deposit density with increasing deposited volume of particles using shallow (5-15 cm) layer filters.

It is possible that the increase in solids content in the deposits observed in this study is created by the fact that new deposit sites continuously are being used as the suspended solids penetrate further down in the filter bed. The contact filtration process has similarities with an adsorption column process, as shown in chapter 6.3.3. This indicate that the increase in deposit volume is not only

created by the growth of already used deposit sites in the upper part of the bed, but also by "new" sites further down in the bed. The increase in slope for filter A/S at the end of the run might indicate that the breakthrough has started, and the assumption of total SS removal is no longer valid. The steeper slope for filter A/S than F/F might be a result of more grains available (more new sites) for solids deposition in this filter, and therefore a more rapid developing increase in solids concentration.

Table 7.2 shows the predicted deposit characteristics for some combinations of raw water and coagulant in the two filters. Mass capacity and solids concentration in deposits are based on 100% suspended solids removal.

Table 7.2 Predicted deposit characteristics and capacities.

Filtered suspension	**Filter**	**Maximum volume capacity** (l deposit/l bed)	**Maximum mass capacity** (g SS/l bed)	**Solids concentration in deposit** (g SS/ l deposit)
RW15 ALS	A/S	0,027	0,51	18,9
RW50 ALS	F/F	0,008		
	A/S	0,007	*(0,37)*	*(51,2)*
RW50 CHI	F/F	0,063	1,72	27,4
	A/S	0,027	0,94	35,0
RW50/3 CHI	F/F	0,046	1,16	25,1
	A/S	0,018	0,74	41,0
RW50/6 CHI	A/S	0,017	1,03	60,0

In the experiments where ALS was used to coagulate RW50, the capacity for mass deposition and the solids concentration in the deposits are not shown for filter F/F due to low removal of suspended solids (higher effluent turbidity). The high solids concentration for the A/S filter indicates that there is a SS leakage also for this filter (effluent turbidity about 0,13 NTU). These experiments are the ones that experience an early breakthrough in turbidity. The predicted deposit volumes for these filter runs show low maximum values. This indicates that breakthrough does not come as a result of high head loss values (i.e. high volume deposits) because it occurs for low values of deposited volume.

Rebhun et al. (1984) found deposit solids concentrations of 20,3 g/l for humic acid coagulated with aluminium sulphate, and as high values as 120 g/l when a

cationic polymer was used to coagulate kaolin clay particles. They measured the solids concentrations in and out of a filter layer to obtain the mass deposited, and stated that the significant differences in maximum mass capacities for a given filter bed must be due to differences in densities between the deposits of different suspensions.

7.2.3 Deposition front advancement

The similarities between fixed bed adsorption columns and contact filtration in deep beds is clearly shown in this study and by others (Adin and Rebhun, 1977). In Figure 7.7 the specific deposit values for the three experiments using CHI with RW50, RW50/3 and RW50/6 is shown for the top sand section (8 cm) of A/S. The curve for RW50 show indications of a deposition front of solids that is moving down the depth of the filter bed, and reach the top sand section after about 3 hours. Deposited volumes are detected in the beginning of the run for RW50/3 and just after start up for RW50/6.

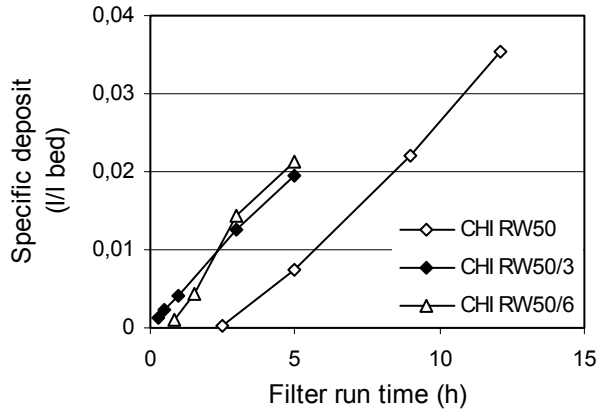

Figure 7.7 Specific deposit for the top section (8 cm) of the sand layer in filter A/S. (CHI with RW50, RW50/3 and RW50/6.

If the filter is compared to an adsorption column, how fast the deposition front advance down the depth of the filter controls breakthrough. The differences in advancement of this front, between the different suspensions, are controlled by the filterability/adsorbability of the flocs formed in the actual filter media.

7.3 Adsorption modelling

In a fixed-bed adsorption column the concentration of the solute that is going to be removed from the suspension, change with time and position in the bed. As the suspension travels through the bed, the concentration in the suspension

drops from the inlet concentration to a minimum concentration over a distance in the bed called the mass transfer zone. This zone moves down the bed leaving the adsorption media saturated with solute. The concentration curve of solute in the fluid, called the breakthrough curve, has after a period of time reached the outlet of the column. The process is stopped when the outlet concentration reaches its maximum permissible level.

7.3.1 Comparison of filtration and adsorption

In depth filtration the mechanisms of particle removal are well described, and can be predicted with the use of mechanistic models. Depth filtration and adsorption have major differences in the development of concentration with time. In filtration the "mass transfer zone" is thought to be stretching from the top to the bottom of the filter depth as shown in Figure 7.8, while adsorption is using a limited depth section which travels down the column. If a filter is made deeper, the effect would clearly be a postponed breakthrough and a lower effluent particle concentration according to the first order relationship proposed by Iwasaki (1937), as shown in Equation (2.18). This is experimentally observed in this study, implying that particle separation by traditional filtration mechanisms plays an important role in contact filtration. The effect of bed depth on run length in filtration is not as easy to predict, and a linear increase of run length with depth (before breakthrough) as in adsorption might occur.

The profiles from Figure 7.8 show that because the adsorption media is equally efficient in the whole depth, and because the C_0 concentration travels down the filter, saturation until $C/C_0 = 1$ is achieved in section after section. In filtration the C_0 concentration is only the incoming concentration for the top layer, therefore a depth filter is less effective further down in the bed. In contact filtration, which seems to behave as a combination of these to processes, saturation of a layer in the filter happens probably before C/C_0 have reached a value of 1. The saturation of a layer and deposition front depth in the bed is probably dependent on factors like grain surface area, filtration rate, coagulant used and suspension. In adsorption it is common to study the breakthrough curve for capacity calculations and scale up design methods.

In Figure 7.9 the C/C_0 breakthrough curves of an experiment using FEC for coagulation of RW50 is shown. The concentration used in this example is on-line effluent turbidity measurements.

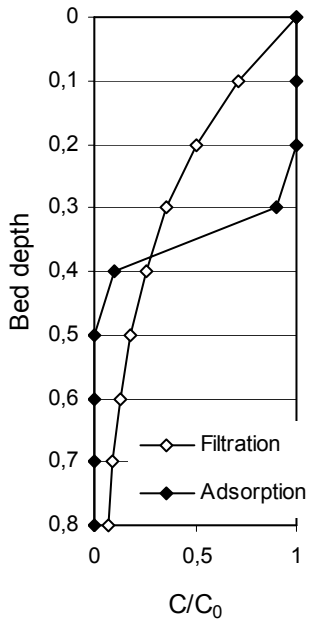

Figure 7.8 Typical concentration profiles in the depth of a filtration column and an adsorption column.

As seen from Figure 7.9, the top peak of the ripening period is chosen as the C_0 concentration. The reason for doing this is that the last peak of the ripening, before a stable condition is obtained, (normally two peaks are seen) is caused by influent solids passing through the filter (Amirtharajah, 1988). Due to the lack of separate flocculation units in contact filtration, floc formation (at least parts of it) is thought to be happening inside the filter bed. Therefore, using a measurement of turbidity that has been exposed to filter pore flocculation might give an indication of available turbidity in the water. Most of the C_0 values used are also confirmed by jar test experiments (with filtration through 13 μm filter paper prior to analysis) using the same suspensions and coagulant doses (Kvinnesland, 2002). After about 2 hours of low effluent turbidity, the breakthrough starts in both filter F/F and A/S. The fluctuations in turbidity during the breakthrough period is due to small variations in the water flow caused by the flow-regulation system, and illustrates the unstable conditions during this phase in the filter run. When the C/C_0 curves approach 1 they flatten out, as would have been expected in an adsorption process when concentration in equals concentration out. Inlet concentration seems to approach the outlet concentration, but it is not known if the breakthrough turbidity is detached particles or inlet particles not able to attach in the filter bed. The removal of

turbidity during the production period is a little higher for filter A/S due to the difference in grain sizes between F/F and A/S.

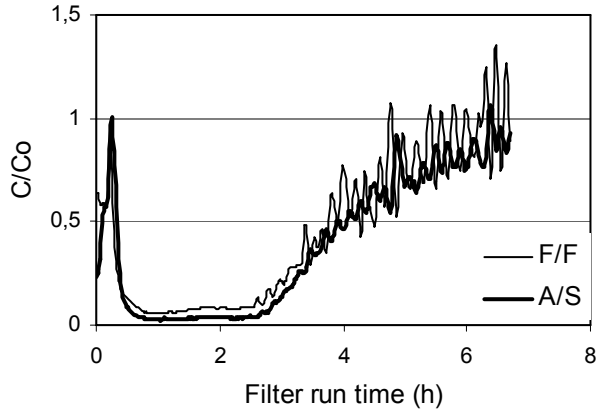

Figure 7.9 Turbidity breakthrough curves for filter F/F and A/S. (RW50, FEC, 7,5 m/h).

In Figure 7.10 breakthrough curves for similar experiments, run in filter F/F and F/F+ are compared. Here PAC was used with or without polymer as filter aid. The experiments with PAC and RW50 without polymer addition show a large difference in the ripening peak between the two filters, with a much smaller peak for the deeper filter. The ripening of a filter bed can be seen as the initial charging of the filter grains, and later in the run it also acts as an adsorption media. The lower peak for the deeper filter can be a result of deeper layers removing turbidity created in the top section of the bed. Knowing that C_0 is the same for the two filters, it is clear that the deep F/F+ has a larger capacity than F/F.

In the experiments where polymer is used as a filter aid, the second peak in the ripening is thought to be turbidity from the incoming suspension. The rate of filter ripening is dependent on filtration rate and the influent water characteristics (Fitzpatrick, 2001). In the examples shown, filter F/F and F/F+ are compared for equal filtration rates, suspension and pre-treatment. This peak has just a slightly higher value for the shallower F/F filter than filter F/F+. Effluent turbidity in the production period is better for the deeper filter, and the run length is considerably longer. When a polymer was used, visible flocs were observed in the water above the filter media (not observed when only coagulant was used). From this the two situations presented in Figure 7.10 are considered

to represent the situations when the filter act as a contact/adsorption filter (left), and as a regular particle removing depth filter (right).

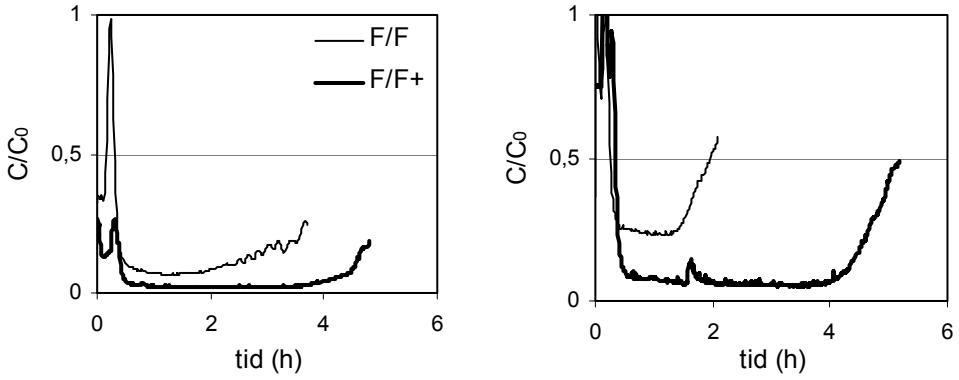

Figure 7.10 Experiments in filters F/F and F/F+ when the filter bed acts as an contact/adsorption filter (left) and as a particle separator (right). (Left: RW50, PAC, 7,5 m/h, Right: RW50, PAC+polymer, 12,5 m/h).

7.3.2 Adsorption capacity

In an adsorption column the capacity of the bed depth can be calculated as time equivalents. The available capacity in the bed is the time equivalent when effluent concentration is below the permissible limit. In this study the effluent turbidity limit is set to 0,3 NTU. The time equivalent is represented by the area between the breakthrough curve and the line $C/C_0 = 1$ as shown in the equation below:

$$t_b = \int_{t_{Turbidity<0,3\,NTU}}^{t_{Turbidity<0,3\,NTU}} (1-\frac{C}{C_0})dt \qquad (7.4)$$

This integral limited by the effluent turbidity level of maximum 0,3 NTU is used to calculate capacities of the filter beds used in this study. An adsorption type of model can be predicted the examples shown in Figure 7.10, if the deeper F/F+ has a capacity that is higher than F/F with a factor of $L_{F/F+}/L_{F/F}$ (bed depth of F/F+/bed depth of F/F). This statement is true for adsorption towers with uniform media in the whole depth of the bed. For the scale up of F/F to F/F+ it should be very similar, the only difference being a smaller fraction of HC material than NC material in F/F+ than in F/F. The difference is assumed to be small if the mechanisms are related to grain surface area. The capacity of the

filter beds for some different combinations of suspension and coagulant was calculated from experimental data according to Equation (7.4). The capacities for filter F/F was then multiplied with the depth ratio for the relationship between F/F and F/F+, and compared to capacities calculated from experimental data achieved for filter F/F+. The results of predicted and experimental capacities for the deep F/F+ filter are shown in Figure 7.11.

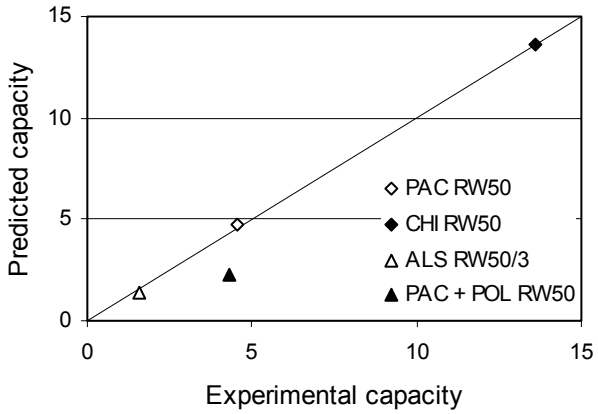

Figure 7.11 Experimental and predicted capacities for filter F/F+, values in time equivalents.

There is good agreement between experimental and predicted capacities for the contact filtration experiments, including the one with turbidity in the raw water. For the experiment with coagulation, reaction/flocculation time and polymer addition before filtration, predicted and experimental values do not agree. The capacity of the contact filtration filter beds can be predicted by the use of adsorption theory for different suspensions and coagulants. This is a strong indication of grain surface area being a limiting factor in contact filtration. The capacity model tested can be used as a simple tool for scale up and dimensioning of filter beds under similar conditions. The under-prediction of the capacity for filter F/F+ when scaling up from filter F/F for the experiments with polymer, indicate that a deeper filter is increasing the capacity more in regular filtration than in contact filtration. This is a bit surprising,

The limited examples shown here can only be regarded as an indication of the behaviour of contact filtration. The good correlation observed when using an adsorption model to predict filtration capacities, does not exclude that contact filtration is based on filtration mechanisms. Filtration of particles by the

transport mechanisms sedimentation, interception and diffusion is an important factor for water quality also in contact filtration.

7.3.3 Grain surface area

Grain surface is significant for the efficiency in a filter bed. An angular grain has more surface area than a spherical grain of the same sieve size. The surface area of grains per bed depth in a bed can be expressed by Equation (7.5), (McEwan (Ed.), 1998).

$$S_A = \frac{6(1-f_0)}{\psi d_g} \tag{7.5}$$

This equation shows that low porosity, low sphericity and smaller grains will increase the surface area. Filter beds with Filtralite grains have a large porosity, but on the other hand the grains are crushed material with a low sphericity. Table 7.3 shows the filter bed and grain characteristics needed in the calculation. The sphericity for anthracite and sand is values found in literature (Ives, 1990). Sphericity for the Filtralite media is calculated using a procedure suggested by Ives (1990).

The results for total surface area in the three filters show that filter F/F+ has a total surface area that is 1,7 times the area in F/F. This is naturally about the same ratio as for the depth of the two filters. In filter A/S the surface area is about 2 times the area in F/F. This is not proportional to the difference in capacity calculated by the adsorption model for different suspensions and coagulants, where ratios between 1,1 and 1,3 were found for contact filtration experiments.

From the calculations of surface area it can be seen that the difference between the media is large. The Filtralite media has a low sphericity, but a high porosity cause that few grains can pack into a given volume. From the listed surface area calculations one can calculate total surface area in the filter beds as shown in Table 7.4.

Table 7.3 Filter bed and grain characteristics

Filter	**Media**	**Layer depths** (m)	**Porosity, f_0**	**Grain diameter, d_g** (mm) (geometric mean of sieve sizes)	**Sphericity, ψ**	**Surface area** (mm^2/mm^3)
F/F	FL NC	0,47	0,7	2,0	0,54	1,7
	FL HC	0,47	0,6	1,13	0,66	3,2
F/F+	FL NC	1,18	0,7	2,0	0,54	1,7
	FL HC	0,60	0,6	1,13	0,66	3,2
A/S	Anth.	0,60	0,55	1,13	0,70	3,4
	Sand	0,35	0,43	0,57	0,85	7,1

Table 7.4 Total surface area of filter grains and ratios.

Filter	**Media**	**Surface area/layer** (m^2)	**Total surface area S_A** (m^2)	**Ratio of $S_A(X)/S_A(F/F)$**
F/F	FL NC	18,0	27,3	1
	FL HC	9,3		
F/F+	FL NC	23,4	46,3	1,7
	FL HC	22,9		
A/S	Anthracite	24,3	53,7	2,0
	Sand	29,4		

The porosity of the Filtralite media is very high, especially for the NC material. If the porosities and sphericities used is correct, the difference in surface area can not alone explain the difference in removal efficiency between filter F/F and A/S. When filter media is the same, the effect of an increase in bed depth of a contact filter can be predicted by using surface area ratios (or bed depth ratios). Comparing two filters with different grain size, the capacity of the filters (in removed turbidity) is not proportional to the total grain surface area.

8 CONCLUSIONS

A series of contact filtration experiments are carried out to investigate the performance of an expanded clay aggregate (Filtralite) filter. It is demonstrated that expanded clay aggregates can be used in dual media down flow filters as the only filtering material. The density difference of Filtralite NC and Filtralite HC is sufficient to prevent intermixing of adjacent layers for the grain sizes used in this study. Due to a more rapid increase in settling velocity with increasing grain size for high density materials, combinations of NC and HC filter grains of greater size than used in this study, is also possible.

Water uptake by the filter grains, measured as increase in settling velocity as a function of time spent in water, was observed for Filtralite HC and NC as well as anthracite. The highly porous NC material experienced a doubling in settling velocity due to water uptake after half a year soaked in water. The initial period of rapid water uptake lasts for about 3-4 weeks, and caution has to be made in this period to avoid loss of material due to washout. For HC material and anthracite, further water uptake was not observed after a few days in water.

The efficiency of all the coagulants tested (aluminium sulphate, iron chloride sulphate, poly-aluminium chloride and chitosan) is strongly pH dependent. The metal coagulants have an optimum pH for removal of organic matter, however this is not always the optimum pH for turbidity removal in the filter and for low metal residuals. In most cases, residual metal limitations determine the coagulant dose and pH requirements, especially for low turbidity humic raw waters. Particles in the raw water enhance hydroxide precipitation, giving increased turbidity removal and lower metal residuals. Poly-aluminium chloride is superior to aluminium sulphate when used as coagulant before filtration in the Filtralite filter, and low residuals of turbidity and metal could be obtained. Chitosan is less effective compared to the metal salts for the removal of organic matter, but there is no metal residual for this coagulant. Due to the lower levels of suspended solids formed during coagulation and the polymeric properties of chitosan, filtrate turbidity is generally very low. The dose of chitosan needed for coagulation decreases with decreasing pH, but higher removals are obtained at higher doses.

Particulate metal hydroxide is the main contribution to residual metal and turbidity in the filtrate from the Filtralite filter, when operating within the normal pH range of a metal salt coagulant. Clay turbidity has a much less

coagulant demand than humic substances. For equal coagulant doses, removal of colour and TOC was in most cases identical for coloured, low turbidity raw water and raw water containing both colour and turbidity.

Raw water containing low levels of colour and turbidity achieved relatively long filter run times, and produced in most cases satisfactory water quality. For the raw water with a higher level of colour, run lengths were short and solids storage capacities were much lower when a metal salt was used for coagulation. Chitosan is superior to the metal salts for all raw waters with respect to filter run times and storage capacities. With this coagulant, as high storage capacity was achieved for raw water with low and high content of organic matter. When used at optimum dose levels there were almost no differences between the coagulants regarding the rate of head loss development for the three filters. This implies that chitosan creates more head loss per solids loaded to the filters, a situation particularly advantages for the coarse Filtralite filter with more head loss available. Raw waters with a higher level of turbidity decrease filter run times in the same way as higher levels of colour. The amount of solids loaded is deciding the capacity of the filter, whether it is coagulated colour or turbidity is of minor importance within the levels tested in this study.

Big differences in initial head loss and rate of head loss development with time are seen between the coarse Filtralite filter and the anthracite/sand filter, due to the difference in grain size. When aluminium sulphate is used alone, the Filtralite filter is not able to produce satisfactory water quality. When the other three coagulants are used the difference in water quality is much smaller, and for chitosan there is almost no difference in filtrate turbidity between the Filtralite and the anthracite/sand filter. Generally a higher fraction of the deposited solids in the filter are stored in the top section of the anthracite/sand filter as compared to the Filtralite filter due to the smaller grain sizes in the former. In the anthracite/sand filter the head loss gradient varies from 5-6 cm/cm bed depth in the top section of the anthracite layer to almost zero in the bottom section of the anthracite. The same trend can be seen for the sand layer. In the Filtralite filter, which is not as effective due to larger grains, the deposits are stored more evenly. Head loss gradients for the Filtralite filter were normally below 1 cm/cm bed depth.

In this study it was observed that it is possible to compensate for a larger grain size by increasing the depth of a filter, but this is dependent on the suspension and the coagulant used.

An increased filtration rate is generally transporting more solids deeper into the filter bed. Water quality is more deteriorated with increasing rate when a metal salt is used for coagulation than when chitosan is used.

The deposition in depth of a contact filter has similarities with an adsorption process. Layers close to the bottom of the filter show no deposition early in the filtration run, but after some time the solids front (or deposition saturation front) have moved further down in the filter. Breakthrough occurs when deposition starts in the bottom section of the filter, indicating that the zone of mass transfer from solution to the filter grains has reached this section.

When a polymer is used as filter aid in combination with a metal salt, the coarse Filtralite filter can produce good water quality and long filter runs, also the available head (loss) is better utilised. Aluminium sulphate gave the best results as primary coagulant when a filter aid was used. The effect of the polymer was dependent on some minutes reaction/flocculation time after coagulant addition before the polymer was added.

Attempts to predict removals in contact filtration of humic waters as a particle separation process, by the use of single collector efficiency models, failed. Generally, the model predicted a lower efficiency in the coarse Filtralite filters than what was observed experimentally.

Model predictions using experimental data, showed strong indications of more voluminous deposits for the coarse filter bed. This implies that the mass per volume deposit is higher in the fine-grained anthracite/sand filter, which might be a result of deposit compaction.

Predicting experimental results from contact filtration experiments by using simple adsorption column models showed good results. This is perhaps an indication of grain surface area being the dominating parameter in contact filtration of humic waters.

REFERENCES

A

Adin, A. and Rebhun, M. (1977) A model to predict concentration and head-loss profiles in filtration, Journal AWWA, Vol 69(8), 444-453.

Amirtharajah, A. (1978) Optimum backwashing of sand filters, Journal of Env. Eng. Div., ASCE, Vol 20(EE5), 917-932.

Amirtharajah, A. (1988) Some theoretical and conceptual views of filtration, Journal AWWA, Vol 80(12), 36-46.

B

Boller, M.A. and Kavanaugh, M.C. (1994) Particle characteristics and headloss increase in granular media filtration, Wat. Res., Vol 29(4), 1139-1149.

British Water (1995) Standard for the specification, approval and testing of granular filtering materials, British Water publication, BW:P.18.93.

C

Camp, T.R. (1968) Floc volume concentration, Journal AWWA, Vol 60, 656-673.

E

Ebie, K. and Amano, S. (1993) Fundamental behaviour of humic acid and kaolin in direct sand filtration of simulated natural surface water, Wat. Sci. Tech., Vol 27(11), 61-70.

Edzwald, J.K. and Van Benschoten, J.E. (1990) Aluminium coagulation of Natural Organic Matter, Proceedings of the 4th Gothenburg Symposium, Springer, October 1-3, Madrid, Spain.

Edzwald, J.K. and Kelly, M.B. (1998) Control of cryptosporidium: from reservoir to clarifiers to filters, Wat. Sci. Tech., Vol 37(2), 1-8.

Edzwald, J.K. and Tobiason, J.E. (1999) Enhanced coagulation: USA requirements and a broader view, Wat. Sci. and Tech., Vol 40(9), 63-70.

Edzwald, J.K., Pernitsky, D.J. and Parmenter, W.L. (2000) Polyaluminum coagulants for drinking water treatment: Chemistry and selection, Proceedings of the 9th Gothenburg Symposium, Springer, October 2-4, Istanbul, Turkey, in H.H.Hahn, E. Hoffmann and H. Ødegaard (Ed.) Chemical water and wastewater treatment VI, 3-13, Springer-Verlag, Berlin, Heidelberg 2000, ISBN 3-540-67574-4.

Eikebrokk, B. (1982) Koagulering/Direktefiltrering for fjerning av humus fra drikkevann (in Norwegian), Dr. of Engineering thesis, NTH, Trondheim, Norway.

Eikebrokk, B. (1998) Optimising coagulation-direct filtration for NOM removal (in Norwegian), Proceedings of the seminar "VAR-Forskningsdagene '98" at NTNU, Trondheim, Norway, Tapir, ISBN 82-519-1347-0.

Eikebrokk, B. (1999) Coagulation-direct filtration of soft low alkalinity humic waters, Wat. Sci. and Tech., Vol 40(9), 55-62.

Eikebrokk, B. (2000) Effects of coagulant type and coagulation conditions on NOM removal from drinking water, Proceedings of the 9th Gothenburg Symposium, October 2-4, Istanbul, Turkey, in H.H.Hahn, E. Hoffmann and H. Ødegaard (Ed.) Chemical water and wastewater treatment VI, 211-220, Springer-Verlag, Berlin, Heidelberg 2000, ISBN 3-540-67574-4.

Eikebrokk, B. and Saltnes, T. (2000) NOM removal from drinking water by chitosan coagulation and filtration through light-weight expended clay aggregate filter, Proceedings: Innovations in conventional and advanced water treatment processes, September 26-29, Amsterdam, The Netherlands.

Eikebrokk B. (2001) Experimental testing of Filtralite for the removal of NOM from drinking water by contact filtration, SINTEF-report: STF66F01106, August 2001, Trondheim, Norway.

F

Folkehelsa (1997) Landsrapport vannverksregisteret, Status for vannforsyning 1994 (In Norwegian), Folkehelsa report nr. 97,July 1997, Oslo, Norway, ISSN 0804-1490.

Fitzpatrick, C.S.B. (2001) Causes of particle breakthrough in filtration, Proceedings of the World Water Congress of IWA, October 15-19, Berlin, Germany.

G

Gjessing, E.T. (1982) Humus i vann-Hva vet vi og hva bør vi vite ? (In Norwegian), Proceeding of the seminar "Vanndagene 1982"at NTH, 26-27 August, Trondheim, Norway.

Graham, N.J.D. (1988) Filter pore flocculation as a mechanism in rapid filtration, Wat. Res., Vol 22(10), 1229-1238.

Gregory, J. (1989) Fundamentals of flocculation, Crit. Rev. in Env. Contr., Vol 19(3), 185-230.

Gregory, J. and Rossi, L. (2000) Dynamic testing of water treatments coagulants, Wat. Sci. Tech.:Wat. Sup., Vol 1(4), 65-72.

H

Helsedepartementet (2001) Forskrift om vannforsyning og drikkevann (Drikkevannsforskriften), (In Norwegian, "Norwegain drinking water regulations"), FOR 2001-12-04, nr 1372.

Hossain, M.D. and Bache, D.H. (1991) Composition of alum flocs derived from a coloured, low-turbidity water, Journal Water SRT-Aqua, Vol 40(5), 298-303.

Hunt, J.R., Hwang, Bor-Chih and McDowell-Boyer, L.M. (1993) Solids accumulation during deep bed filtration, Env. Sci. Tech., Vol 27(6), 1099-1107.

I

Ives, K.J. and Sholji, I. (1965) Research on variables affecting filtration, Journal of the San. Eng. Div., Vol 91(SA4), 1-18.

Ives, K.J. (1975) Mathematical models of deep bed filtration, Proceedings of the NATO advanced study institute, in K.Ives (Ed.) The Scientific Basis of Filtration, July 2-20, 1973, Cambridge, U.K., Noordhoff I.P.

Ives, K.J. (1970) Rapid filtration, Wat. Res., Vol 4, 201-223

Ives, K.J. (1980) Deep bed filtration: Theory and practice, Filt. & Sep., Vol 17(2), 157-166.

Iwasaki, T. (1937) Some notes on sand filtration, Journal AWWA, Vol 29,1591-1597.

J

Jekel, M.R. and Heinzmann, B. (1989) Residual aluminium in drinking-water treatment, Journal of Wat. Sup. Res. and Tec.-AQUA, Vol 38, 281-288.

K

Kawamura, S. (1991) Integrated design of water treatment facilities, 211, John Wiley and Sons, New York, USA.

Klute, R. (1990) Destabilisation and aggregation in turbulent pipe flow, Proceedings of the 4th Gothenburg Symposium, October 1-3, Madrid, Spain, in H.H.Hahn and R.Klute (Eds.) Chemical water and wastewater treatment, 33-54, Springer-Verlag, Berlin, Heidelberg 1990, ISBN 3-540-53181-5.

Kvinnesland, T. (2002) Personal communication.

L

Letterman, R.D. (Ed.) (1999) Water quality and treatment, fifth edition, AWWA, McGraw-Hill, USA.

Logan, B.E., Jewett, D.G., Arnold, R.G., Bouwer, E.J., O'Melia, C.R. (1995) Clarification of clean-bed filtration models, Journal of Env. Eng., Vol 121(12), 869-873.

M

Machenbach, I. (2002) Personal communication.

Mackie, R.I. (1989) Rapid gravity filtration-Towards a deeper understanding, Filtration & Separation, Vol 26(1), 32-35.

McEwan, J. Brock. (Ed.) (1998) Treatment process selection for particle removal, AWWARF/IWSA-report, Denver, Co. USA.

Mints, D.M. and Krishtul, V.P. (1960) Investigation of the process of filtration of a suspension in a granular bed, Journal of Appl. Chem. USSR, Vol 33, 303-314.

Moran, D.C., Moran, M.C., Cushing, R.S., Lawler, D.F. (1993a) Particle behavior in deep-bed filtration: Part 1-Ripening and breakthrough, Journal AWWA, Vol 85(12), 69-81.

Moran, M.C., Moran, D.C., Cushing, R.S., Lawler, D.F. (1993b) Particle behavior in deep-bed filtration: Part 2-Particle detachment, Journal AWWA, Vol 85(12), 82-93.

O

Odegaard, H., Eikebrokk, B. and Storhaug, R. (1999) Processes for the removal of humic substances from water - An overview based on Norwegian experiences, Wat. Sci. Tech., Vol 40(9), 37-46.

O'Melia, C.R. and Shin, J.Y. (2000) Removal of particles using dual media filtration: modelling and experimental studies, Wat. Sci. Tech.:Wat. Sup., Vol 1(4), 73-79.

P

Parthasaraty, N. and Buffle, J. (1985) Study of polymeric aluminium (III) hydroxide solutions for application in waste water treatment. Properties of the polymer and optimal conditions of preparation, Wat. Res., Vol 19(2), 25-36.

R

Rajagopolan, R. and Tien, C. (1976) Trajectory analysis of deep-bed filtration with the sphere-in-a-cell porous media modell, Am. Inst. of Chem. Eng. Journal, Vol 22(3), 523-533.

Ratnaweera, H., Gjessing, E. and Oug, E. (1999) Influence of Physical-Chemical Characteristics of Natural Organic Matter (NOM) on Coagulation Properties: An Analysis of Eight Norwegian Water Sources, Wat. Sci. Tech., Vol 40(9), 89-96.

Rebhun, M., Fuhrer, Z. and Adin, A. (1984) Contact flocculation-filtration of humic substances, Wat. Res., Vol 18(8), 963-970.

Ribas, F., Bernal, A. and Perramon, J. (2000) Elimination of Giardia cysts, Cryptosporidium oocysts, turbidity and particles in a drinking water treatment plant with clarification and double filtration, Wat. Sci. Tech., Vol 41(7), 203-211.

S

Sembi, S.S. (1984) Optimization of size-graded filters, Dr. of Philosophy thesis, University College London, London, U.K.

Singer, P.C. (1999) Humic substances as precursors for potentially harmful disinfection by-products, Wat. Sci. Tech., Vol 40(9), 25-30.
Specht, C.H., Kumke, M.U. and Frimmel, F.H. (2000) Characterisation of NOM adsorption to clay minerals by size exclusion chromatography, Wat. Res., Vol 34(16), 4063-4069.
Strand P., S. (2001) Interactions between chitosans and bacteria: flocculation and adhesion, Dr. of Engineering thesis, Dept. of biotechnology, NTNU, Trondheim, Norway.

T

Tambo, N. and Kamei, T. (1998) Coagulation and flocculation on water quality matrix, Wat. Sci. Tech., Vol 37(10), 31-41.
Thorsen, T. (1999) Fundamental studies on membrane filtration of coloured surface water, Dr. Technicae thesis, NTNU, Trondheim, Norway.

U

US EPA (1998) National Primary Drinking Water Regulations: Disinfectants and Disinfection Byproducts; Final Rule, 40 CFR Parts 9, 141, and 142.

V

Van Benschoten, J.E. and Edzwald, J.K. (1990a) Chemical aspects of coagulation using aluminium salts-I. Hydrolytic reactions of alum and polyaluminum chloride, Wat. Res., Vol 24(12), 1519-1526.
Van Benschoten, J.E. and Edzwald, J.K. (1990b) Chemical aspects of coagulation using aluminium salts-II. Coagulation of fulvic acid using alum and polyaluminum chloride, Wat. Res., Vol 24(12), 1527-1535.
Van der Hoek, J.P., Hofman, J.A.M.H. and Graveland, A. (1999) The use of Biological Activated Carbon Filtration for the Removal of Natural Organic Matter and Organic Micropollutants from Water, Wat. Sci. Tech., Vol 40(9), 257-264.
Vigneswaran, S. (1983) Analysis of mathematical models for deep bed filtration: Microscopic and macroscopic approaches, Journal of IWWA, Vol 15(3), 249-257.

Y

Yao, K.M., Habbibian, M.T., O'Melia,C.R. (1971) Water and waste water filtration: Concepts and applications, Envir. Sci. Tech., Vol 5(11), 1105-1112.

APPENDIX A

Sammendrag på norsk (Summary in Norwegian)

Denne oppgaven omhandler kontaktfiltrering av humusholdig råvann i et filter bestående av ekspanderte leire aggregater (Leca, Filtralite). Målsettingen med oppgaven var å identifisere filtermediets egenskaper og optimalisere bruken av det i et dybde-filter for behandling av vann. Hovedvekt i oppgaven er lagt på fjerning av organisk materiale (humus) fra drikkevann.

Humus i vann
Humus er store molekyler som dannes ved nedbrytning av planter og dyr i naturen. Humus vaskes ut fra bakken og ender opp i elver og vann, og forårsaker en brunfarging av vannet. Vann som inneholder humusstoffer er ikke nødvendigvis skadelig å drikke, men giftstoffer kan være assosiert med humusen. Ved desinfeksjon av humusholdig vann med klor eller ozon, dannes det kreftfremkallende stoffer.

Fordi humus er molekyler må de gjennomgå en koagulering for å skape partikler som lar seg fjerne i et filter. Ved dybdefiltrering i granulære filtre fjernes partikler hovedsakelig ved at de sedimenterer på, henger seg opp i, eller diffunderer bort til et filterkorn. Siling er uønsket i et dybdefilter fordi det fører til dårlig utnyttelse av lagringskapasiteten nedover i en filterseng. Direktefiltrering er en behandlingsprosess som inneholder koagulering, flokkulering for å skape filtrerbare partikler og filtrering. Ved kontaktfiltrering er flokkuleringen utelatt, og partiklene som skal fjernes dannes for en stor del i filter porene.

Filtermediet
I denne oppgaven er ekspanderte leire-aggregater (Filtralite) brukt som filtermateriale i dybdefilter for kontaktfiltrering. Ved å måle synkehastigheten til filterkorn av forskjellig kvalitet (forskjellig tetthet), så man at det var mulig å sette sammen et to-media filter bestående av bare leire-aggregater. I nedstrømsfiltrering er man avhengig av å ha de største filterkornene på toppen av filteret og de minste kornene på bunnen for å øke effektiviteten til filteret. Etter endt filtrering vaskes filteret ved å reversere vannstrømmen. For å opprettholde den ønskede lagdeling av filteret etter vasking, må de store kornene på toppen ha en lavere tetthet en de små kornene på bunnen.

På grunn av den porøse strukturen adsorberer filtermaterialet vann. Vann-opptaket ved fukting, målt som økning i synkehastighet som funksjon av tid i vann, ble undersøkt for Filtralite NC (normal tetthet, knust), HC (høy tetthet, knust), antrasitt og sand. Det mest porøse materialet Filtralite NC, viste en dobling av synkehastigheten etter fukting i et halvt år. De første 3-4 ukene av denne perioden økte synkehastigheten raskt, og her må filtermediet vaskes ved lave spylevanns-hastigheter for å unngå utvasking av materiale. Økning av synkehastigheten for HC materialet og antrasitt ble observert i de første dagene, før den var stabil. Sand viste som forventet ingen økning i synkehastighet som følge av vannopptak.

Forsøksanlegget

Forsøk som er beskrevet ble utført i et filtreringsanlegg i pilotskala. Anlegget besto av to parallelle filterkolonner som ved hvert forsøk mottok vann som hadde vært igjennom den samme forbehandlingen. Råvannet som ble brukt var kranvann som i enkelte forsøk ble tilsatt små mengder humuskonsentrat og/eller bentonitt-leire. Vannet ble først pH justert med saltsyre, før tilsetting av koagulant i en hurtigmikser. Vannet ble så ledet inn til de to filterkolonnene. Det ene filteret besto av et topplag av 47 cm Filtralite NC (1,6-2,5 mm) og et bunnlag av 47 cm Filtralite HC (0,8-1,6 mm). Det andre filteret, som ble brukt som et referanse filter, besto av et topplag av 60 cm antrasitt (0,8-1,6) og et bunnlag av 30 cm sand (0,4-0,8 mm). I senere forsøk ble dybden av lagene i Filtralite filteret økt, for å se om den økt dybden kunne kompensere for en større kornstørrelse. Turbiditet, pH, filtreringshastighet og trykktap i filtersenga ble målt kontinuerlig og data lagret på PC. Vannprøver av råvann, koagulert vann og filtrert vann ble tatt ut ved hvert forsøk og analysert i laboratoriet.

Optimaliseringsforsøk

For å finne optimale pH- og koagulantdose- betingelser for Filtralite filteret ble det utført en rekke forsøk ved forskjellige betingelser for fire forskjellige råvann. Disse forsøkene viste at fjerning av organisk materiale for alle koagulantene (aluminiumsulfat, jernkloridsulfat, pre-polymerisert aluminiumklorid og bio-polymeren kitosan) var sterkt pH-avhengig. De metallbaserte koagulantene har en optimal pH for fjerning av organisk materiale, som kan være forskjellig fra optimal pH for fjerning av turbiditet og lave restmetall konsentrasjoner. Restmetall-begrensninger er i de fleste tilfeller bestemmende for koaguleringsbetingelser, spesielt for råvann med høyt innhold av humus og lav turbiditet. For råvann med høyere turbiditet, vil partiklene i vannet øke utfellingen av metallhydroksid, som igjen fører til økt turbiditets-fjerning og lavere restmetall-konsentrasjoner. Ved å bruke pre-polymerisert aluminiumklorid som koagulant i steden for aluminium sulfat, oppnås en lav

utløpsturbiditet og restmetall-konsentrasjon fra det grovkornede Filtralite-filteret. Kitosan er mindre effektivt for fjerning av organisk materiale, målt som farge og TOC, enn de metallbaserte koagulantene. Restmetall er selvfølgelig ikke et problem for denne koagulanten. På grunn av at denne koagulanten skaper mindre suspendert stoff ved koagulering og dens egenskaper som polymer, oppnås en særdeles lav utløpsturbiditet. Ved lave kitosandoser økes fjerningen av organisk materiale ved å senke pH, men høyere fjerning kan oppnås ved høyere kitosan doser.

Partikulært metall gir det største bidraget til restmetall og turbiditet i utløpsvannet fra Filtralite filteret, når en metallbasert koagulant blir brukt innenfor sitt normale pH område. Leire-partikler har et mye mindre koagulant behov enn humus, og like god fjerning av organisk materiale kan oppnås for råvann med og uten turbiditet, ved den samme koagulantdosen.

Filtreringsforøk
Forsøk viste at lange filtersykluser og i de fleste tilfeller god vannkvalitet kunne oppnås for råvann med lavt innhold av humus og turbiditet. For råvann med høyt humusinnhold koagulert med et metallsalt, ble syklusene særdeles korte og lagringskapasiteter for filtrene var vesentlig lavere enn for råvann med lite humus. Kitosan viste seg å være overlegen alle metallsaltene med hensyn til sykluslengde og lagringskapasitet for alle råvann. For denne koagulanten ble like stor lagringskapasitet oppnådd ved høyt som ved lavt innhold av organisk materiale. Trykktapsutviklingen over filteret med tid viste liten forskjell mellom koagulantene, noe som betyr at kitosan skaper et høyere trykktap i filteret per mengde suspendert stoff tilsatt. Dette er særdeles gunstig i kombinasjon med Filtralite-filteret, hvor det er mye trykktap tilgjengelig. Råvann med høyere turbiditet forkorter sykluslengden på samme måte som råvann med høyt humusinnhold. Det er mengden suspendert stoff tilført (og om koagulanten er kitosan eller et metallsalt) som bestemmer syklusslengden, om det er koagulert humus eller turbiditet er av mindre betydning.

Det ble observert store forskjeller i initialt trykktap og utvikling med tid mellom det grovkornede Filtralite filteret og antrasitt/sand filteret som følge av forskjellen i kornstørrelse. Dersom aluminiumsulfat blir brukt som koagulant produserer Filtralite-filteret en dårligere vannkvalitet enn antrasitt/sand-filteret. For de andre koagulantene er denne forskjellen mindre, og spesielt for kitosan er vannkvaliteten tilsvarende god for de to filtrene. Generelt blir en større andel av avsetningene lagret i toppen av antrasitt/sand filteret enn for Filtralite filteret som følge av en mindre kornstørrelse. For antrasitt/sand filteret kan trykktapsgradienten (cm trykktap/cm sengedybde) variere fra 5-6 cm i toppen

av antrasitten til tilnærmet null i nederste del, det samme kan sees for sand-laget men der er gradientene mindre. I Filtralite-filteret er avsetningene lagret jevnere i dybden av senga, på grunn av at effektiviteten er redusert ved å øke kornstørrelsen.

Det er mulig å kompensere for en større kornstørrelse ved å øke dybden av filtersenga. Detter ble observert i en rekke forsøk hvor lagdybden i Filtralite-filteret ble øket til 118 cm for topplaget og 60 cm for bunnlaget. Dybdene ble valgt ut fra at forholdet mellom lagdybde og korndiameter skulle være det samme som for antrasitt/sand filteret. Utløpsturbiditeten var for de fleste råvann og koagulanter bedre fra det dype Filtralite filteret enn fra antrasitt/sand filteret, men ved bruk av aluminiumsulfat kunne fremdeles ikke en tilsvarende vannkvalitet produseres.

Ved å øke filtreringshastigheten transporteres en større del av avsetningene lenger ned i filtersenga. Vannkvaliteten blir mer forringet ved økt filtreringshastighet når en metalbasert koagulant brukes enn ved kitosan koagulering.

Avsetningsforløpet av fast stoff i dybden av et kontaktfilter har likhetstrekk med forholdene i en adsorpsjonskolonne. Filterlag nær bunnen i et filter viser ingen avsetninger tidlig i syklusen fordi innkommende konsentrasjon til disse lagene er svært lav. Det er en avsetningsfront i filteret som beveger seg nedover og etterlater seg filtermateriale mettet med avsetninger. Gjennombruddet kommer når denne avsetningsfronten har nådd nederste lag i filteret. Hastigheten som den beveger seg nedover i filteret med, er avhengig av vannet som kommer inn på filteret, filtreringshastigheten og filtersengens oppbygging.

Ved å bruke en polymer som filtreringshjelpemiddel sammen med et metallsalt, oppnås lange filtersykluser og god vannkvalitet i Filtralite-filteret. Polymeren lager større og sterkere fnokker av humus metall-aggregatene, og de blir dermed mer filtrerbare i det grovkornede Filtralite-filteret. Aluminiumsulfat ga best virkning når den ble brukt sammen med en polymer. Effekten av filtreringshjelpemiddelet var avhengig av noen minutters reaksjonstid for koagulanten før tilsetning av polymer. Polymerdosen kan varieres for å optimalisere lagringskapasitet til filteret.

Modellering

Forsøk på å modellere effektiviteten av de forskjellige kontaktfiltrene med en modell basert på partikkelfjernings-mekanismer, ga ikke resultater som samsvarte med eksperimentelle data. Generelt ble effektiviteten av de

grovkornede Filtralite-filtrene predikert dårligere enn vist i forsøkene. Dette viser kanskje at et kontaktfilter ikke er en ren partikkelfjerningsprosess, og at andre mekanismer også innvirker.

Det ble funnet sterke indikasjoner på at avsetningene i et grovkornet filter (høyere porøsitet) er mer voluminøse enn avsetninger i et finkornet filter. Dersom filtrene fjerner like mye suspendert stoff fører dette til at tettheten på avsetningene er høyere i det finkornede filteret.

Det viste seg å være mulig å beregne kapasiteten til det dype Filtralite-filteret ut fra eksperimentelle verdier for det grunne filteret ved bruk av enkle adsorpsjonskolonne-modeller. Eksperimentelle og predikerte verdier samsvarte godt for noen kontaktfiltreringsforsøk, men ikke for et forsøk med polymer-tilsetting. Dette kan indikere at ved polymer-tilsetting fungerer filteret mer som et rent partikkelfjerningsfilter.